ISTITUTO NAZIONALE DI FISICA NUCLEARE

Sezione di Tieste

INFN-TC-05-12
14 Settembre 2005

CHARACTERISATION AND TEST OF THE POWER SUPPLY SYSTEM OF THE PAMELA EXPERIMENT

Valter Bonvicini[1], Stefano Ciano[1]

1) INFN- Sezione di Trieste, Laboratori c/o Area di Ricerca Padriciano 99, I-34012, Trieste

Abstract

This work describes the measurements and tests performed in Trieste in order to fully characterize the performance of the Power Supply System (PSS) of the space experiment PAMELA. The PSS behavior has been analyzed by means of an *ad hoc* designed set-up reproducing the electrical experimental conditions specified in the PAMELA ICD (Interface Control Document) and expected during the three-year lifetime of the mission.

PACS.: 84.70.+p

Published by ***SIS–Pubblicazioni***
Laboratori Nazionali di Frascati

1 INTRODUCTION

The space experiment PAMELA (a Payload for Antimatter-Matter Exploration and Light-nuclei Astrophysics) is scheduled to be launched on a Russian satellite Resurs-DK1 at the end of 2005. Details about the various PAMELA detectors and the scientific goals of the mission can be found through Refs.[1-5]. In a satellite-borne experiment, the power supply system represents one of the most crucial items of the whole apparatus. It has to provide all the required "clean" and stable supply voltages for each sub-system of the apparatus (detectors, front-end and read-out electronics) starting from the unregulated primary voltage supplied by the satellite batteries/accumulators system. Moreover, the power supply system should be immune to all kind of glitches, pulses and low and high-frequency disturbances occurring on the unregulated satellite primary power buses, which can be due to many possible causes, such as switching on/off of antennas and radio links, different satellite operations, etc.

An oversimplified block scheme[1] of the PAMELA PSS is sketched in Appendix E. The power lines from the Resurs-DK1 satellite are interfaced with the first stage of the PSS, consisting of 6 Input Protection Modules (IPMs), via a set of input filters (manufactured by CAEN) and a Relay Board, manufactured by Kayser[6], which is also connected to telemetry signals coming directly from Resurs-DK1. The basic unit of the first stage of the PAMELA PSS is the CAEN S9008 dc/dc converter, called Input Protection Module[7]. This is a push-pull type dc/dc converter, which provides +17 V dc floating output voltage when supplied with a +22 V ÷ +32 V input voltage. The unit is provided with input over/under voltage control, output over current control and maximum duty cycle control in order to keep parameters within safety limits. For the purpose of redundancy, there are 6 IPMs in the PSS, 3 "hot" (IPM1, IPM3 and IPM5) and 3 "cold" (spares: IPM2, IPM4 and IPM6). The outputs of the IPMs are connected to the inputs of 64 dc/dc converters (32 hot and 32 cold), of 7 different types, also manufactured by CAEN[7], which provides all high and low voltages necessary for the power supply of the PAMELA sub-detectors. This set of dc/dc converters constitutes the second stage of the PSS. The main characteristics of the dc/dc converters (type, input voltage range, output voltage, and maximum output power) are summarized within Appendix E.

Section 2 reports the requirements to the PAMELA PSS contained in the PAMELA Interface Control Document. The basic measurement set-up used throughout the paper is described in section 3 (possible variations for particular measurements are described from time to time). Test results on the main PSS units (IPMs and dc/dc converters) are reported in section 4. Tests on a "complete" PSS, including cables and connectors identical to those used in the satellite, are detailed in section 5.

2 REQUIREMENTS SET BY THE INTERFACE CONTROL DOCUMENT

The requirements set to the PSS by the PAMELA Interface Control Document (ICD) are described in Section 9.4 of the ICD itself [6]. In particular, the PSS is required to function nominally in presence of the following conditions and occurrences:

- "Voltage at input power buses normally between 23 and 32 V, with possible sags down to 22 V of duration up to 200 ms".

[1] The scheme reported in Appendix E is not complete (some parts of the system are not shown) for the purpose of simplicity, its scope being only to illustrate the basic units and working principle.

- "Occurrence of supply rushes and slumps (within the 23 V - 32 V range) with amplitude of maximum 5 V with pulse rise time up to 10 μs and repetition frequency between 10 Hz and 20 kHz".

- "Switching-induced dumping pulses with a duration of up to 20 ms and an amplitude of up to ± 10 V (of supply voltage level), frequency of pulse filling vibrations is up to 10 MHz, minimum oscillation frequency 150 kHz".

- "Single voltage pulse rushes of up to 10 μs duration and an amplitude of up to 80 V for each power bus with respect to the shell of the vessel".

3 MEASUREMENT SET-UP

3.1 General description

A measurement set-up was conceived and prepared at INFN-Trieste in order to perform the measurements required. It includes:

- a DC high power supply (HP Harrison 6269A, 0-40 V, 0-50 A), used to emulate the DC power from the satellite;
- a Noise Generator (NG), which was designed and realized in Trieste to generate all kinds of disturbances required by the ICD and described in the previous section;
- a set of differential probes LeCroy DXC100A, attenuation 1:10:100, frequency up to 250 MHz, max. voltage 500 V;
- a differential amplifier with internal generator LeCroy DA1855A, used together with the DXC100A probes;
- a Tektronix 1X probe Tek P6101A;
- a current probe LeCroy AP015;
- 3 PAMELA IPM modules mounted inside shielded boxes. These units are push-pull type dc/dc converters that provide a + 17 V DC floating output voltage when supplied with a + 22 V ÷ + 32 V input voltage.[2]

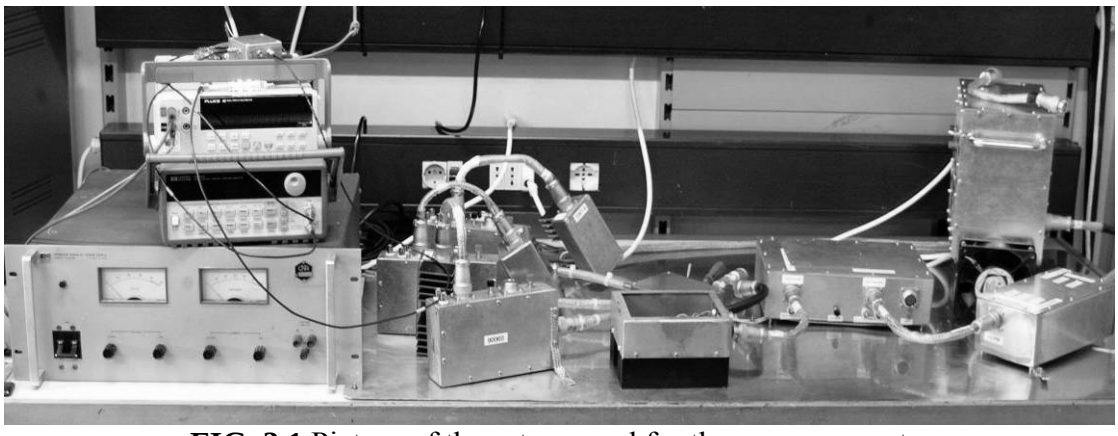


FIG. 3.1 Picture of the set-up used for the measurements.

- a set of PAMELA dc/dc converters in shielded boxes (manufactured by CAEN) that could be connected at the outputs of the IPMs. These units are push-pull type

[2] In all measurements done with the NG, only one IPM unit at a time could be operated due to the NG output power limitation.

converters used to generate the various voltages needed for the PAMELA sub-detectors from the regulated + 17 V DC supplied by the IPMs;
- a splitter to allow the output of the IPM to be connected simultaneously up to 4 different dc/dc converters and/or to resistive loads;
- a set of resistive loads to emulate different power consumption situations.
- a Kayser Relay Board, used to connect or disconnect the primary of the various IPMs to the input power lines;
- an input filter, manufactured by CAEN, placed between the input power lines and the Kayser relays board, before the IPM input;
- a LeCroy 9354A oscilloscope;
- a LeCroy 960 oscilloscope;
- a Fluke 45 digital multimeter;
- a set of shielded cables.

Initially, the measurements were performed with ad-hoc realised shielded cables of about 1 m length. Later, the real Russian cables foreseen for PAMELA were used. The type of cables used for a particular measurement will always be indicated throughout the paper.

In Fig. 3.1 it is possible to see a partial view of the set-up used for the first measurements. Fig. 3.2 shows the Caen input filter while Fig. 3.3 shows the three dc/dc converters Caen IPM S9008 used at the input of the supply chain.

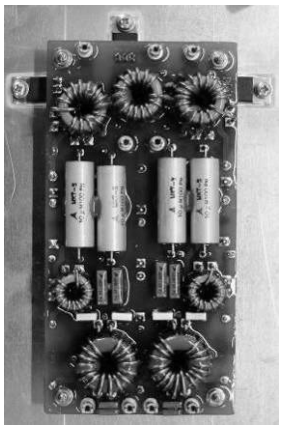


FIG. 3.2 CAEN filter.

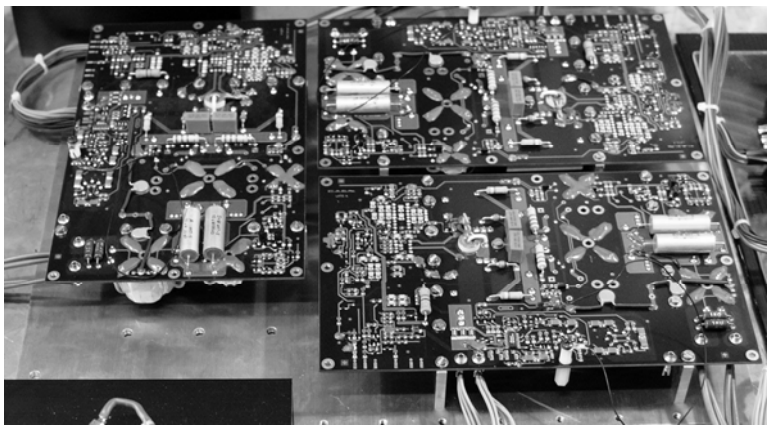


FIG. 3.3 The three IPM S9008 used in the tests.

3.2 Characteristics of the Noise Generator (NG)

In order to fully comply with the test conditions listed in section 2, we have designed and realized an electronic module (called “Noise Generator”, NG) capable of emulate all types of disturbances and glitches on the primary power lines described in the PAMELA ICD. A block scheme of the NG is given in Fig. 3.4.

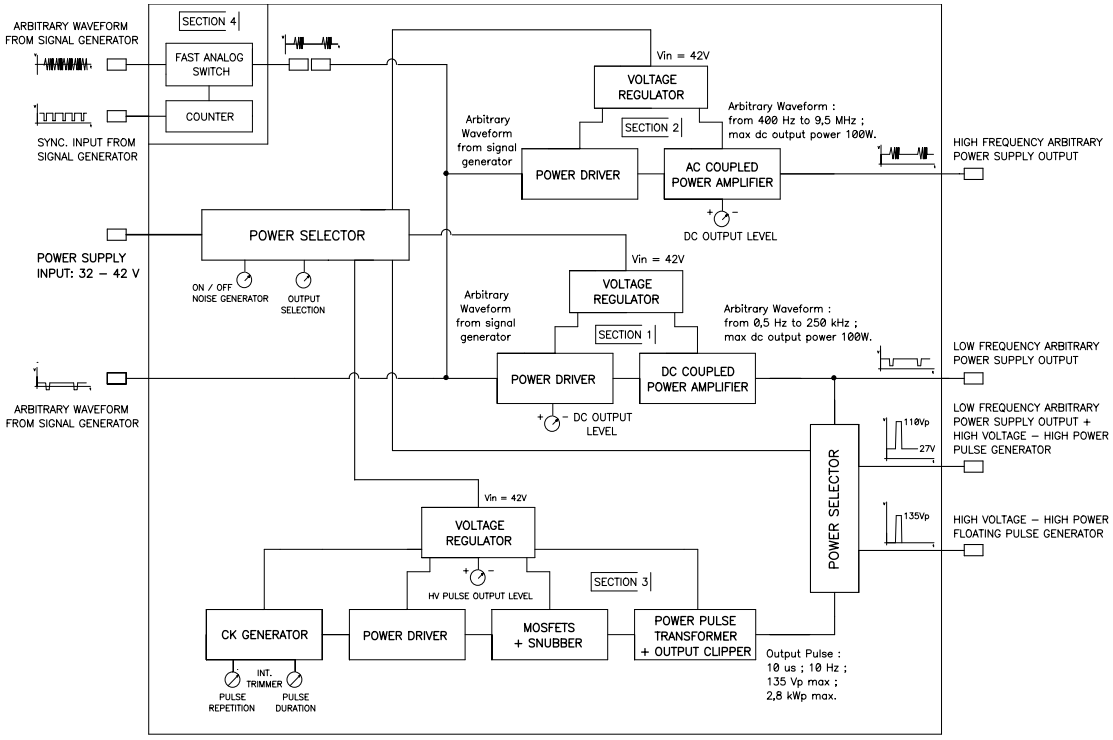


FIG. 3.4 Block diagram of the NG.

The NG is functionally divided into 4 sections. Their specifications are as follows:

NG Section 1 - Low frequency arbitrary power supply

Input characteristics : Vdc from 32 to 42V
Output characteristics :
dc level: adjustable from 23 to 37V; Max dc output Power = 100W;
ac level: adjustable from 0 to14 Vpp;
modulation: external source input (signal out / signal in = 0,5);
output Bandwidth at 10 Vpp: from 0.5 Hz to 250 KHz (Tr ~ 1,5 µs).

NG Section 2 - High frequency arbitrary power supply:

Input characteristics : Vdc from 32 to 42V
Output characteristics :
dc level: adjustable from 19 to 39V; Max dc output Power = 100W;
ac level: adjustable from 0 to 35 Vpp;
modulation: external source input (signal out /signal in = 2);
output Bandwidth at 20 Vpp: from 400 Hz to 9,5 MHz (Tr ~ 40 nS).

NG Section 3 - High voltage - high power floating pulse generator:

Input characteristics : Vdc from 35 to 42V
Output characteristics :
pulse level: adjustable from 32 to 135V ; max peak pulse power: 2,8 kWp;
pulse duration : 10μS ; pulse repetition 10Hz ; (Tr ~ 5 ms).
dc level: in addiction with section1 adjustable from 23 to 37V;
max dc output power = 100W

NG Section 4 - Counter + analog switch (external circuit):

High frequency analog switch with output disable synchronized with trigger input.

A picture of the NG module is shown in Fig. 3.5.

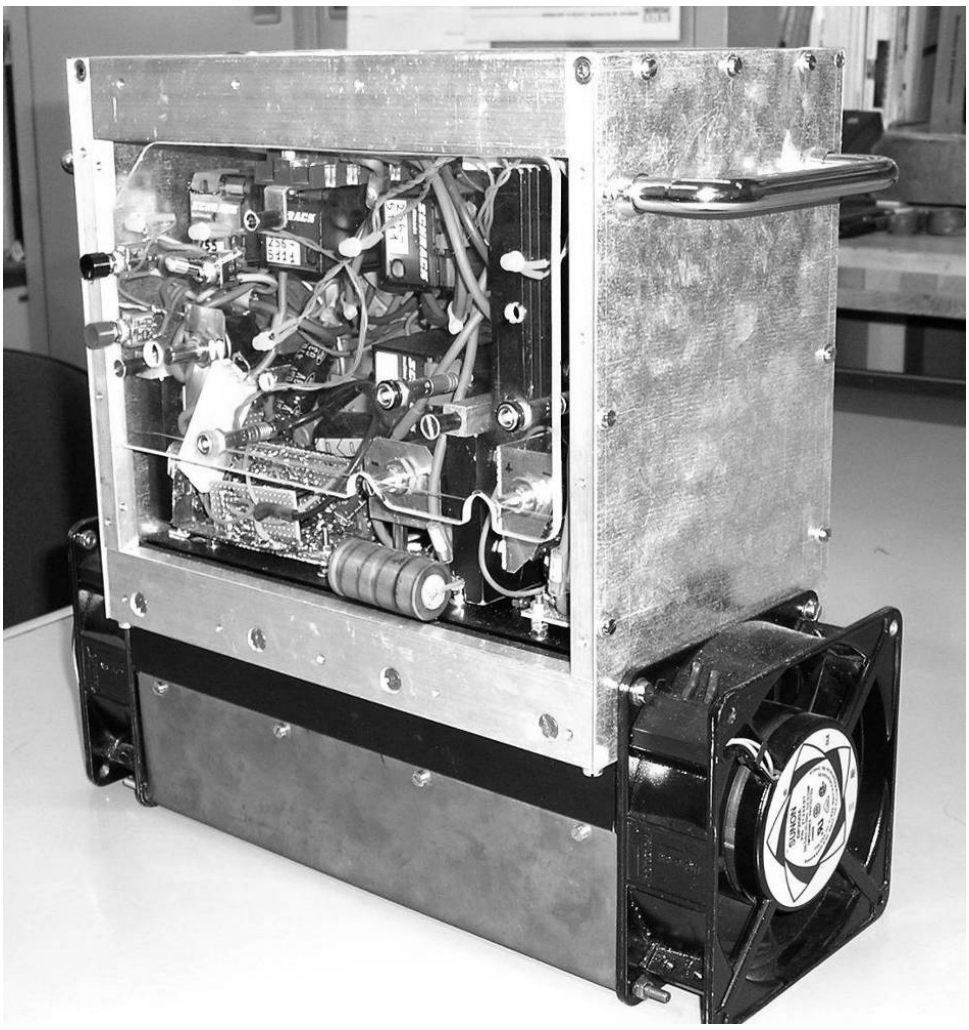


FIG. 3.5 Picture of the Noise Generator module

4 MEASUREMENTS WITH NON-RUSSIAN CABLES

4.1 Load regulation of the IPM

The first test was to ascertain if the IPM units met the load regulation capability specified by the manufacturer and needed by the PAMELA experiment, that is 1% at V_{in} = + 28 V and P_{out} = 20 ÷ 85 W. Tab. 4.1 summarizes the results of the measurements.

LOAD, [Ω]	OUTPUT VOLTAGE, [V]
∞	20.15
1000	18.97
500	18.50
250	17.84
200	17.61
100	17.21
50	17.03
6.8 (HALF POWER)	16.88
3.4 (FULL POWER)	16.82

TAB. 4.1 Measured load regulation capability on three S9008 IPM units (the reported output voltage is an average of the outputs of the three values, which were anyway virtually equal).

We can therefore conclude that the specified 1% load regulation is achieved.

4.2 Ripple and noise measurements in nominal conditions (i.e. no disturbances applied to the input power lines) with a resistive load at the output of the IPM

The set up used for these measurements is depicted in Fig. 4.1. The differential probe DXC100A was used to measure the ripple and noise at different points of the chain: at the input of the CAEN filter, at the IPM input and at the IPM output.

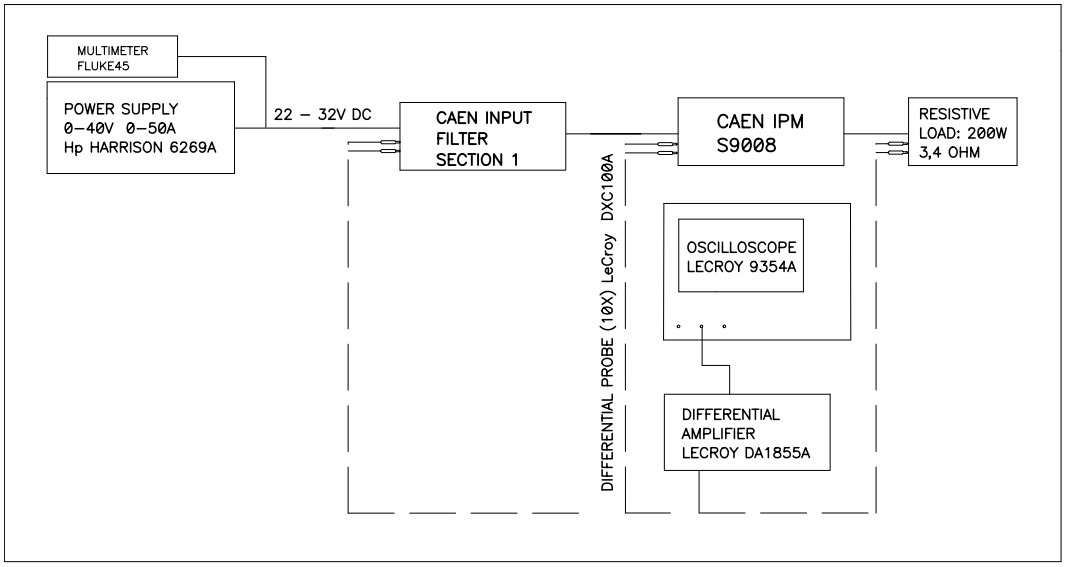


FIG. 4.1 Block scheme of the set up used for the measurements described in this subsection.

Fig. 4.2 shows the measured AC noise at the input of the CAEN filter (conditions: V_{in} = 25 V, $R_{LOAD\ IPM}$ = 3.4 Ω (full power), scope bandwidth limit 20 MHz. The peak-to-peak ripple voltage is about 25 mV.

Fig. 4.3 shows the measured AC noise at the input of the IPM (conditions: V_{in} = 25 V, $R_{LOAD\ IPM}$ = 3.4 Ω (full power), scope bandwidth limit 20 MHz). There are high frequencies noise components giving fast noise peak pulses up to 2.5 V. Anyway, these components are cut off by the CAEN filter, so that they do not appear towards the satellite's power lines, as shown in Fig. 4.2.

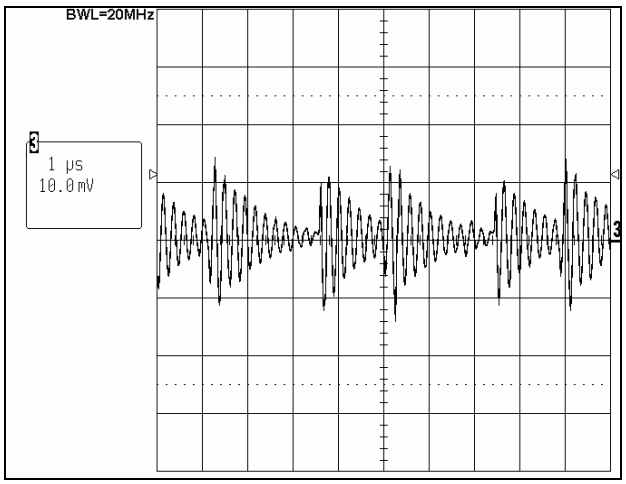


FIG. 4.2. Measured AC noise at filter's input.

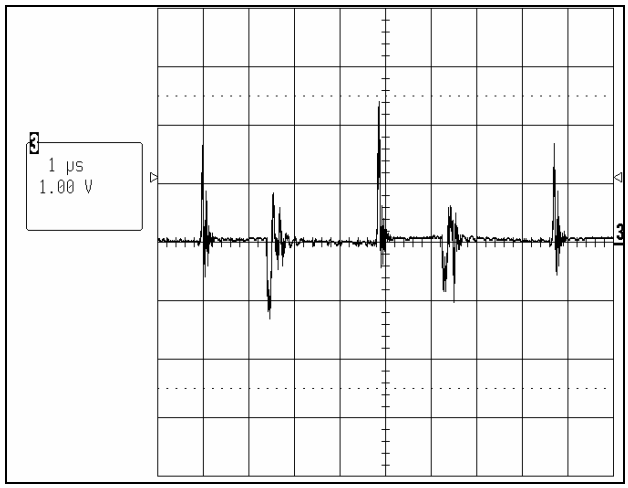


FIG. 4.3 Measured AC noise at the IPM input.

Fig. 4.4 shows the measured AC noise at the output of the IPM (conditions: V_{in} = 32 V, $R_{LOAD\ IPM}$ = 3.4 Ω (full power), scope bandwidth limit 20 MHz. Low frequency and high frequency noise components are present, the high frequency noise giving max. peak-to-peak ripple up to 270 mV. This noise level is considered acceptable for PAMELA, because the following dc/dc converter stages will further filter it effectively.

Fig. 4.5 shows the low frequency part of the noise at the output of the IPM (conditions: V_{in} = 32 V, $R_{LOAD\ IPM}$ = 3.4 Ω (full power), scope bandwidth limit 1 MHz). As it can be seen, once eliminated the high frequency components, the peak-to-peak ripple is about 30 mV.

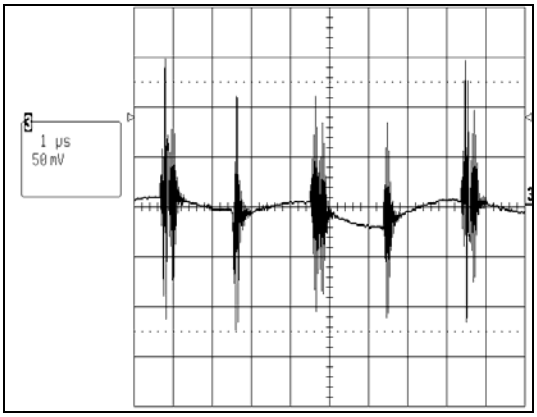


FIG. 4.4 AC noise at the IPM output

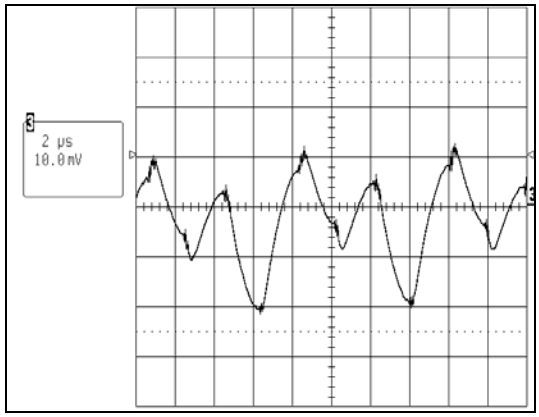


FIG. 4.5 Low-frequency part of the noise shown in Fig.4.4.

Fig. 4.6 shows in the upper part again the noise waveform of Fig. 4.5 (conditions like in Figure 4.5, only V_{in} = 25 V in this case), but with a different time scale (20 µs/div), while in the lower part it displays the spectral components of the noise waveform, obtained with a FFT (Fast Fourier Transform) with Flat Top Filter. The most important spectral component is at 130 kHz.

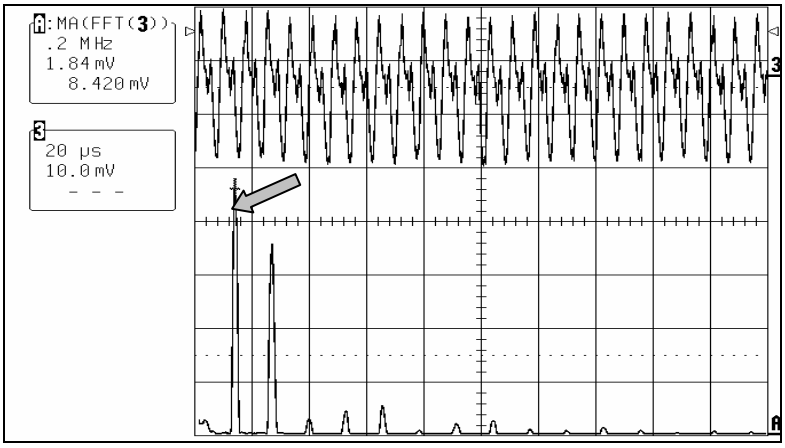


FIG. 4.6 Upper waveform: low-frequency part of the noise at the IPM output; Lower waveform: FFT (Fast Fourier Transform) of the upper waveform.

4.3 Ripple and noise measurements in nominal conditions (i.e. no disturbances applied to the input power lines) with dc/dc converters connected at the output of the IPM

Preliminary tests were performed in order to verify if the outputs of the dc/dc converters for the PAMELA sub-detectors were clean enough when supplied by the IPM at full load. To perform these basic measurements, a splitter was connected at the output of the IPM[3] in Fig. 4.1. One of the outputs of the splitter was connected to a 6.8 Ω resistive load (accounting for half-power consumption of the IPM), another one was connected, once at a time, to the input of 3 different types of dc/dc converters (S9006, S9004 and S9019), while the remaining two outputs of the splitter were left not connected (Fig. 4.7).

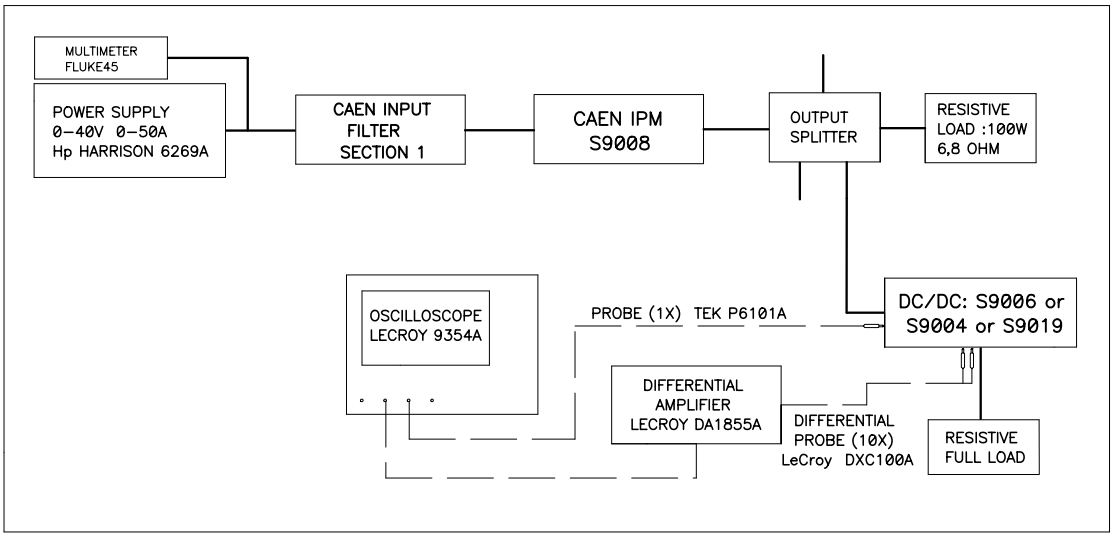


FIG. 4.7 Block diagram of the set-up used for the measurements described in sub-section 4.3.

The AC noise, measured with the normal, non differential probe of the oscilloscope (BWL was set at 15MHz) at the input of the S9006 dc/dc converter is shown in the the upper waveform (channel 2) of Fig. 4.8, while the lower waveform (channel 3) in the same figure is the noise at the output of the S9006 unit, measured with the differential probes DXC100A and under the following conditions: input voltage of the IPM V_{in} = 32 V, $R_{LOAD\ S9006}$ = 0.6 Ω (full power), scope bandwidth limit 20 MHz. The output noise has peak-to-peak values of less than 15 mV, corresponding to the switching frequency of the unit.

Fig. 4.9 displays again the AC noise at the S9006 output, but with a time division of 10 ms/div.

[3] The noise at the input of the CAEN filter and at the input of the IPM did not change with respect to the measurements described in the previous subsection.

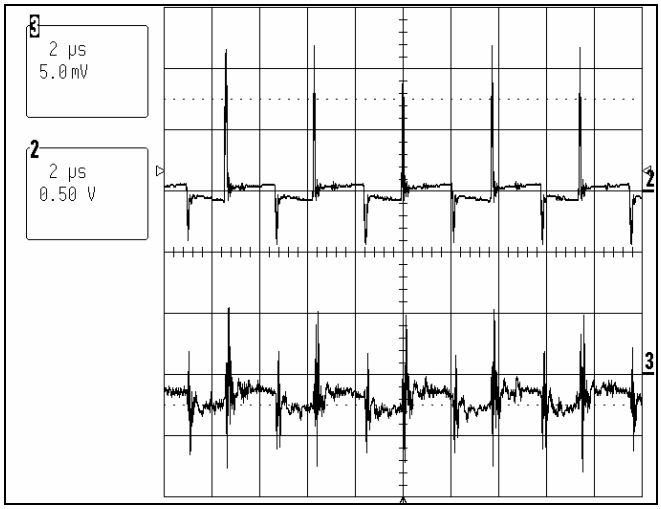


FIG. 4.8 Upper waveform: AC noise at the S9006 input. Lower waveform: AC noise at the S9006 output.

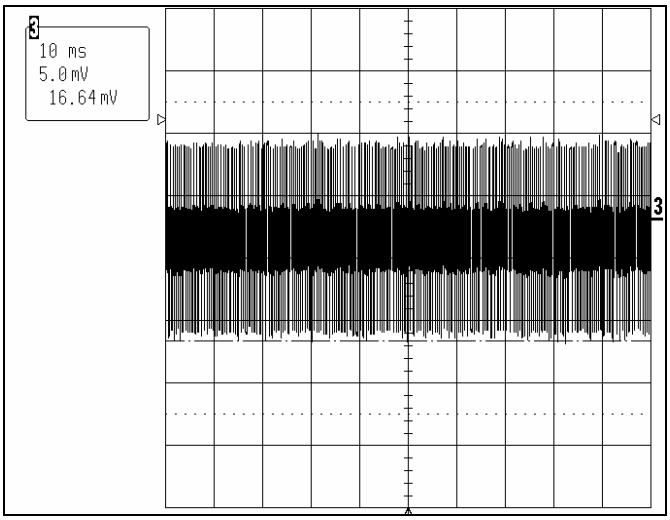


FIG. 4.9 AC noise at the S9006 output (time scale 10 ms/div.)

Fig. 4.10 is a FFT of the spectral contents of the noise at the output of the unit S9006, showing the principal peak at 270 kHz (corresponding to the switching frequency), followed by harmonics.

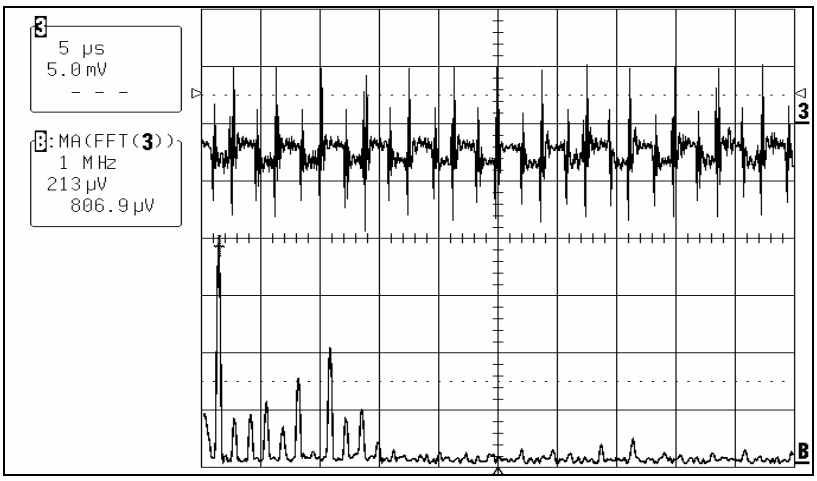


FIG. 4.10 AC noise at the S9006 output (up) and its FFT content (lower waveform)

In Fig. 4.11 the upper waveform (channel 2) is the measured AC noise at the input of the S9004 dc/dc converter measured with the normal, non differential probe of the oscilloscope (BWL 15 Mhz), while the lower waveform (channel 3) is the noise at the positive output of the S9004 (+ 5.7 V DC), measured with the differential probes DXC100A (conditions: input voltage of the IPM V_{in} = 32 V, $R_{LOAD\ S9004}$ = 7.5 Ω = full power, scope bandwidth limit 20 MHz). The output noise has a peak-to-peak value of about 20 mV, at a frequency corresponding to the switching frequency of the unit.

Figure 4.12 displays the same quantities for the negative output of the S9004 (- 5.7 V DC).

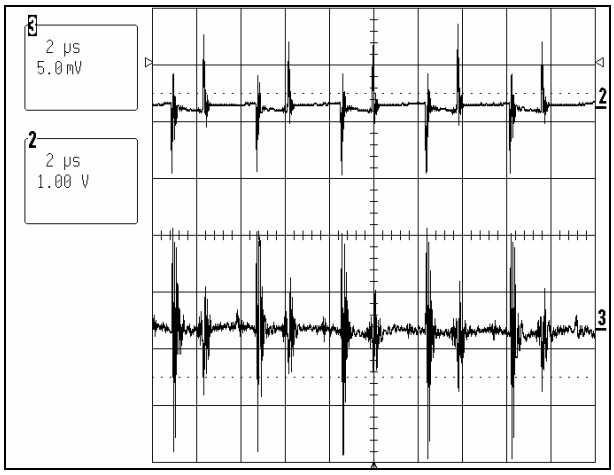


FIG. 4.11 Upper waveform: AC noise at the S9004 input. Lower waveform: AC noise at the S9004 positive output (+ 5.7 V).

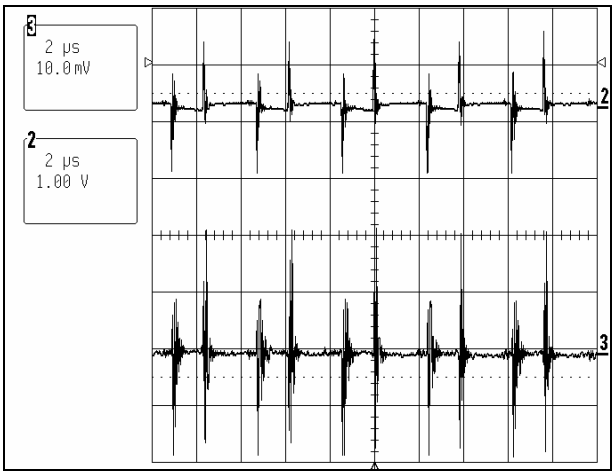


FIG. 4.12 Same as for Fig. 4.11, the lower waveform is now the AC noise at the S9004 negative output (- 5.7 V).

In Fig. 4.13 the upper waveform (channel 2) is the measured AC noise at the input of the S9019 dc/dc converter measured with the normal, non differential probe of the oscilloscope (BWL 15 Mhz), while the lower waveform (channel 3) is the noise at the + 6.7 V DC output of the S9019 measured with the differential probes DXC100A (conditions: input voltage of the IPM V_{in} = 32 V, $R_{LOAD\ S9019/\pm 6.7V}$ = 60 Ω = full power), scope bandwidth limit 20 MHz). Vertical scale for channel 3 is 5 mV/div.

Fig. 4.14 is analogous to Fig. 4.13, for the – 6.7 V DC output of the S9019. Vertical scale for channel 3 is 10 mV/div.

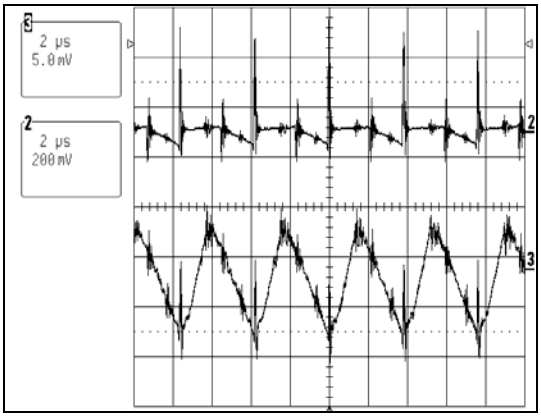


FIG. 4.13 Upper waveform: AC noise at the S9019 input. Lower waveform: AC noise at the S9019 + 6.7 V output.

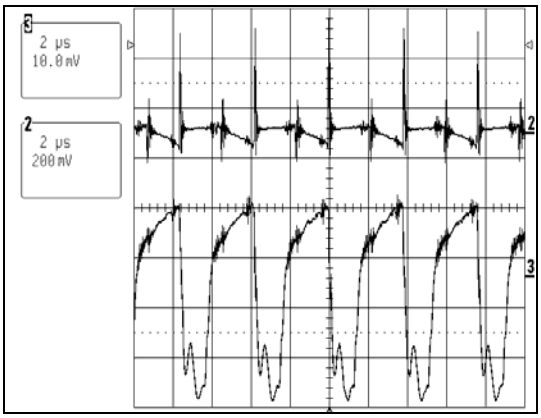


FIG. 4.14 Same as Fig. 4.13 for the – 6.7 V output of the S9019 dc/dc converter.

Fig. 4.15 and Fig. 4.16 are the same as Fig. 4.13 and Fig. 4.14, respectively, but with a time division of 10 ms/div.

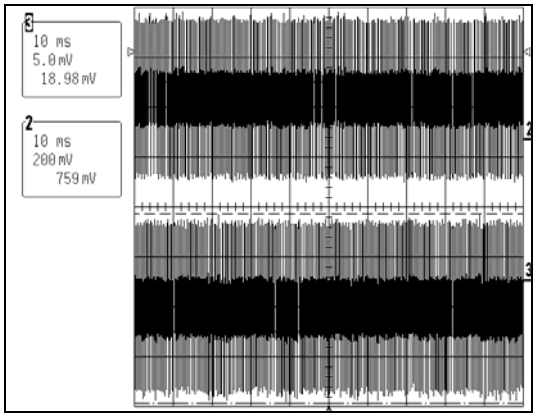


FIG. 4.15 (see text)

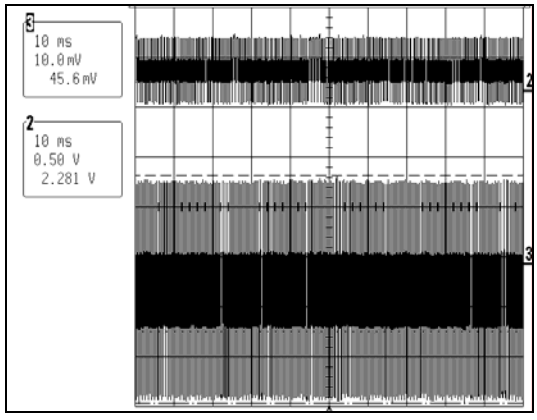


FIG. 4.16 (see text)

The spectral contents of the noise at the + 6.7V and -6.7V outputs of the S9019 unit is reported in Figs. 4.17 and 4.18, respectively.

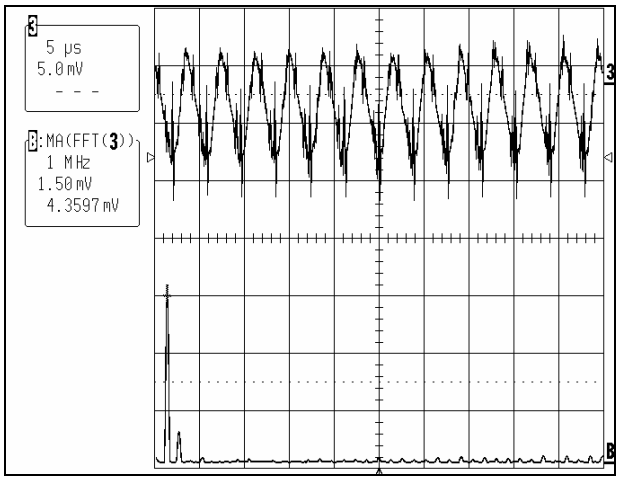


FIG. 4.17: Lower waveform: FFT of the spectral contents of the noise at the + 6.7 V output of the unit S9019 (depicted again in the upper waveform), showing the principal peak at 260 kHz, followed by harmonics.

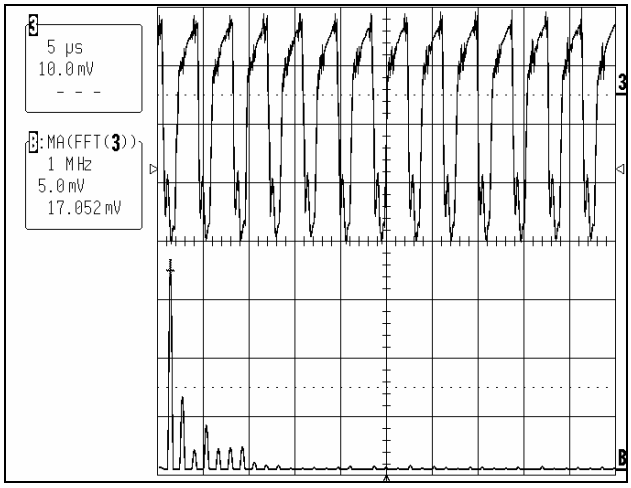


FIG. 4.18: Lower waveform: FFT of the spectral contents of the noise at the - 6.7 V output of the unit S9019 (depicted again in the upper waveform), showing the principal peak at 260 kHz, followed by harmonics.

In Fig. 4.19 the upper waveform (channel 2) is the measured AC noise at the input of the S9019 dc/dc converter measured with the normal, non differential probe of the oscilloscope (BWL 15 Mhz), while the lower waveform (channel 3) is the noise at the + 120 V DC output of the same unit, measured with the differential probes DXC100A (conditions: input voltage of the IPM V_{in} = 32 V, $R_{LOAD\ S9019/+120V}$ = 13.5 kΩ = full power, scope bandwidth limit 20 MHz). Vertical scale for channel 3 is 20 mV/div.

In Figure 4.20 are reported the same waveforms of Fig. 4.19, but with a time scale of 10ms/div.

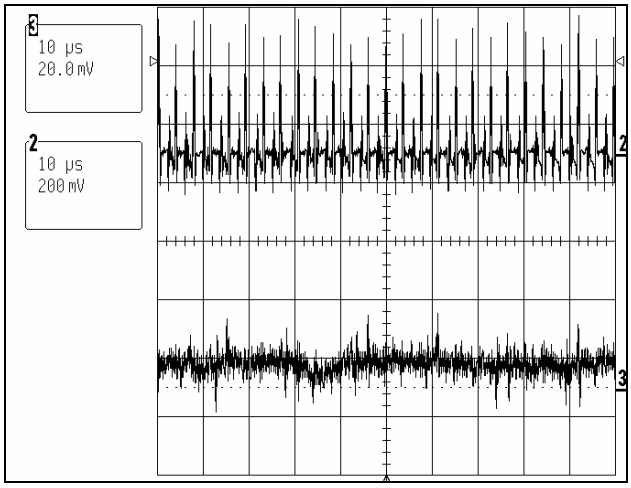


FIG. 4.19 Upper waveform: AC noise at the S9019 input. Lower waveform: AC noise at the S9019 + 120 V output.

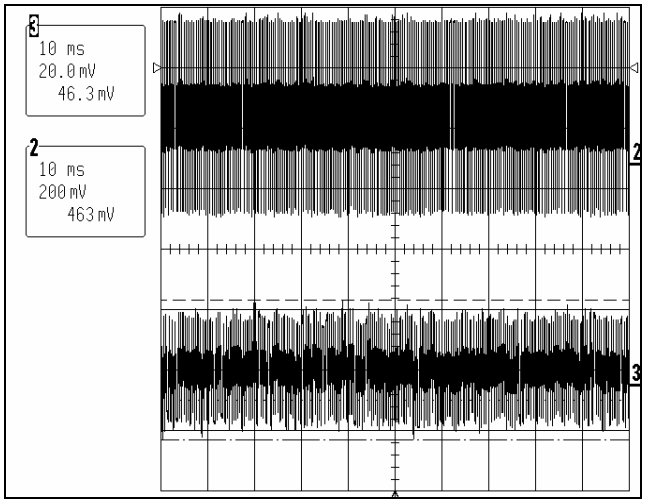


Fig. 4.20 Same as in the Fig. 4.19, with a time scale of 10 ms/div.

4.4 Measurements in presence of "voltage sag in one-time transient modes for time duration up to 200 ms"

4.4.1 Preliminary tests on the NG.

The effective ability of the NG to give the required voltage drops was tested by means of the set up depicted in Fig. 4.21. A 6.8 Ω load was placed directly at the NG output. Fig. 4.22 shows the measured voltage across the load when setting a 10 V voltage drop (from +32 V to +22 V). Fig. 4.23 shows the current delivered to the load by the NG.

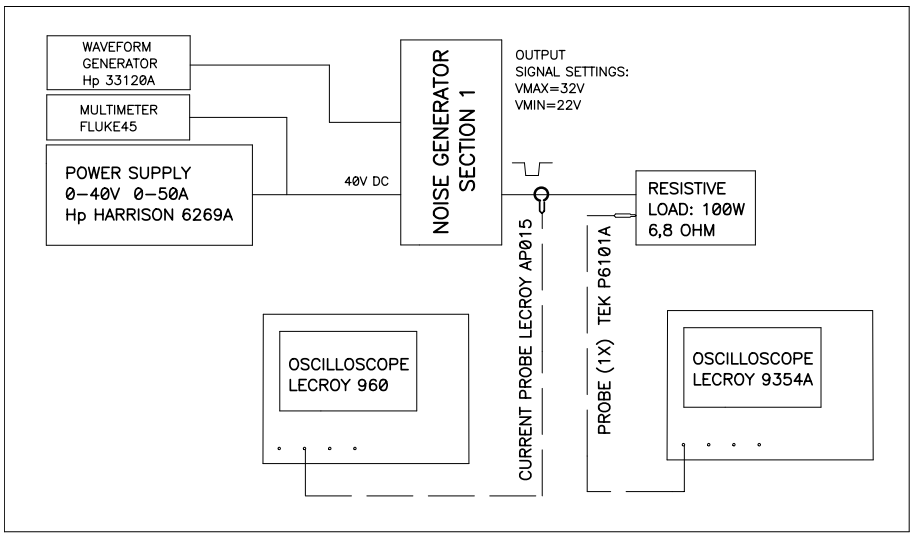


FIG. 4.21 Block diagram of the set-up for the NG preliminary test

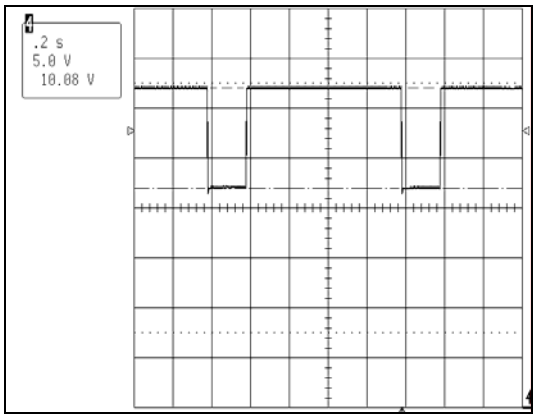


FIG. 4.22 Voltage across the load for a 10 V voltage drop from + 32 V to + 22 V.

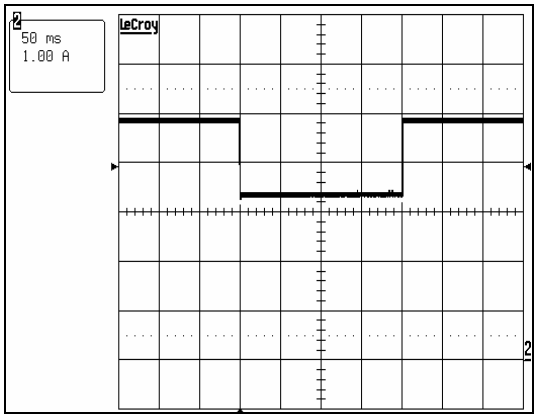


Figure 4.23 Current delivered to the load.

Fig. 4.24 and Fig. 4.25 are details of the falling and raising edges (respectively) of the voltage pulses shown in Fig. 4.22.

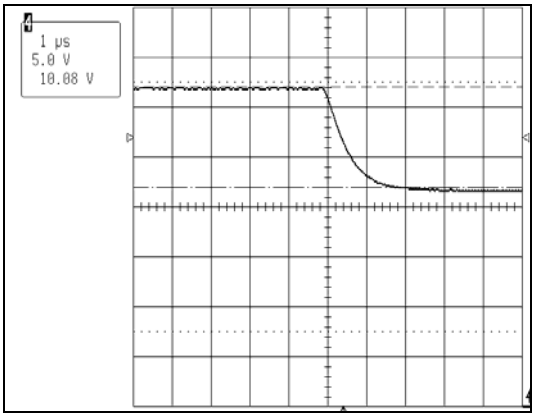


FIG. 4.24 (see text)

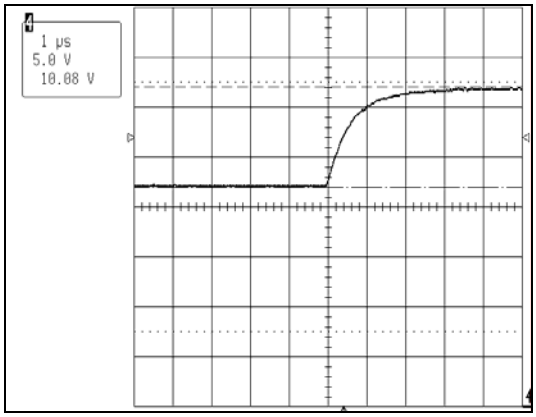


FIG. 4.25 (see text)

4.4.2. Tests with the IPM connected to a resistive load

After this preliminary test, a measurement with both CAEN filter and IPM module at full load was performed (see the set-up depicted in Fig. 4.26). This test is extremely important for the operation of PAMELA, since this voltage drops occurring on the primary satellite power bus could, in principle, turn off the IPMs.

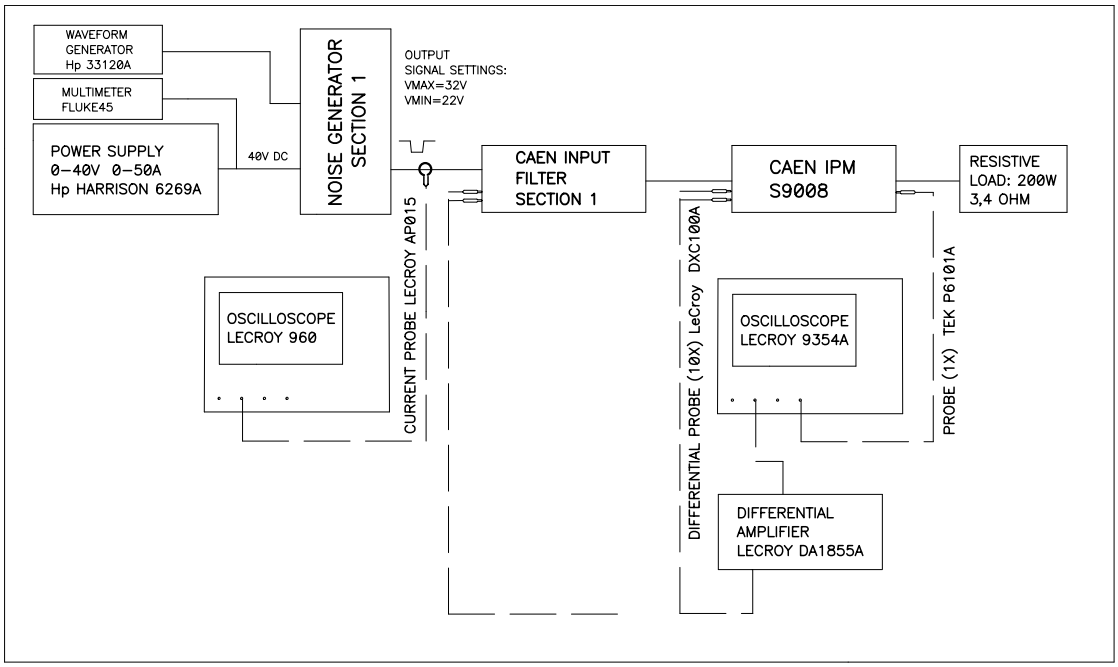


FIG. 4.26 Schematic diagram of the measurement

Fig. 4.27 shows on channel 3 the voltage at the input of the CAEN filter, which exhibits a drop of 10 V (from + 32 to + 22 V) with a 200 ms duration. On channel 2 of the same picture it is shown the IPM output voltage, which is not affected by the given disturbance. The IPM doesn't switch off and continues to operate in presence of this disturbance on the input line.

Fig. 4.28 shows, for the same conditions of Figure 4.27, on channel 3 (upper waveform) the voltage at the IPM's input (BWL set at 100 kHz). On channel 2 of the same picture (lower waveform) there is again the IPM output voltage. This picture clearly shows that there is a voltage drop of almost 1 V between the input and output of the CAEN filter, so that at the input of the IPM the effective voltage, when such a 10 V drop

is delivered to the primary line, is not + 22 V, but slightly more than + 21 V. This, and the fact that the unit does not switch off anyway, are important informations in view of the operational use of the PSS within PAMELA.

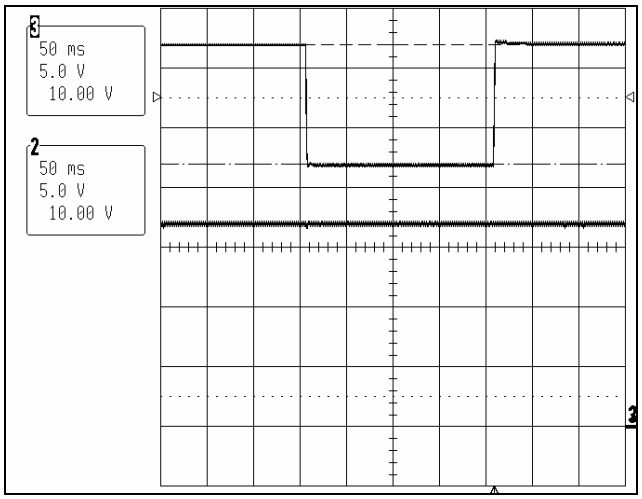


FIG. 4.27 Upper trace: voltage at Caen filter's input; lower trace: IPM output.

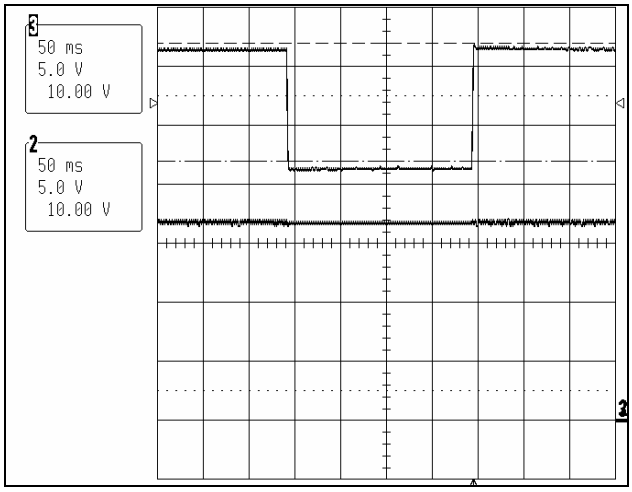


FIG. 4.28 Upper trace: IPM input; lower trace: IPM output.

Another important issue to be analyzed are the current spikes induced by these voltage sags at the input of the Caen filter, because they can, in principle, damage the unit. Fig. 4.29 shows the input current of the CAEN filter. The variation of the current dc level due to the voltage drop on the line as well as the current spikes (up to about 4 A) corresponding to the transients are clearly visible. No problems were reported in the filter as a consequence of these spikes.

Fig. 4.30 displays on channel 3 (upper waveform) the voltage at the input of the IPM (BWL set at 20 MHz), on channel 2 (lower waveform) the voltage at the IPM output[4], while channel C (central waveform) is the enhanced resolution view of channel 2 (i.e. filtered with an upper bandwidth limit of 40 kHz), showing in detail the effect of the fronts of the disturbance on the IPM output, which is negligible.

[4] The peak-to-peak noise shown here in channel 2 is not significant because it was measured with the non-differential probe and is therefore affected by ground pick-up.

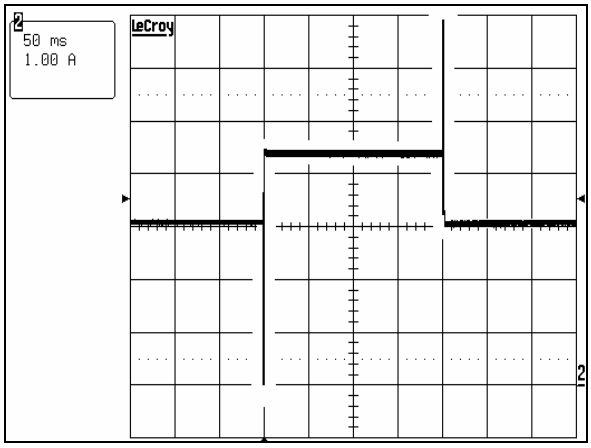


FIG. 4.29 Filter's input current

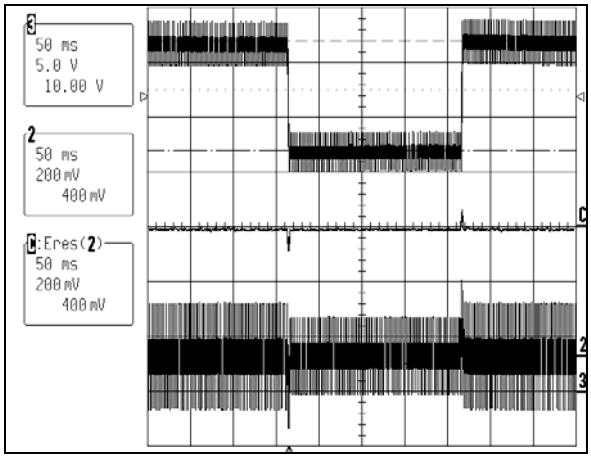


FIG. 4.30 Upper trace: IPM input; lower trace: IPM output (wide bandwith); central trace: enhanced resolution view of IPM output.

Fig. 4.31 and 4.32 are magnified views of the effect of the falling and rising edges of the pulse (respectively) on the IPM output voltage (waveforms are as described for Fig. 4.30).

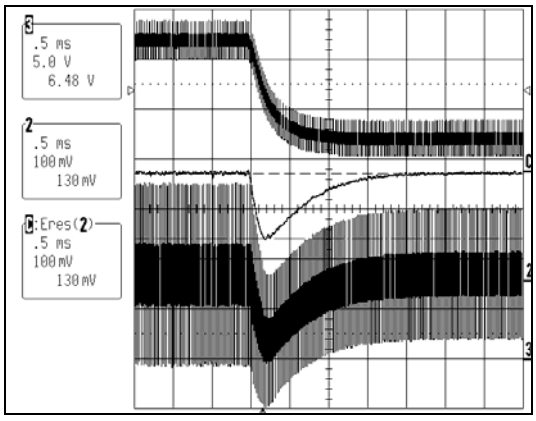


FIG. 4.31 See text.

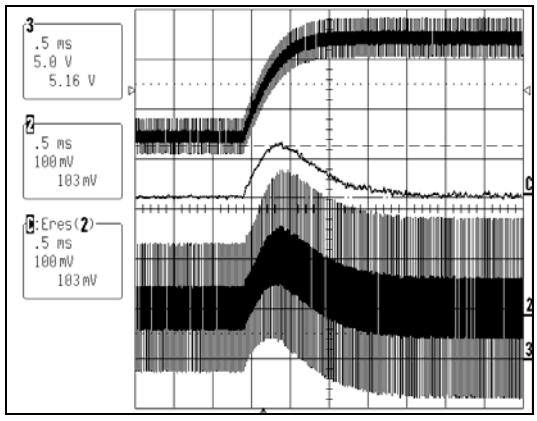


Figure 4.32 See text.

4.4.3. Tests with the IPM connected to a resistive load and 3 dc/dc converters

Fig. 4.33 shows the set up used to test the system for "voltage drops" disturbances with the IPM connected, via the splitter, to a resistive load (6.8 Ω, corresponding to half power) and 3 dc/dc converters simultaneously: an S9004, an S9006 and an S9019. Each dc/dc converter was fully loaded with a resistive load. With this set up we used the differential probe DXC100A to measure the voltage at the CAEN filter's input, the current probe LeCroy AP015 to measure the input current of the CAEN filter and the non-differential 1X TEK P6101A probe to measure the voltage at the input of the S9006 unit.

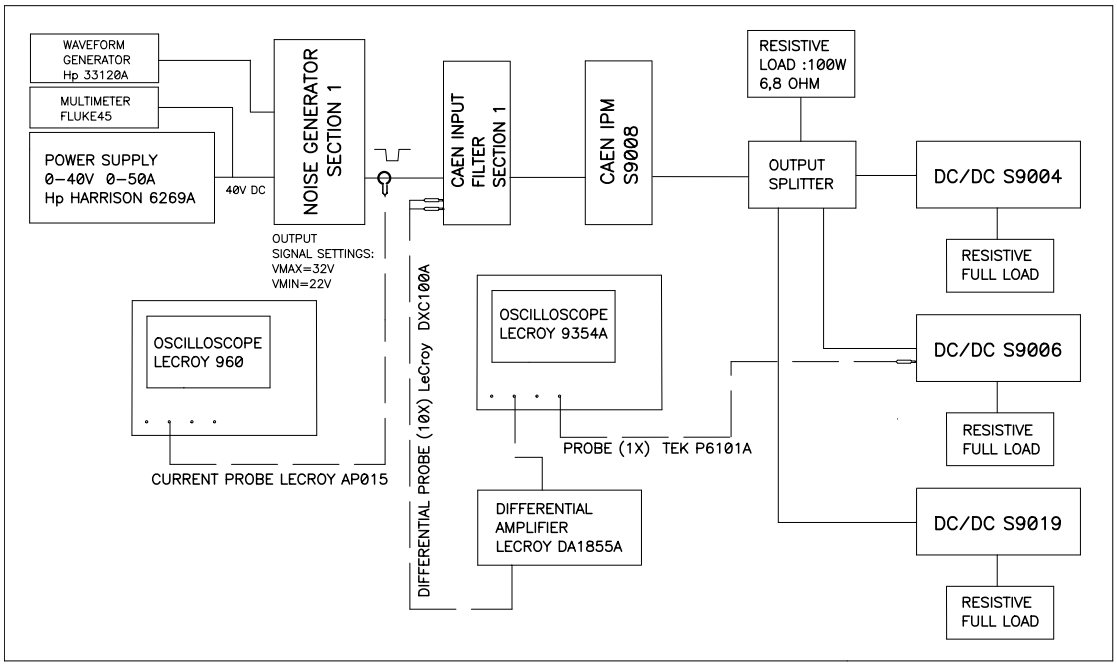


FIG. 4.33 Set-up used to obtain the results shown in Figs. 4.34 and 4.35.

In Fig. 4.34, the upper waveform (channel 3) is the falling part of the disturbance (a + 32 to + 22 V sag of duration 200 ms) at the filter's input, the lower waveform (channel 2) is the AC voltage at the input of the S9006 (N.B.: the peak-to-peak noise shown here in channel 2 is not significant because it was measured with the non-differential probe and is therefore subject to ground pick-up), while the central waveform (channel C) is the enhanced resolution view of channel 2 (filtered with an upper bandwidth limit of 40 kHz), showing in detail the effect of the front of the disturbance at the S9006 input.

Fig. 4.35 is analogous to Fig. 4.34 for the other (rising) front of the disturbance.

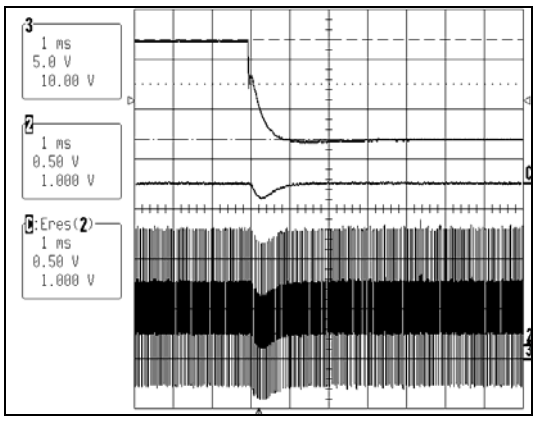


FIG. 4.34 See text.

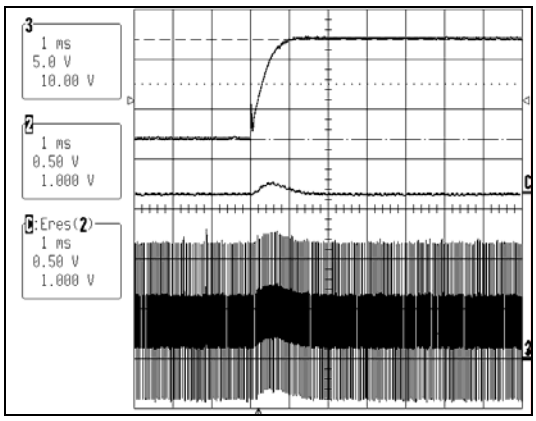


Figure 4.35 See text.

Fig. 4.36 shows the set up used to measure the noise at the output of the S9006. The chain is the same as before (Fig. 4.33), with the exception that now we have used the DXC100A differential probe to measure the voltage noise at output of the dc/dc converter.

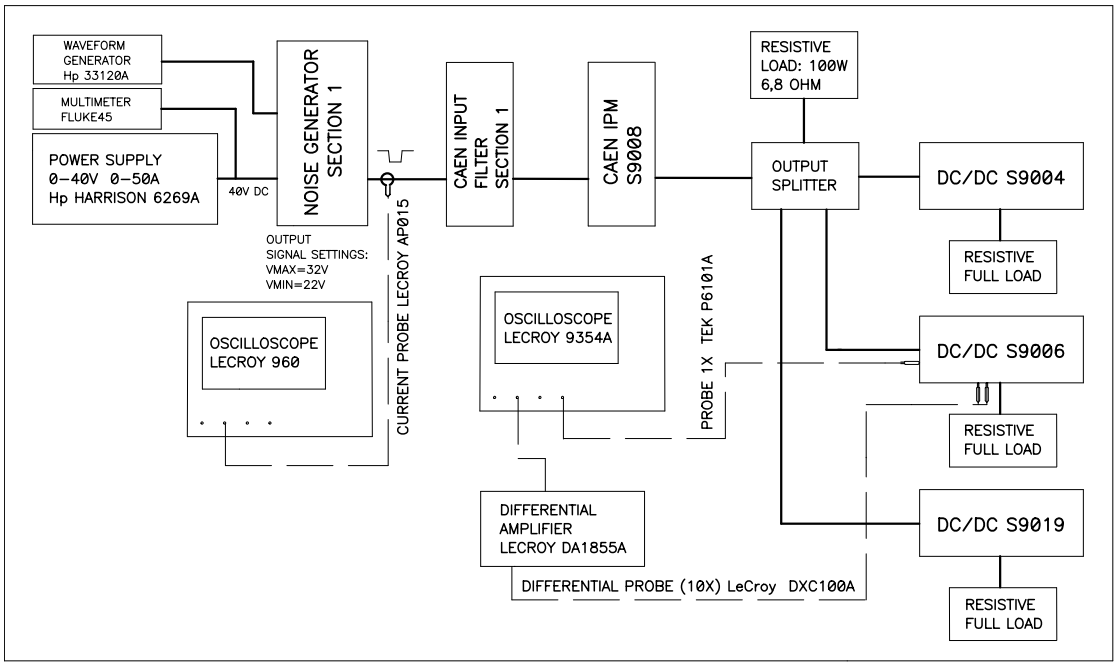


FIG. 4.36 Set-up used to measure the noise at the S9006 output.

In Fig. 4.37 the lower waveform (channel 2) is the voltage measured at the input of the S9006 (with the non-differential probe), the central waveform (channel C) is the enhanced resolution view of channel 2 (filtered with an upper bandwidth limit of 40 kHz), showing in detail the effect of the falling front of the disturbance at the S9006 input, while the upper waveform (channel 3) is the AC noise measured at the output of the S9006, showing that the peak-to-peak noise due to the disturbance is less than 2 mV, and therefore negligible for the PAMELA normal operations.

Fig. 4.38 is analogous to Fig. 4.37 for the other (rising) front.

These two last pictures clearly show that the effect of the fronts of this disturbance is negligible at the output of the S9006 dc/dc converter.

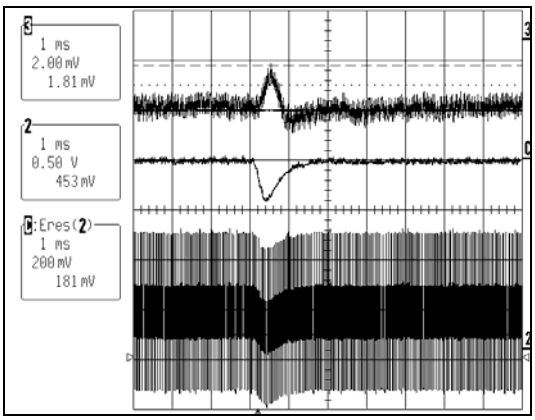


FIG. 4.37 See text.

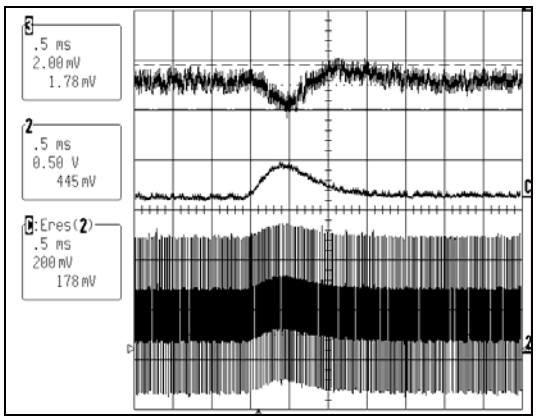


Figure 4.38 See text.

Fig. 4.39 shows the set up used to evaluate the effect of the disturbance at the input of the S9004 dc/dc converter. We used the differential probe DXC100A to measure the voltage at the CAEN filter's input, the current probe LeCroy AP015 to measure the input current of the CAEN filter and the non-differential 1X TEK P6101A probe to measure the voltage at the input of the S9004 unit.

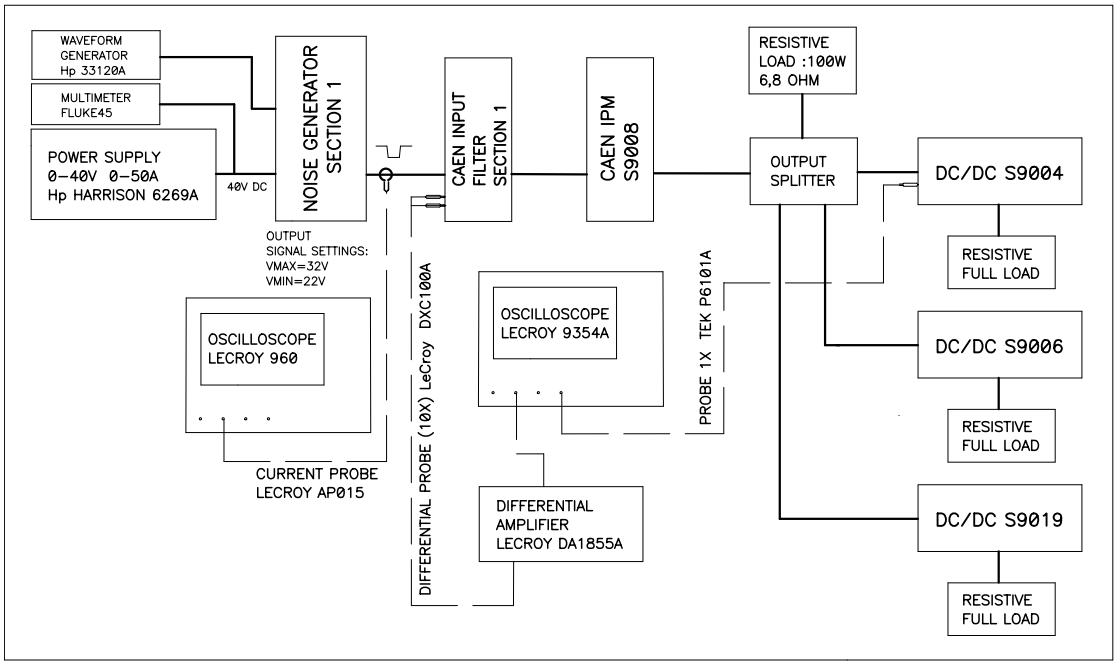


FIG. 4.39 Set-up relative to the measurements shown in Figs. 4.40 and 4.41

In Fig. 4.40 the upper waveform (channel 3) is the falling front of the disturbance (always a + 32 V to + 22 V drop of duration 200 ms) at the filter's input, the lower waveform (channel 2) is the AC voltage at the input of the S9004, while the central waveform (channel C) is the enhanced resolution view of channel 2 (filtered with an upper bandwidth limit of 40 kHz), showing in detail the effect of the front of the disturbance at the S9004 input.

Fig. 4.41 is similar to Fig. 4.40 for the other (rising) front of the disturbance.

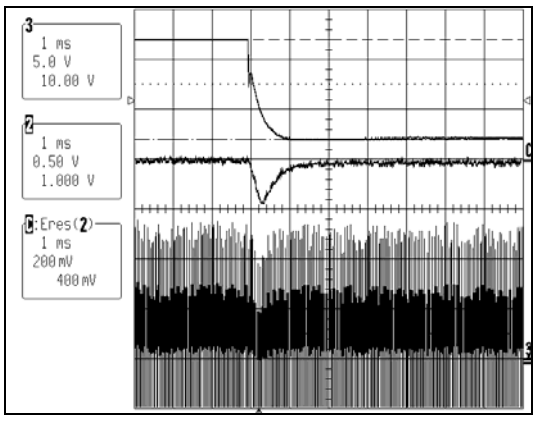


FIG. 4.40 See text.

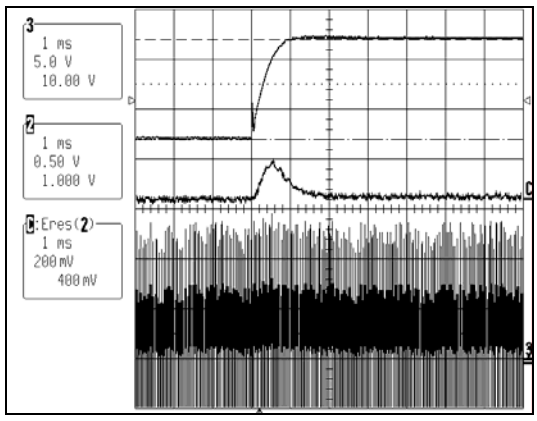


FIG. 4.41 See text.

Fig. 4.42 shows the set up used to measure the noise at the output of the S9004 dc/dc converter. The chain is the same as before, while now we have used the DXC100A differential probe to measure the voltage noise at output of the S9004.

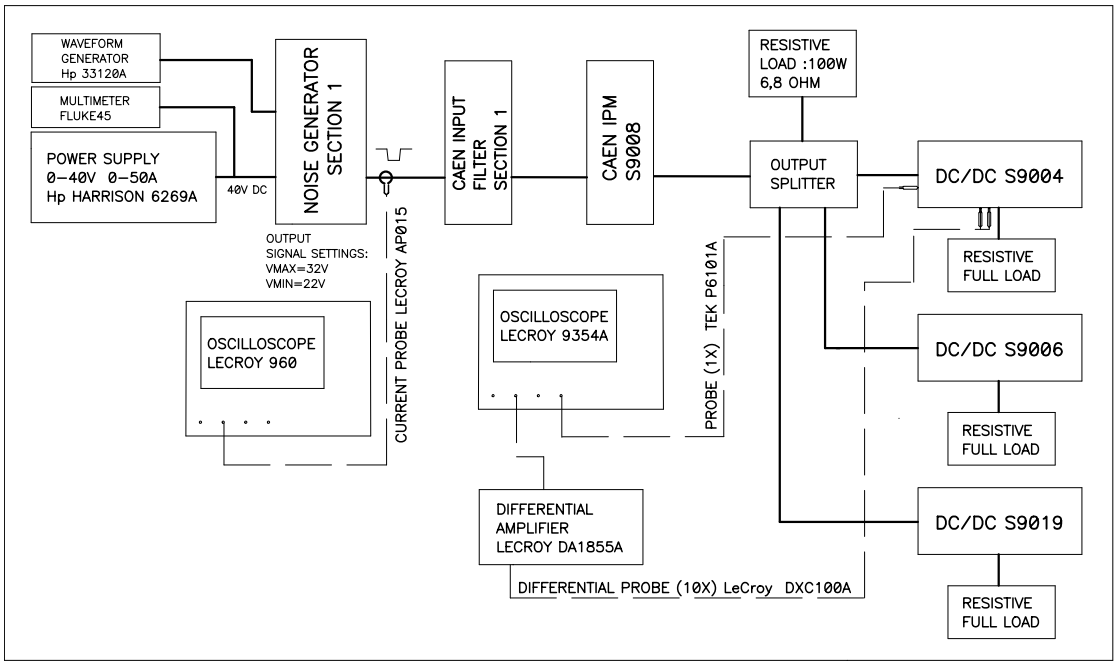


FIG. 4.42 Set-up used to pertain to the results shown in Figs. 4.43 and 4.44

In Fig. 4.43 the lower waveform (channel 2) is the voltage measured at the input of the S9004 (with the non-differential probe), the central waveform (channel C) is the enhanced resolution view of channel 2 (filtered with an upper bandwidth limit of 40 kHz), showing in detail the effect of the falling front of the disturbance at the S9004 input (a peak of ~ 0.2 V), while the upper waveform (channel 3) is the AC noise measured at the + 5.7 V DC output of the S9006 unit, showing a peak-to-peak noise of about 1 mV.
Fig. 4.44 is similar to Fig. 4.43 for the other (rising) front.

These two last pictures clearly show that the effect of the fronts of this disturbance is totally negligible at the + 5.7 V DC output of the S9004 dc/dc converter. Very similar results were obtained for the – 5.7 V DC output of the unit.

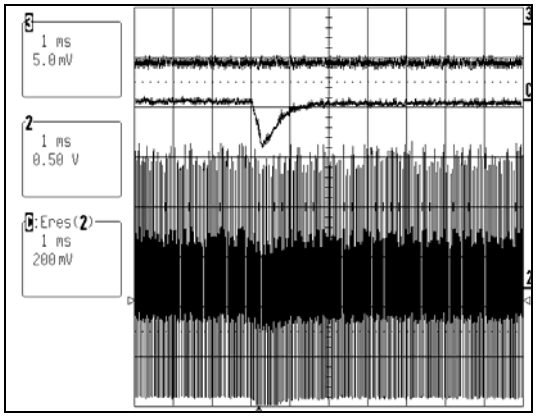


Figure 4.43 See text.

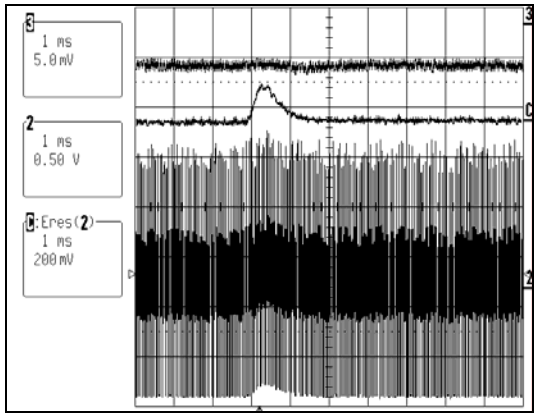


Figure 4.44 See text.

Fig. 4.45 shows the set up used to evaluate the effect of the disturbance at the input of the S9019 dc/dc converter. Again, we used the differential probe DXC100A to measure the voltage at the CAEN filter's input, the current probe LeCroy AP015 to measure the input current of the CAEN filter and the non-differential 1X TEK P6101A probe to measure the voltage at the input of the S9019 unit.

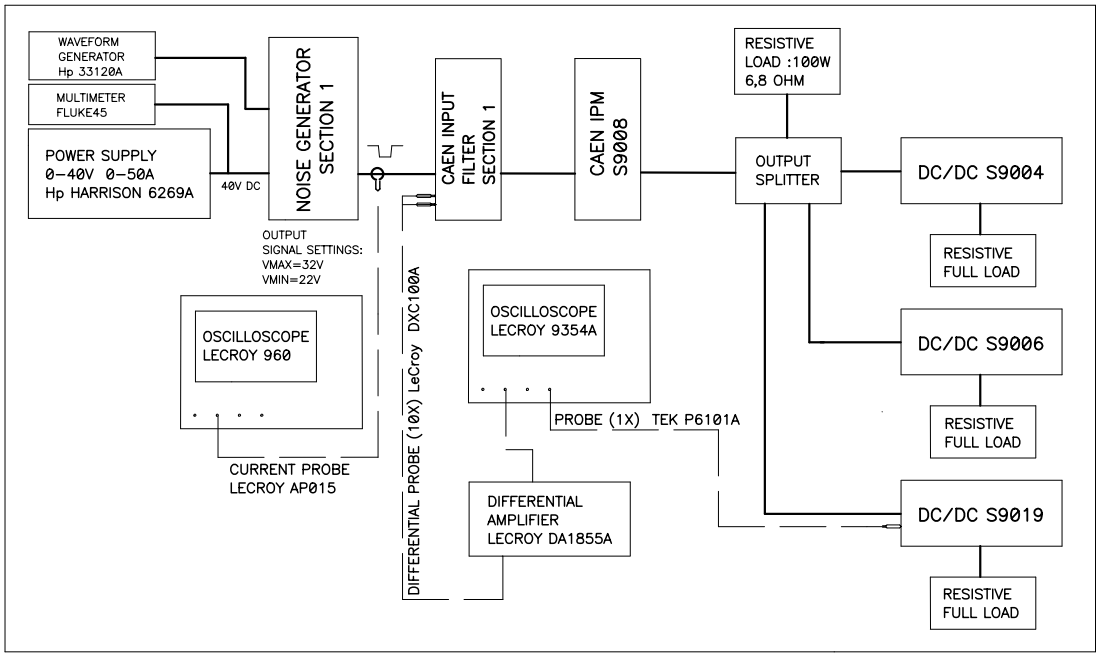


FIG. 4.45 Set-up relative to the measurements shown in Figs. 4.46 and 4.47

Fig. 4.46 the upper waveform (channel 3) is the falling front of the disturbance (always a + 32 to + 22 V drop of duration 200 ms) at the filter's input, the lower waveform (channel 2) is the AC voltage at the input of the S9019 (measured with the non-differential probe), while the central waveform (channel C) is the enhanced resolution view of channel 2 (filtered with an upper bandwidth limit of 40 kHz), showing in detail the effect of the front of the disturbance at the S9019 input (a peak of ~ 0.15 V).

Fig. 4.47: same as in Figure 4.48 for the other (rising) front of the disturbance.

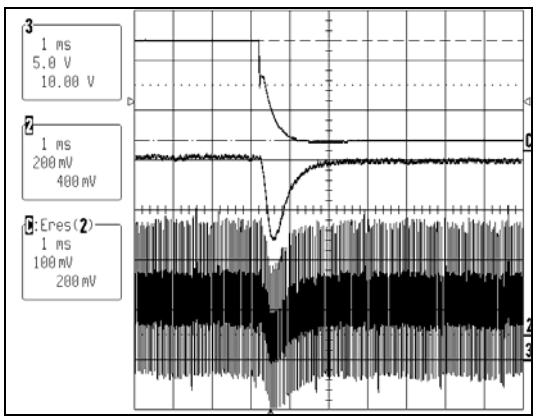


Figure 4.46 See text.

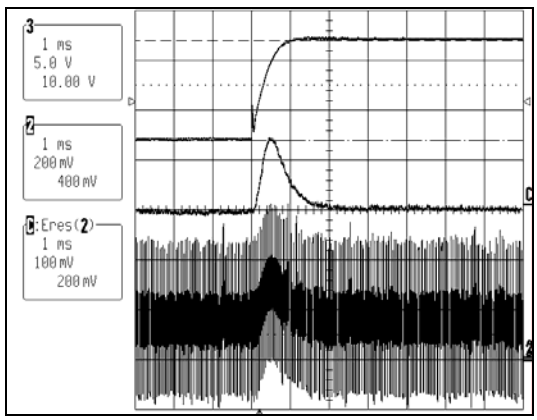


Figure 4.47 See text.

Figure 4.48 shows the set up used to measure the noise at the output of the S9019. The chain is the same as before, while now we used the DXC100A differential probe to measure the voltage noise at output of the S9019.

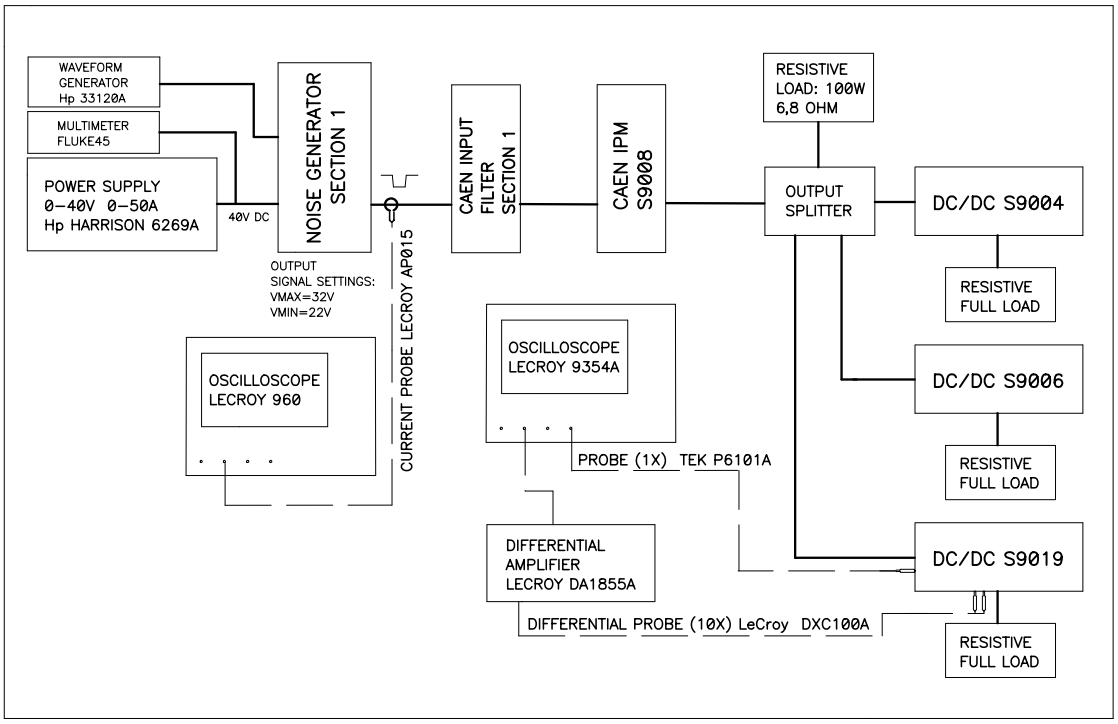


Figure 4.48 Set-up used to pertain to the results shown in Figs. 4.49 and 4.50

The lower waveform (channel 2) in Fig. 4.49 is the voltage measured at the input of the S9019 (with the non-differential probe), the central waveform (channel C) is the enhanced resolution view of channel 2 (filtered with an upper bandwidth limit of 40 kHz), showing in detail the effect of the falling front of the disturbance at the S9019 input (a peak of amplitude ~ 150 mV), while the upper waveform (channel 3) is the AC noise measured at the + 120 V DC output of the S9019, showing a 10 mV peak-to-peak glitch in correspondence of the front. Fig. 4.50 is analogous to Figure 4.49 for the other (rising) front.

These two last pictures clearly show that the effect of the fronts of this disturbance is negligible for PAMELA at the + 120 V DC output of the S9019 dc/dc converter. Very similar results were obtained for the ± 6.7 V DC outputs of the unit.

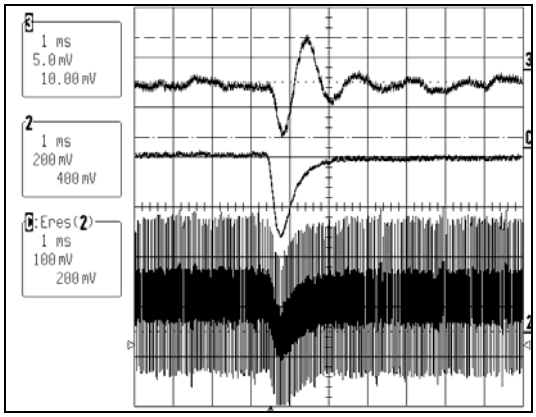


FIG. 4.49 See text.

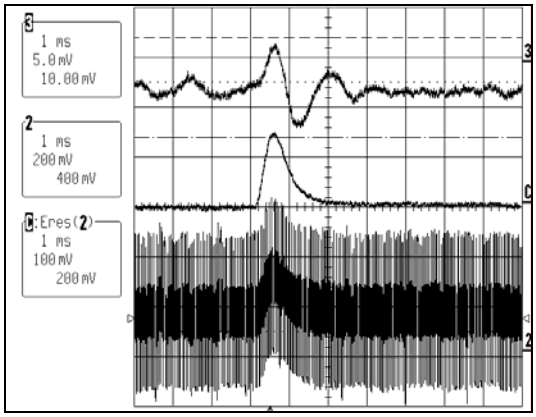


FIG. 4.50 See text.

4.5 Measurements in presence of "multiplexing dumping pulses (inducing) with a duration of up to 20 ms and an amplitude of up to ± 10 V (of supply voltage level), frequency of pulse filling vibrations is up to 10 MHz, minimum oscillation frequency 150 kHz".

4.5.1 Preliminary tests on the set up.

The effective ability of the NG to give the required disturbances was tested by means of the set-up sketched in Fig. 4.51. A 6.8 Ω load was placed directly at the NG output. We used an HP 33120A Waveform Generator and an analog switch connected like indicated in the scheme. In this way it was possible to give 20 V_{pp} pulses (± 10 V with respect to the DC supply level) with a frequency sweep from 140 kHz to 10.5 MHz and duration of the sweep of 22 ms.

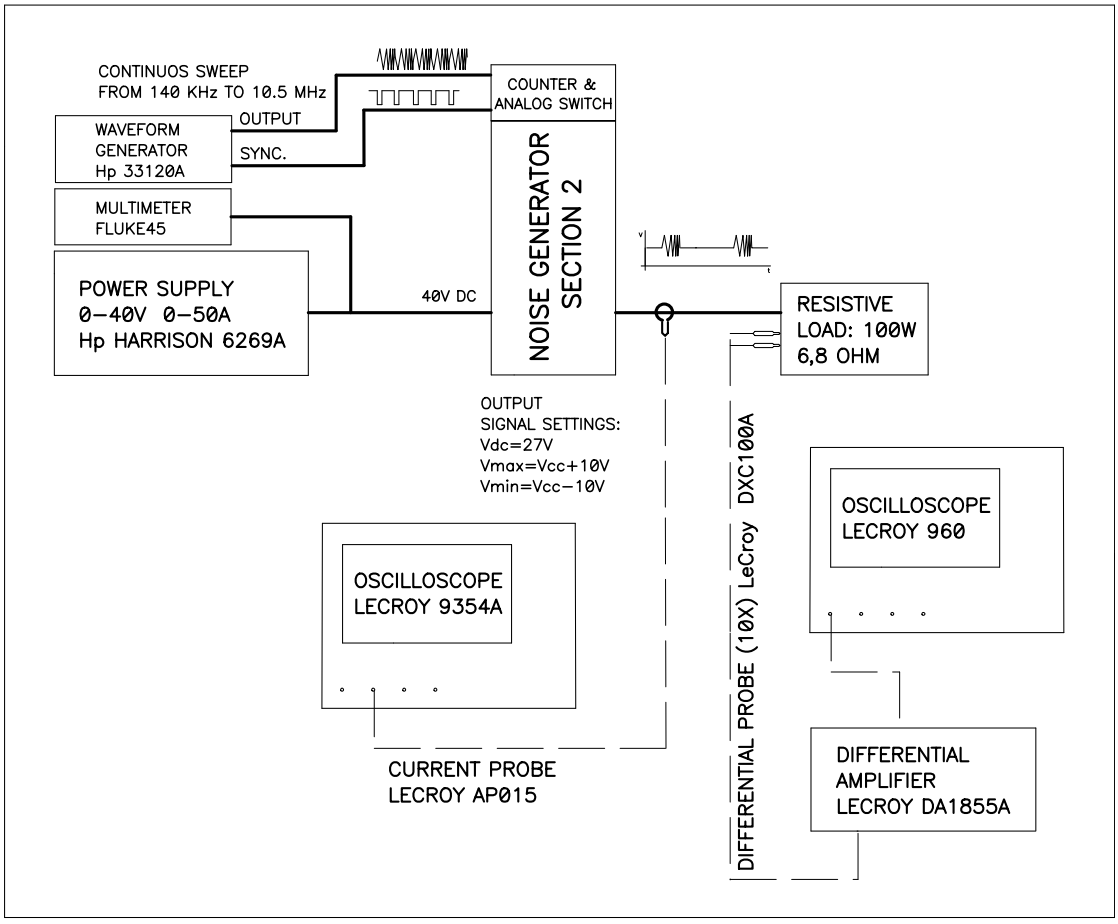


FIG. 4.51 Block diagram of the set-up used for the preliminary tests on the NG

In Figure 4.52 it is reported the output voltage across the load measured with the differential probe. The period between two consecutive sweeps is 1.1 s and the peak-to-peak voltage is 20 V. Figure 4.53 shows a detail of one sweep with a time scale of 5 ms/div. We can therefore conclude that this type of disturbance, required by the ICD, could be correctly generated with our set-up.

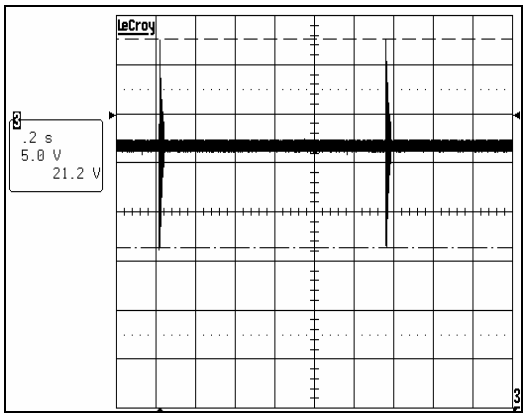


FIG. 4.52 See text.

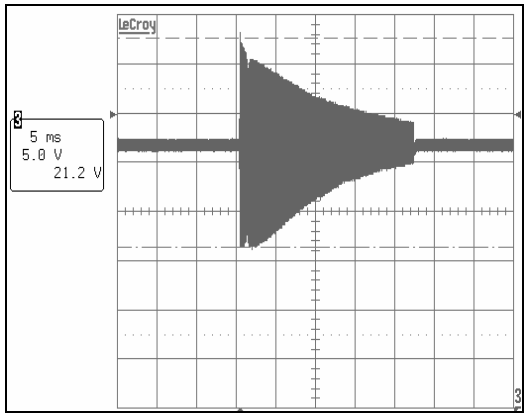


FIG. 4.53 See text.

4.5.2. Tests with the CAEN filter connected to a resistive load.

After this preliminary test, the CAEN filter was introduced in the circuit and connected to a 6.8 Ω resistive load (see the set up depicted in Fig. 4.54). The differential probe DXC100A was used to sense the voltage at the input of the filter (i.e. towards the power lines). Sweeps with the characteristics described in the previous sub-section were given to the system.

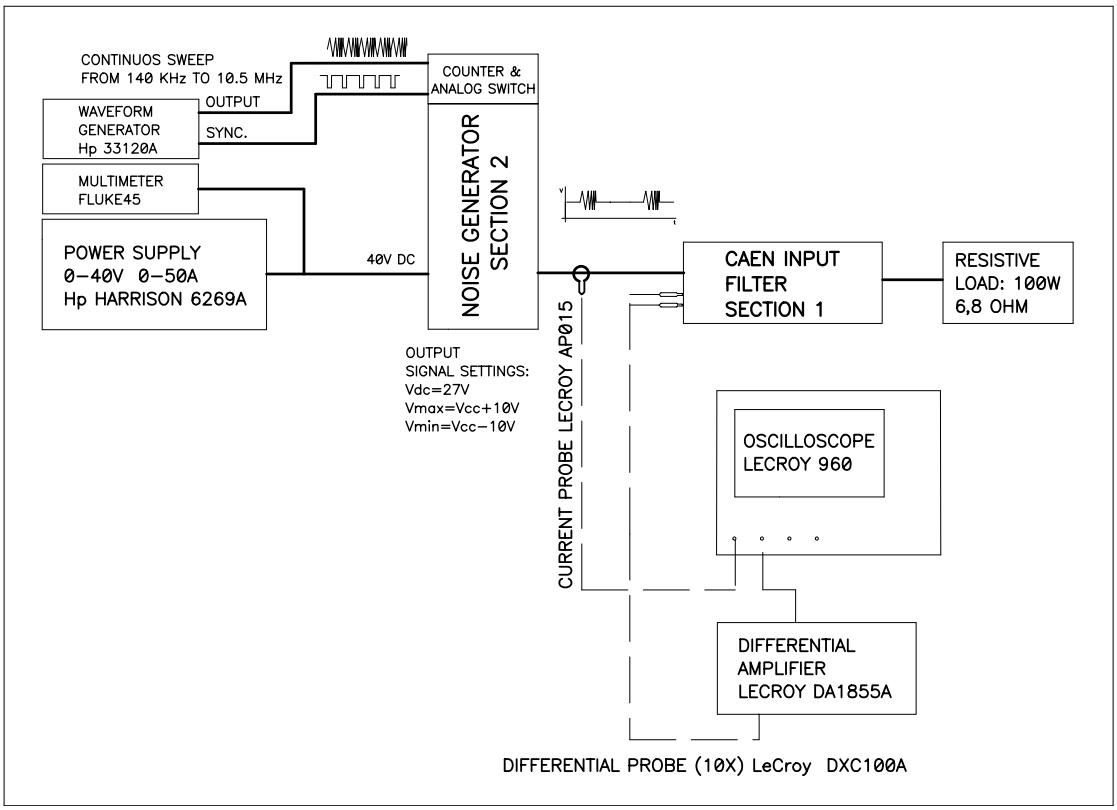


FIG. 4.54 Set-up for the test on the input of the CAEN filter.

The lower waveform (channel 3) in Fig. 4.55 shows the measured voltage at the input of the CAEN filter, which exhibits a resonance peak with a peak-to-peak voltage of about 50 V (vertical scale is 10 V/div). So this type of disturbance excites the CAEN filter and gives at its input a possible interference towards the power lines. Since the peak-to-peak amplitude of the sweep was about 12 V, the Q of this resonance is about 4.17. The

resonance peak occurs at a frequency of about 5.7 MHz. The upper waveform (channel 1) is the input current of the filter, displaying a resonance at the same frequency with a peak-to-peak value of about 4 A.

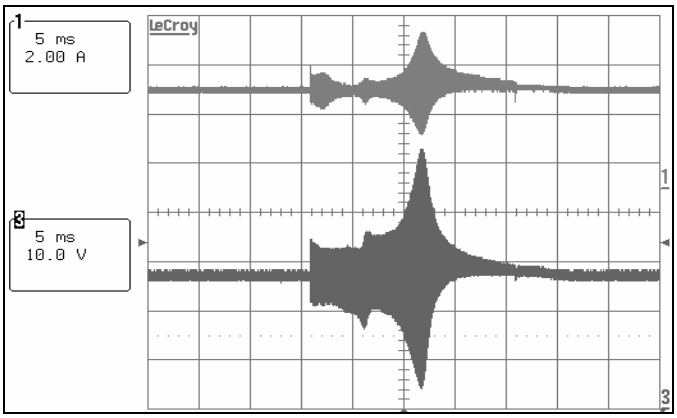


FIG. 4.55 Lower waveform: voltage at the input of the CAEN filter when the "frequency sweep" disturbance is applied to the power lines; upper waveform: corresponding current at the filter's input.

Fig. 4.56 shows the set-up used to sense the effect of the sweep at the output of the CAEN filter. Here the differential probe was connected to the output of the filter.

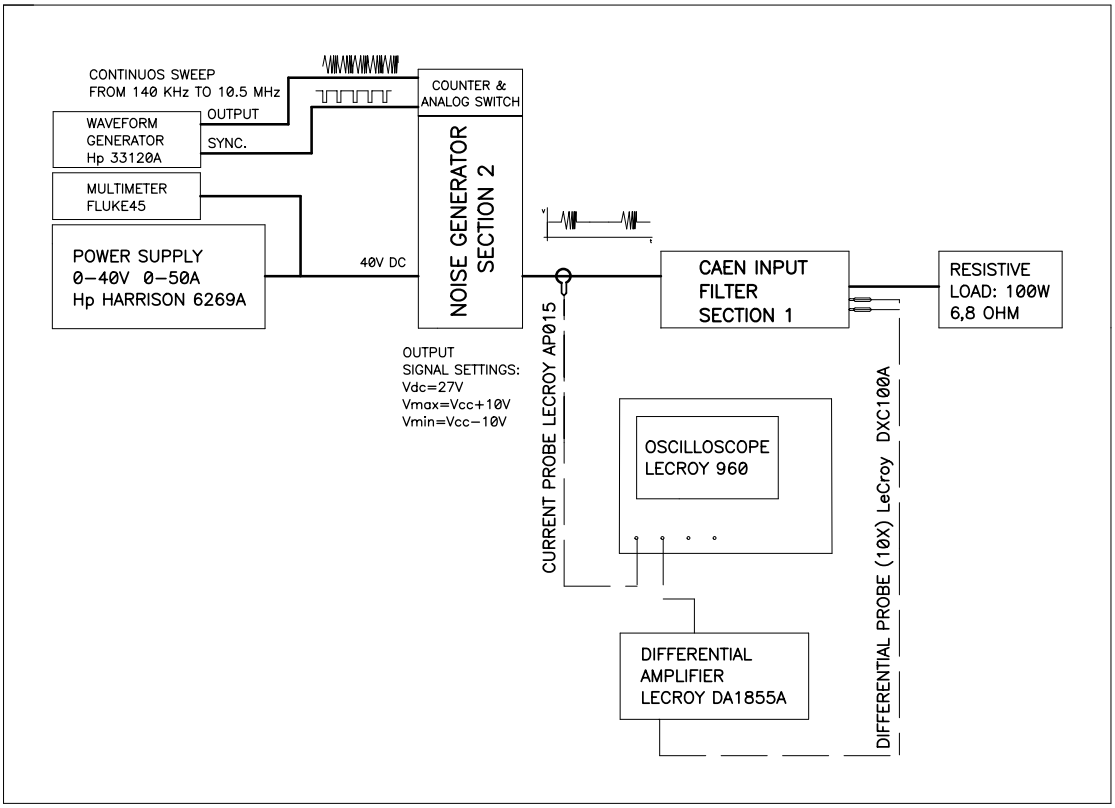


FIG. 4.56 Set-up for the test on the output of the CAEN filter.

In Fig. 4.57 the upper waveform (channel 3) is the AC voltage at the output of the filter, while the lower waveform (channel 1) is again the input current of the filter. From the upper trace it is clear that the effect of the resonance is not significantly transmitted towards PAMELA. On the other hand, this test has shown that the PAMELA PSS can

transmit some noise towards the satellite when excited with this type of disturbance coming from the primary satellite lines. This should be investigated during the EMI/EMC tests foreseen in Russia during the integration of the apparatus in the satellite.

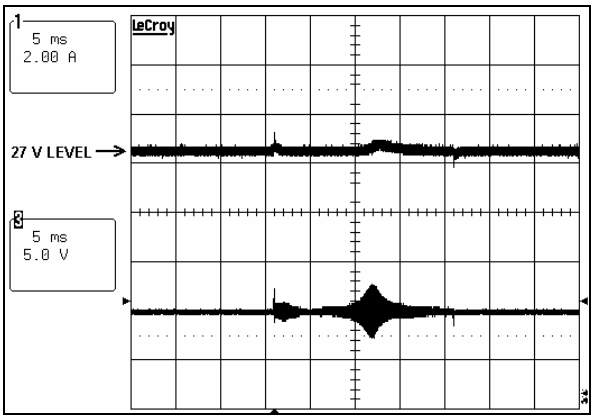


FIG. 4.57 Upper waveform: voltage at the output of the CAEN filter when the "frequency sweep" disturbance is applied to the power lines; lower waveform: current at the filter's input.

4.5.3. Tests with the IPM connected to a resistive load.

After these measurements, a test with an IPM connected at the output of the CAEN filter was performed (see the set up depicted in Fig. 4.58). The IPM had a resistive load corresponding to full power operation (3.4 Ω).

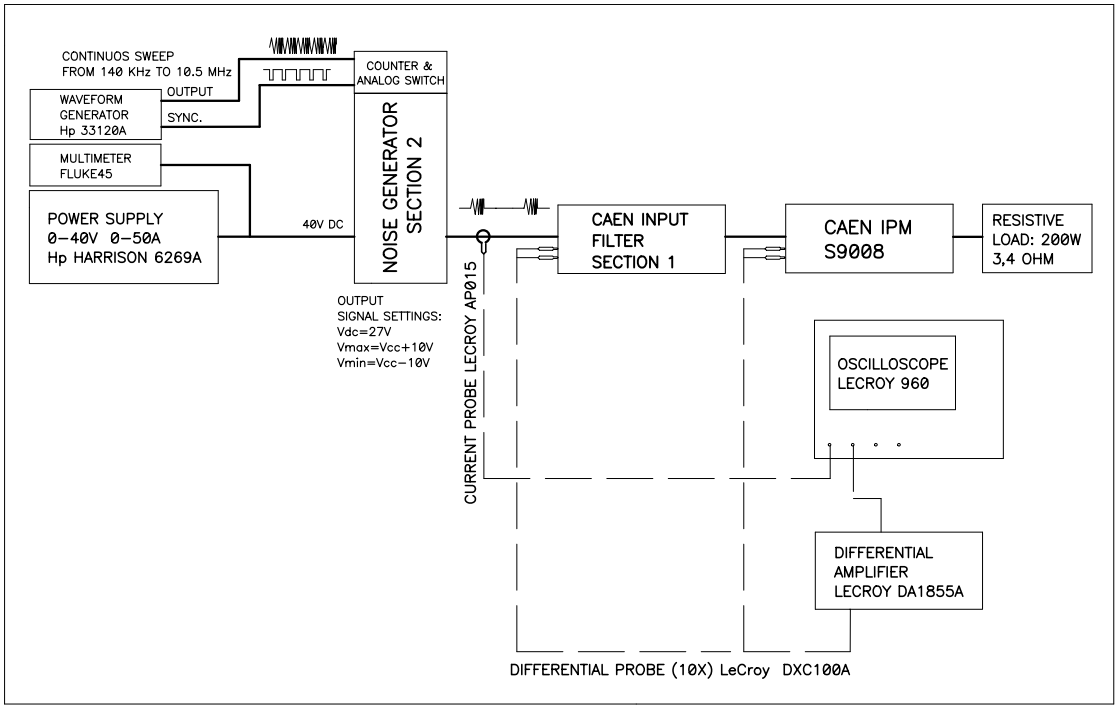


Figure 4.58 Set-up used to probe the input of the CAEN filter when connected to a fully-loaded IPM.

In Fig. 4.59 the upper waveform (channel 3) is the voltage measured with the differential probe at the input of the filter (vertical scale 5 V/div, DC-coupling), while the lower waveform (channel 1) is the filter input current. The different values of the resonance voltage and current peaks with respect to those of Fig. 4.55 are due to the fact that, in the measurements of Fig. 4.59 we used an excitation level half of that used for the measurements of Fig. 4.55.

In Fig. 4.60 the upper waveform (channel 3) is the voltage at the IPM input (scope BWL 100 kHz), while the lower waveform (channel 1) is again the input current of the filter.

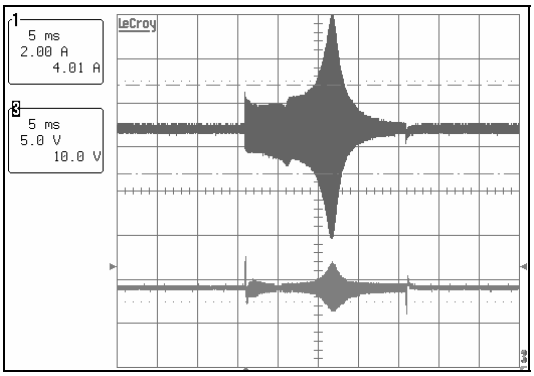


FIG. 4.59 See text.

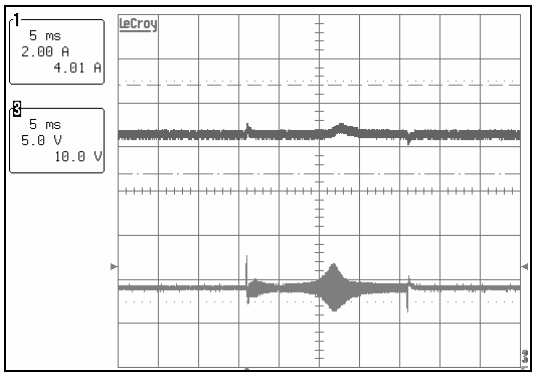


FIG. 4.60 See text.

To probe the IPM output**,** the differential probe was connected like shown in Fig. 4.61.

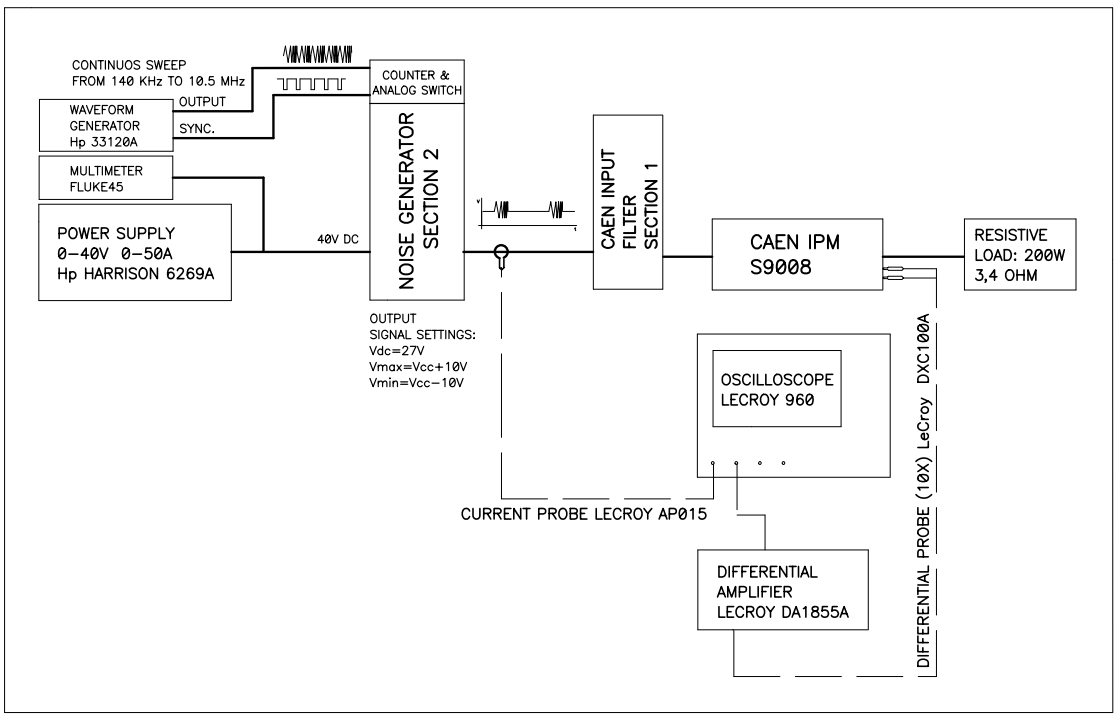


FIG. 4.61 Set-up used to probe the output of a fully-loaded IPM

Fig. 4.62 displays in the upper waveform (channel 3) is the AC voltage measured at the IPM output (BWL 20 MHz). There is practically no effect due to the resonance after the IPM. The lower waveform is again the input current in the filter.

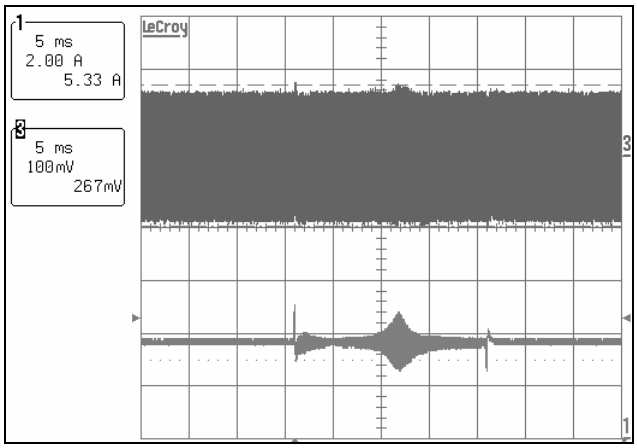


FIG. 4.62 Upper waveform: AC voltage at the output of the IPM; lower waveform: current at the input filter.

4.5.4. Tests with the IPM connected to a resistive load and 3 dc/dc converters.

For this set of measurements, the IPM was connected, via the splitter, to a resistive load (6.8 Ω, corresponding to half power) and to 3 dc/dc converters simultaneously: an S9004, an S9006 and an S9019 (Fig. 4.63). Each dc/dc converter was fully loaded with a resistive load. No difference was found (as expected) for the voltage and current at the filter's input with respect to the results of Fig. 4.59.

The results have shown that the noise at the output of the dc/dc converters was unaltered by the presence of this disturbance with respect to the results previously shown in section 4.3.

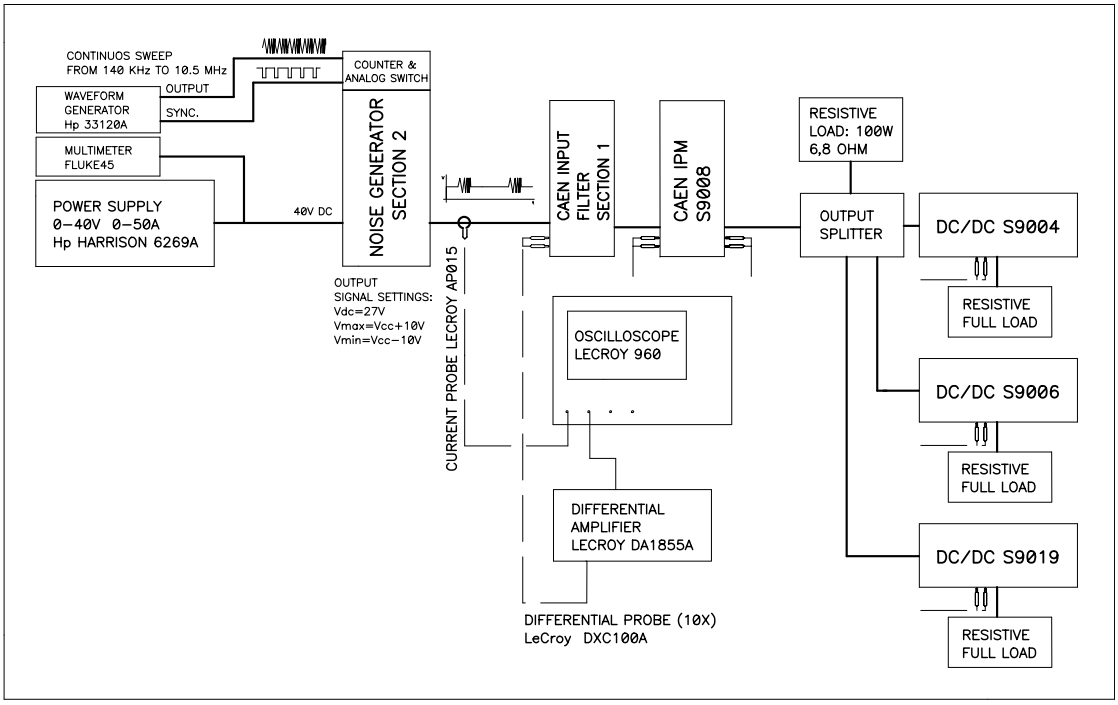


FIG. 4.63 Set-up used to probe the dc/dc converters output.

4.6 Measurements in presence of "supply voltage rushes and slumps (within its tolerance) by amplitude of maximum 5 V with a pulse rise time of over 10 µs and repetition frequency between 10 Hz and 20 kHz".

4.6.1 Tests with the IPM connected to a resistive load and 3 dc/dc converters.

Fig. 4.64 shows the set up used for this measurement: the IPM output was connected, via the splitter, to a resistive load (6.8 Ω, corresponding to half power) and to the usual set of 3 dc/dc converters, each of them was fully loaded with a resistive load.

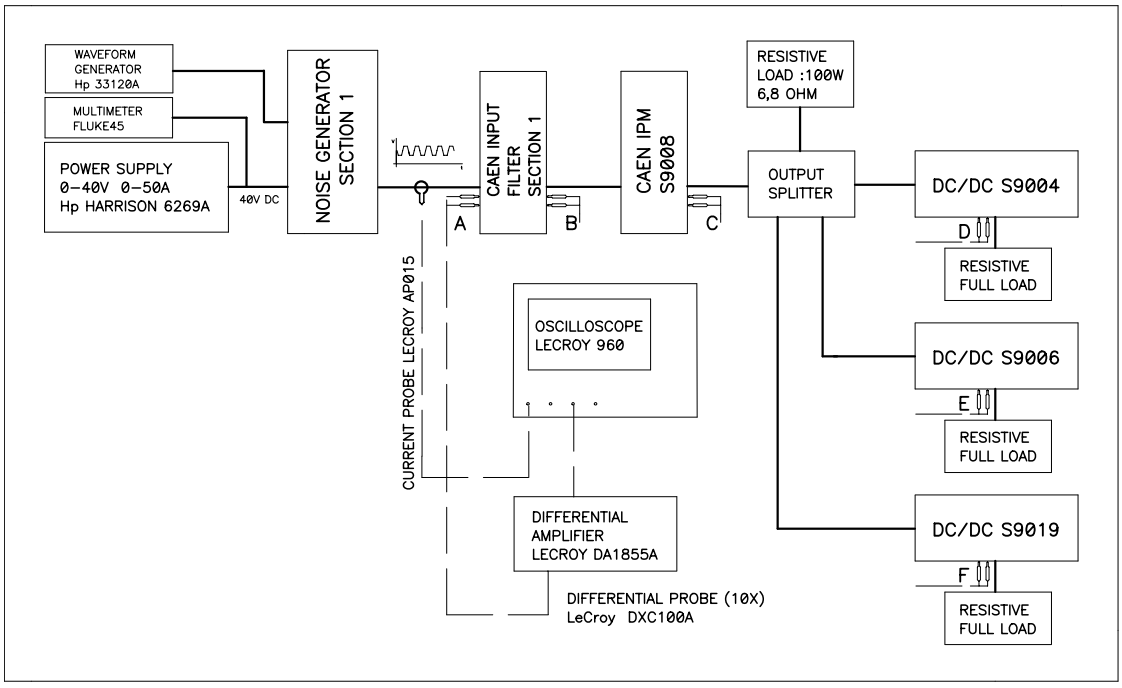


FIG. 4.64 Set-up used to measure the IPM undervoltage and overvoltage thresholds

The first set of measurements (disturbances close to the upper limit) was performed by setting square-wave disturbances, having different repetition frequencies, with amplitudes between 27V and 32V (5Vpp).

The second set of measurements (disturbances close to the lower limit) was performed by setting square-wave disturbances, having again different repetition frequencies, with amplitudes between 22V and 27V (5Vpp).

All voltage measurements described in this subsection were performed with a differential probe.

Concerning the first set of measurements, Figs. 4.65 to 4.70 were obtained with a square-wave disturbance frequency of 21 kHz.

Fig. 4.65 shows, in the upper trace (channel 3), the voltage measured at the input of the CAEN filter (point A in Fig. 4.64), vertical scale 5 V/div, DC, BWL = 20 MHz. The lower waveform (channel 1) is the filter input current.

Fig. 4.66 displays, in the upper trace (channel 3), the voltage measured at the output of the CAEN filter (point B in Fig. 4.64), vertical scale 200 mV/div, AC, BWL = 1 MHz. The lower waveform in the same figure (channel 1) is the filter input current.

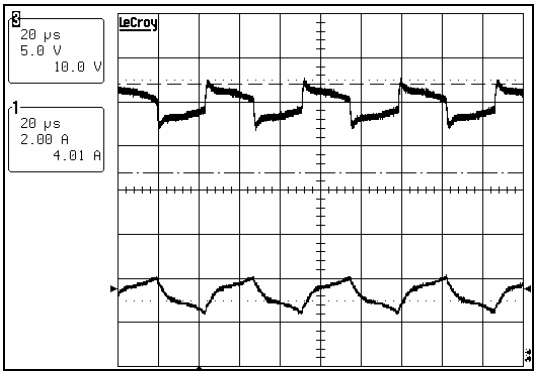


FIG. 4.65 See text.

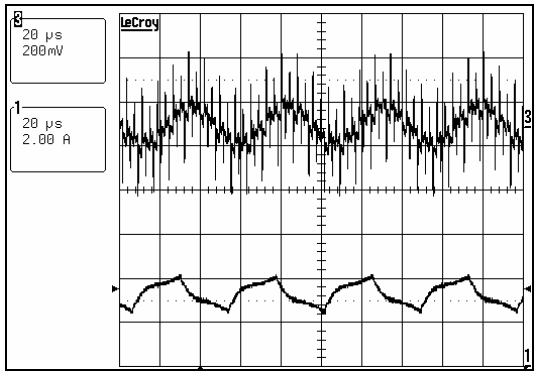


FIG. 4.66 See text.

Fig. 4.67 displays the voltage measured at the IPM input (upper trace, channel 3), i.e. at point C in Fig. 4.64, vertical scale 10 mV/div, AC, BWL = 1 MHz. The lower waveform (channel 1) is the filter input current.

Fig. 4.68 shows the voltage measured at the +120V output of the S9019 dc/dc converter, that is at point F in Fig. 4.64 (upper trace, channel 3). The conditions are: vertical scale 5 mV/div, AC, BWL = 20 MHz. The lower waveform (channel 1) is again the filter input current.

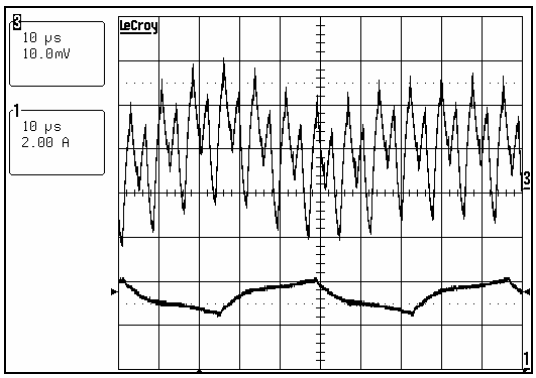


FIG. 4.67 See text.

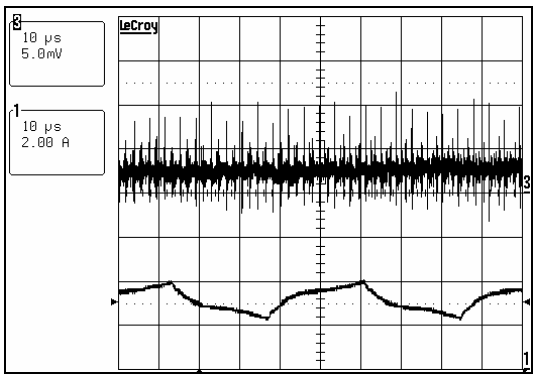


FIG. 4.68 See text.

In Fig. 4.69, the upper trace (channel 3) shows the voltage measured at the +3.4V output of the S9006 dc/dc converter (point E in Fig. 4.64), vertical scale 5 mV/div, AC, BWL = 20 MHz. The lower waveform (channel 1) is the filter input current.

Fig. 4.70 displays in the upper waveform the voltage measured at the +5.7V output of the S9004 dc/dc converter (point D in Fig. 4.64), vertical scale 10 mV/div, AC, BWL = 20 MHz. The lower waveform (channel 1) is the filter input current.

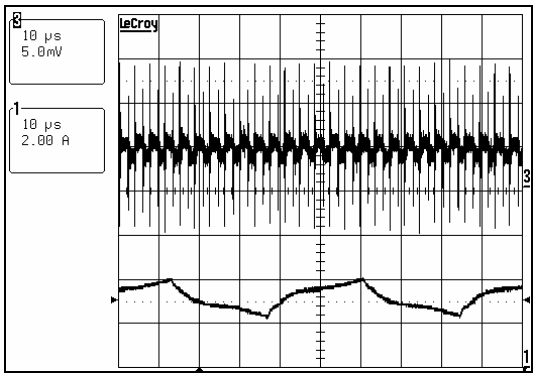


FIG. 4.69 See text

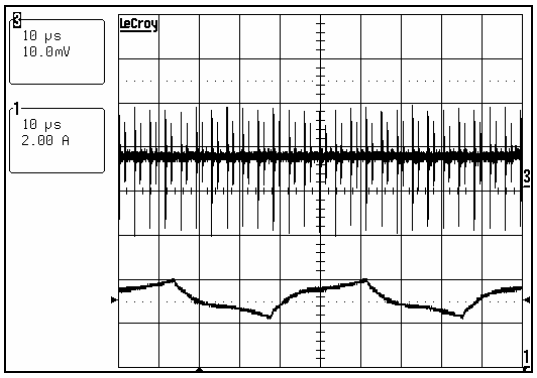


FIG. 4.70 See text

It can be noticed that the presence of such a disturbance on the power line does not provoke appreciable noise at the dc/dc converters' outputs.

Figs. 4.71 and 4.72 refer to the second set of measurements (disturbances close to the lower limit) and were obtained with a square-wave disturbance frequency of 21 kHz.

In Fig. 4.71 are displayed the voltage measured at point A of Fig. 4.64 (upper trace, channel 3, vertical scale 5 V/div, DC, BWL = 20 MHz) and the filter input current (lower trace, channel 1).

In Fig. 4.72 are displayed the voltage measured at point F of Fig. 4.64 (upper trace, channel 3, vertical scale 5 mV/div, AC, BWL = 20 MHz) and the filter input current (lower trace, channel 1).

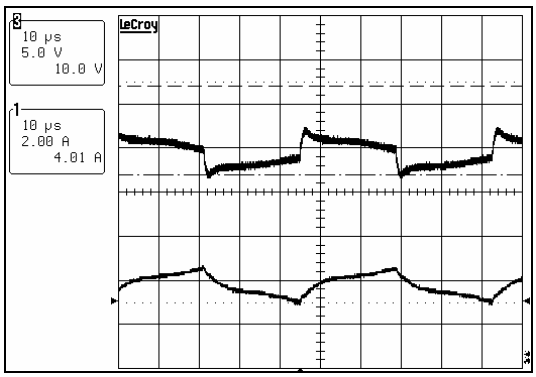


FIG. 4.71 See text

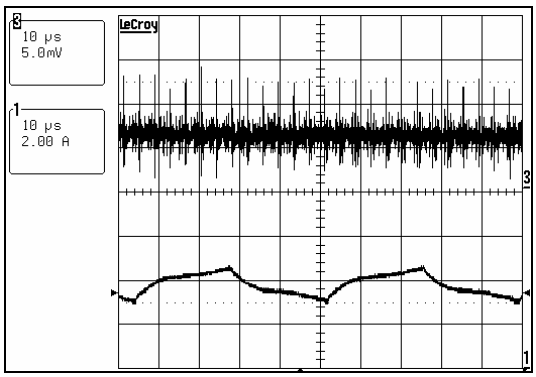


FIG. 4.72 See text

Similarly to the result of Fig. 4.72, which refers to the +120V output of the S9019 module, no noise problems were detected on the outputs of the other dc/dc converters (points D and E in Fig. 4.64).

Other measurements, similar to those described in this subsection and conducing to analogous results, were performed at frequencies of 10 Hz, 1 kHz and 6 kHz.

4.6.2 Undervoltage and overvoltage

This type of disturbance can provoke an "undervoltage" or an "overvoltage" status of the IPM if occurring when the DC level of the input voltage is significantly below or above 27 V DC, respectively. Since the occurrence of both these conditions provoke a switching-off of the IPM, it is therefore extremely important to measure the effective IPM thresholds for undervoltage and overvoltage conditions, as well as the effective switch-off and recovery times of the IPM.

In Fig. 4.73 the upper waveform (channel 3) is the input voltage of the filter, showing that when the undervoltage threshold for this IPM is reached (19.3 V, dashed line), it takes about 0.8 ms for the IPM to switch-off. The switching off of the IPM is clearly visible from the lower waveform (channel 1), which is the filter input current, that starts dropping to zero after about 0.8 ms after the input voltage has reached the undervoltage threshold.

Figure 4.74: the upper waveform (channel 3) is the input voltage of the filter, showing that when the overvoltage threshold for this IPM is reached (33.4 V, dashed line), it takes about 0.8 ms for the IPM to switch-off. The overvoltage was provoked by a positive pulse on the power line of duration 1.5 ms. The switching off of the IPM is clearly visible from the lower waveform (channel 1), which is the filter input current, that starts dropping to zero after about 0.8 ms after the input voltage has reached the overvoltage threshold.

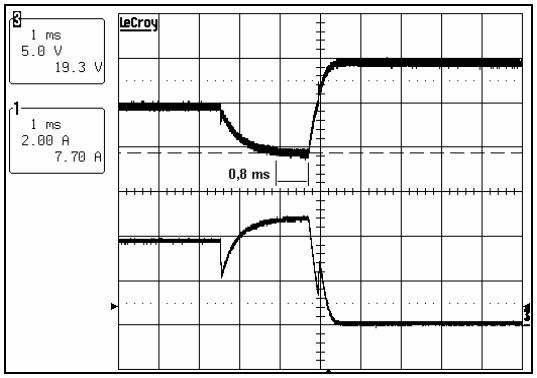


FIG. 4.73 IPM undervoltage test (see text).

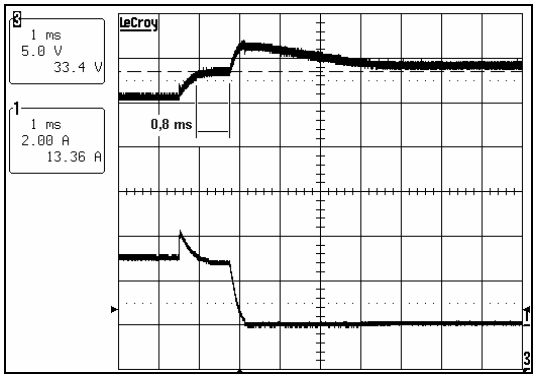


FIG. 4.74 IPM overvoltage test (see text)

Fig. 4.75 shows the result of an overvoltage + recovery test. In this case the pulse on the power line allowed the IPM to recover its normal operation by bringing the input voltage down across the 33.5 V threshold after the overvoltage condition (upper waveform, channel 3). The central waveform (channel 1) is the filter input current, while the lower waveform (channel 2) is the IPM output voltage, showing that the normal + 17 V DC output voltage is recovered about 2 ms after crossing of the threshold.

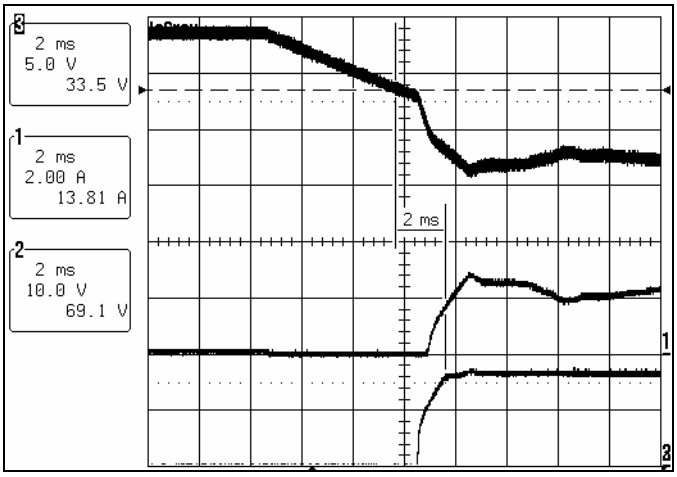


FIG. 4.75 Upper waveform: IPM input voltage; central waveform: filter input current; lower waveform: IPM output voltage, showing the recovery time of ≈ 2 ms.

4.7 Measurements in presence of "single voltage pulse rushes of up to 10 μs duration and an amplitude of up to 80 V for each power bus with respect to the shell of the vessel" (i.e. common mode disturbance)

4.7.1 Preliminary tests on the set up.

First of all it was necessary to check the actual performance of the noise generator, since this type of pulses is difficult to reproduce. We used a measurement set-up illustrated in the block diagram of Fig. 4.76. A 10 kΩ resistor was used to load the NG output. The differential probe DXC100A was used to sense the pulses on the terminals of a 24 V battery with respect to the shell, while the current probe was used to monitor the current at the NG output. The arrangement depicted in Figure 4.76 allowed giving common mode pulse rushes to the battery's terminals.

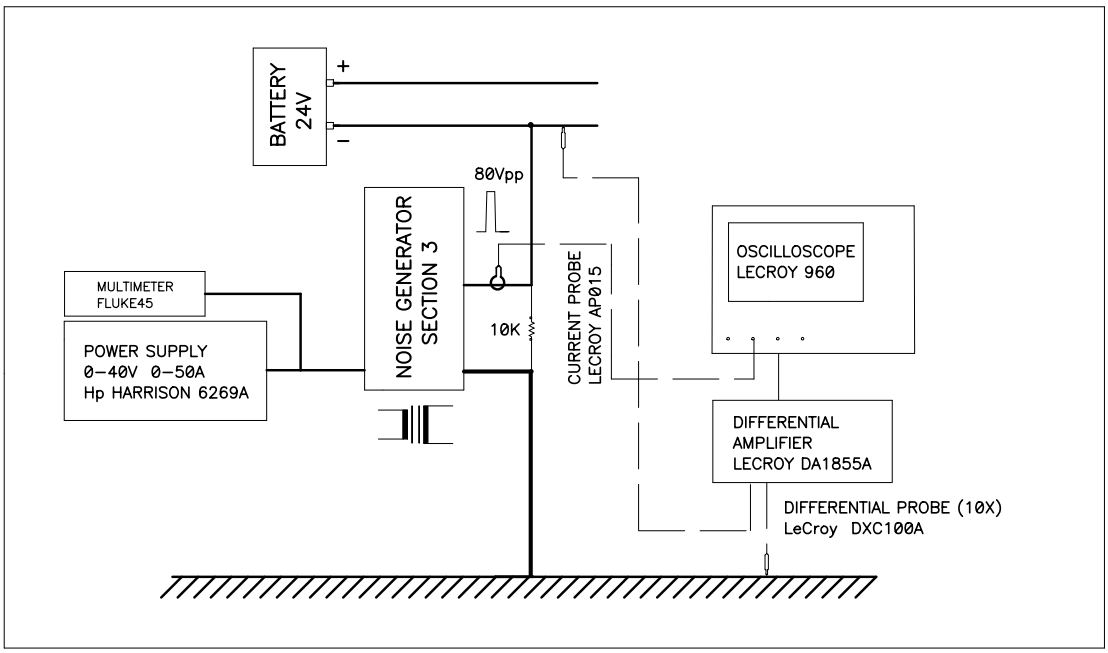


FIG. 4.76 Block diagram of the set-up used to test the "80 V voltage pulse rushes" disturbance.

In Fig. 4.77 the upper waveform (channel 2) is the current at the NG output, while the lower waveform (channel 3) is the 80 V pulse appearing at the battery's terminal with respect to the shell. We therefore conclude that this type of voltage rush could be adequately reproduced.

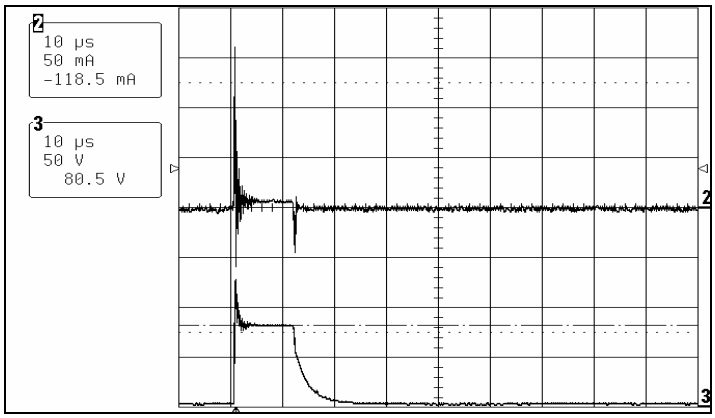


FIG. 4.77 Upper waveform: NG output current; lower waveform: battery's voltage.

Since this type of disturbance occurring on the power lines could, in principle, lead to permanent damage or break-up of the CAEN filter and the IPM, its effects should be carefully tested.

4.7.2. Tests with the CAEN filter connected to a resistive load

Fig. 4.78 describes the set up used to test the behaviour of the CAEN filter for this type of disturbance. The filter was loaded with a 6.8 Ω load. The 24 V battery terminals were connected to the filter's inputs, the negative terminal being "hanged" to the NG output. The filter's ground contact was connected to the shell.

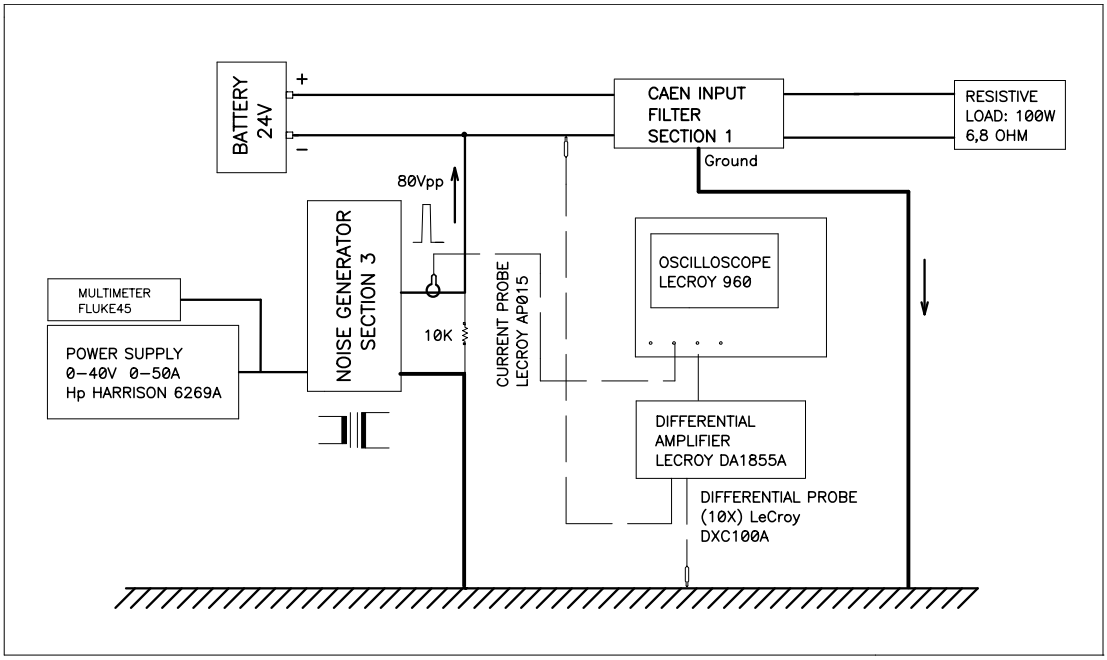


FIG. 4.78 Block-diagram of the measurements on the CAEN filter.

A Fig. 4.79 show, in the upper waveform (channel 2), the current at the NG output, and in the lower waveform (channel 3), the voltage appearing at the filter's input with respect to the shell.

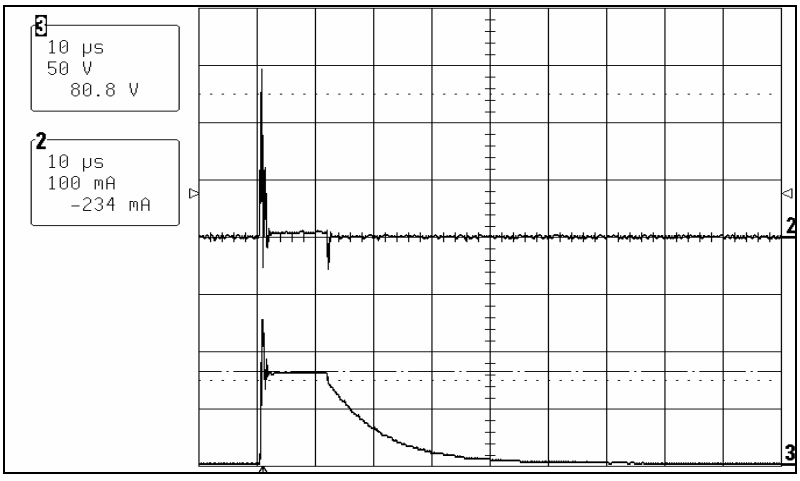


FIG. 4.79 Upper waveform: NG output current; lower waveform: CAEN filter input voltage with respect to the shell.

4.7.3. Tests with the IPM connected to a resistive load

After these preliminary measurements, a test with an IPM connected to the output of the CAEN filter was performed (see the set up depicted in Fig. 4.80). The IPM had a resistive load corresponding to half-power operation (6.8 Ω).

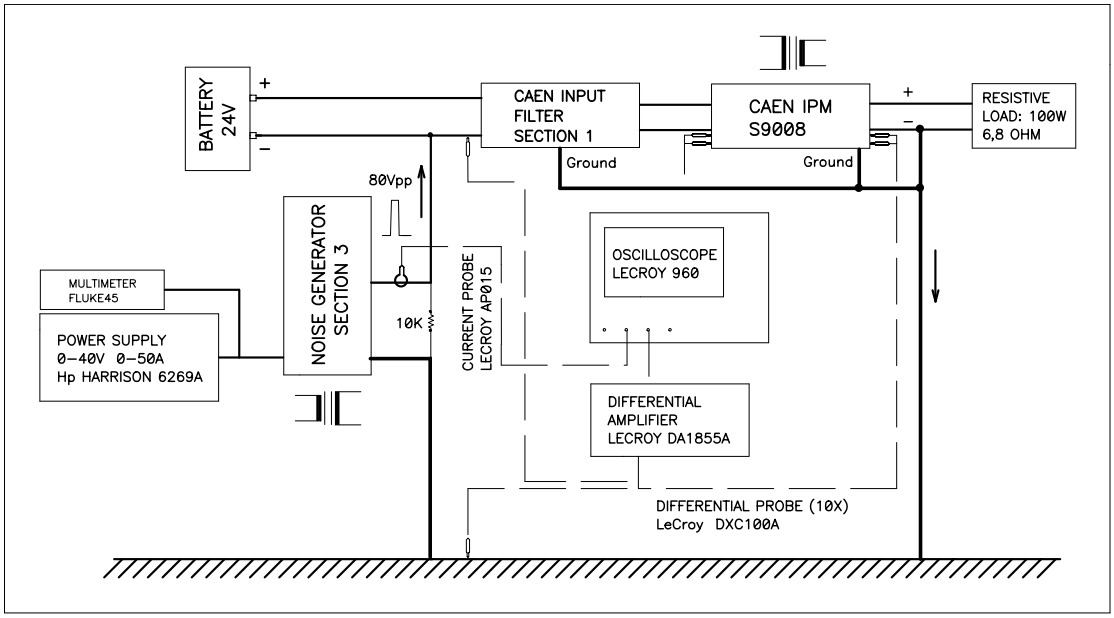


FIG. 4.80 Measurement set-up used in this sub-section

In Fig. 4.81 the lower waveform (channel 3) is the voltage appearing at the filter's input with respect to the shell. The amplitude of the applied pulse was 80 V, like shown in Fig. 4.79. An over elongation is present in this case (i.e. with the IPM connected to the filter), while such elongation was absent without IPM connected (see Fig. 4.79). The upper waveform in Fig. 4.81 (channel 2) shows the measured current at the output of the NG. In these conditions, the peak-to-peak current amplitude is 121 mA.

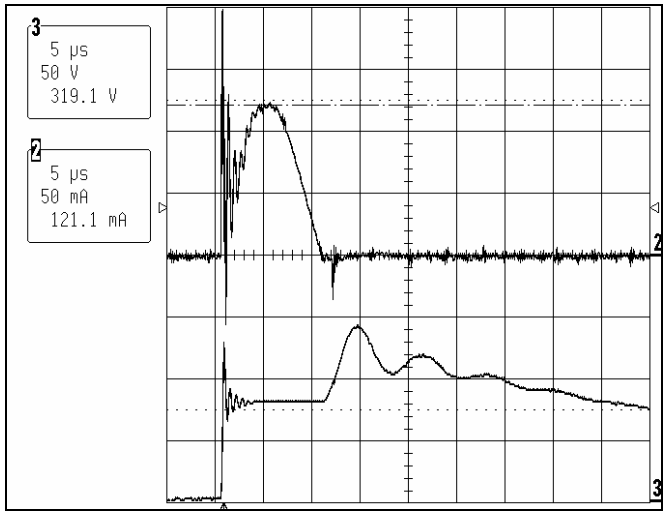


FIG. 4.81 Lower waveform: voltage at the filter's input for an 80 V common-mode voltage pulse on the input power line; upper waveform: measured NG output current.

Fig. 4.82 shows, in the upper waveform (channel 2), again the current at the NG output, while the lower waveform (channel 3) is the voltage, measured with the differential probe, appearing at the IPM input (see Fig. 4.80).

In Figure 4.83 the upper waveform (channel 2) is again the current at the NG output, while the lower waveform (channel 3) is the voltage, measured with the differential probe, appearing at the IPM output (BWL = 1 MHz).

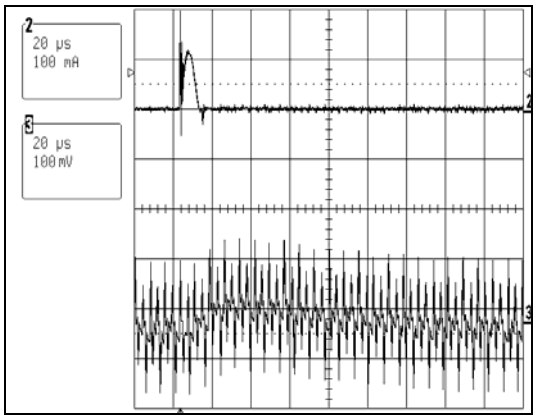


FIG. 4.82 See text.

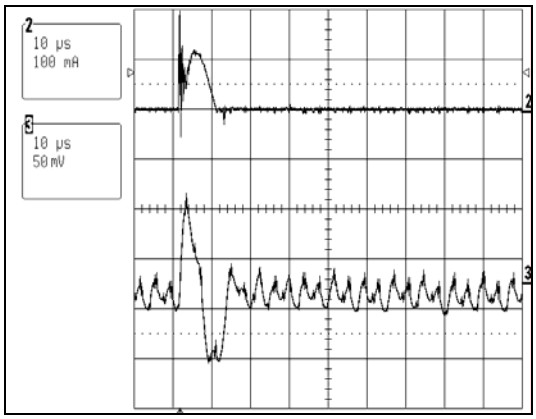


FIG. 4.83 See text.

We can therefore conclude that:

1. The input filter and the IPMs are not damaged by this type of voltage rush on the input power lines;
2. The effect of the pulse at the IPM output is a voltage glitch of about 160 mV peak-to-peak, which does not constitute a problem for PAMELA.

4.7.4. Tests with the IPM connected to a resistive load and 3 dc/dc converters

For this set of measurements, the IPM was connected, via the splitter, to a resistive load (6.8 Ω, corresponding to half power) and 3 dc/dc converters simultaneously: an S9004, an S9006 and an S9019. Each dc/dc converter was fully loaded with a resistive load. The set up is depicted in Fig. 4.84.

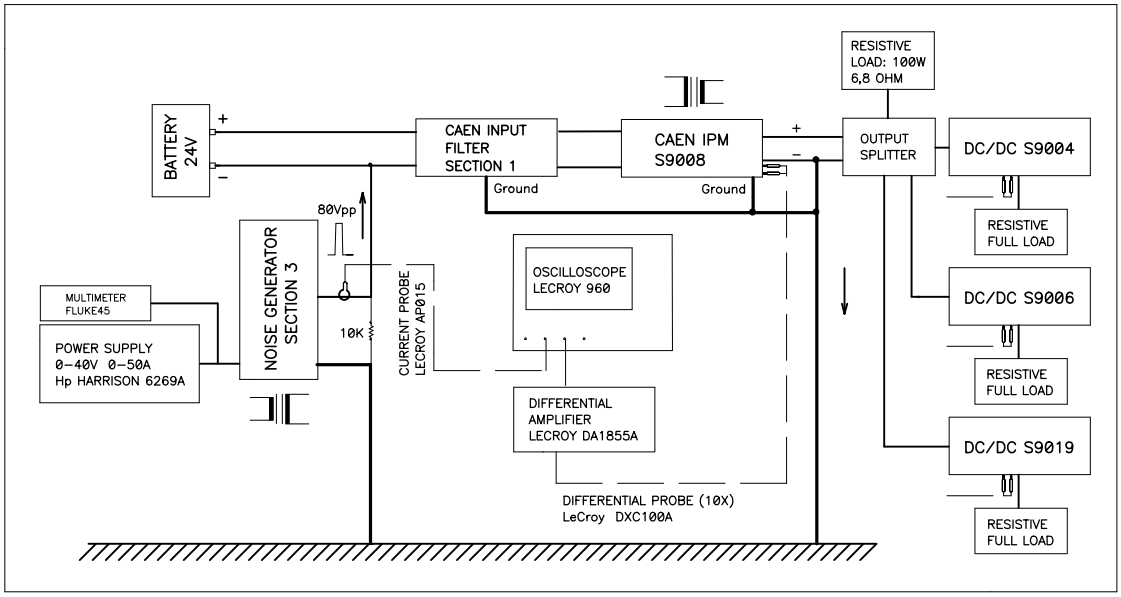


FIG. 4.84 Set-up used for the measurements with IPM and dc/dc converters.

Fig. 4.85 shows, in the upper waveform (channel 2) the current at the NG output, and in the lower waveform (channel 3) the voltage, measured with the differential probe, appearing at the IPM output across the 6.8 Ω load (BWL = 20 MHz). The situation is not significantly different from that of Figure 4.83 (i.e. without the dc/dc converters).

In Fig. 4.86 the upper waveform (channel 2) is again the current at the NG output, while the lower waveform (channel 3) is the noise, measured with the differential probe, at the S9006 dc/dc converter's output. As clearly shown, the effect of the 80 V common mode pulse at the dc/dc converter's output is totally negligible, and this was found to be the case also for the S9004 and S9019 units.

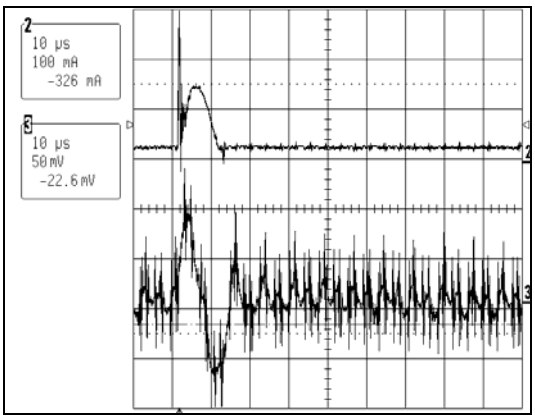


FIG. 4.85 See text.

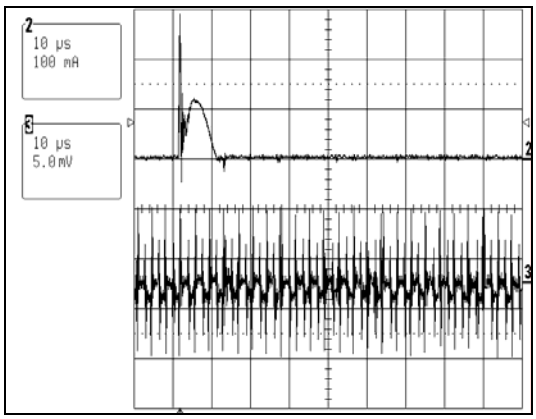


FIG. 4.86 See text.

4.8 Measurement of the in-rush currents

In-rush current measurements were performed both at the input of the filter and at the input of the IPM.

4.8.1 In-rush currents at the filter's input

These measurements were performed by placing a switch on the power lines between the HP power supply and the filter. A fully-loaded IPM was connected at the filter's output, to reproduce a realistic situation.

In Fig. 4.87 the upper waveform (channel 3) is the voltage, measured with the differential probe, at the input of the CAEN filter. The commutation from 0 V to 27 V DC is clearly evident. There are some bounces of the voltage due to the switch. The lower waveform (channel 1) is the input current of the filter. The maximum peak level reached is about 10 A.

In Fig. 4.88 the upper waveform (channel 1) is again the input current of the filter (here the time scale is 5 ms/div, however). The lower waveform (channel 3) is the output voltage of the IPM. Here one can see that the 17 V DC output level of the IPM is reached after a time of about 2 ms from the commutation of the line (closing of the switch).

Fig. 4.89 refers to a measurement done with the dc/dc converters connected to the IPM output. The lower waveform (channel 3) is the output voltage of the S9006 dc/dc converter. The 3.4 V DC output level of the S9006 is reached after a time of about 22 ms from the commutation of the line (closing of the switch). The upper waveform (channel 1) is the input current of the filter (here the time scale is 10 ms/div).

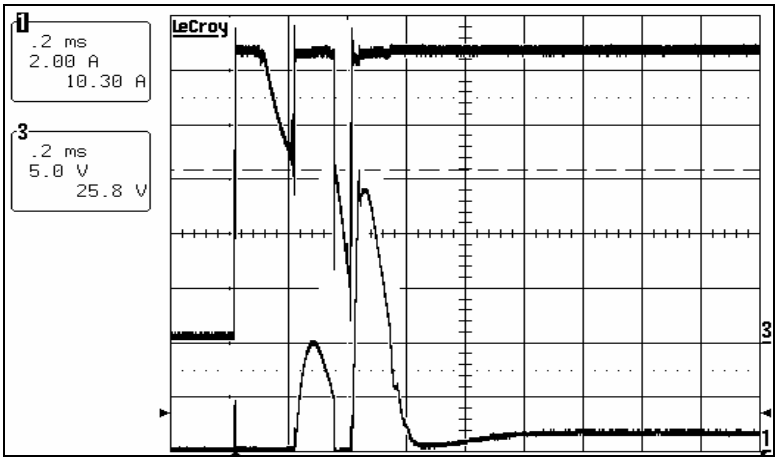


FIG. 4.87 In-rush current at the filter's input (see text).

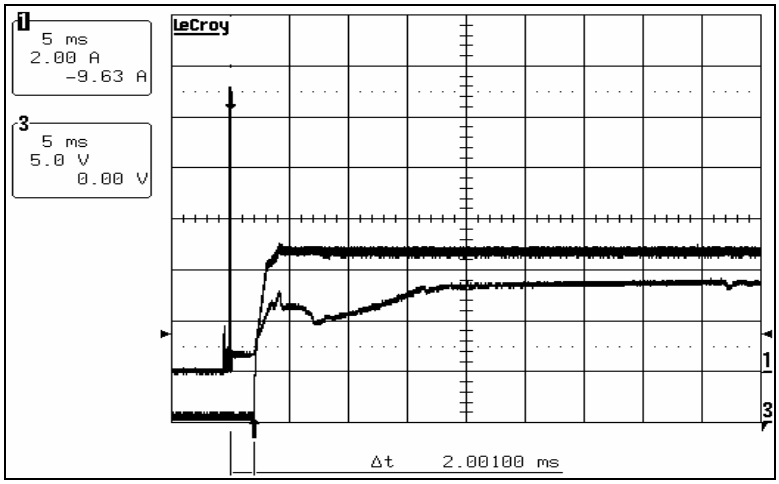


FIG. 4.88 Upper waveform: in-rush current at the filter's input (5 ms/div scale); lower waveform: IPM output voltage

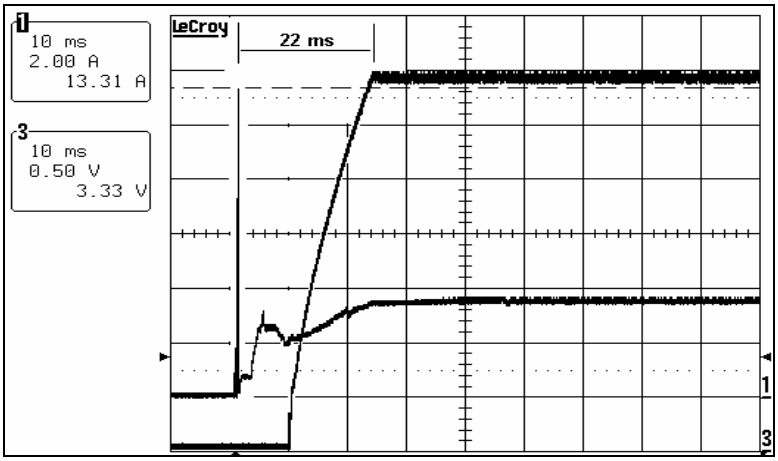


FIG. 4.89 Upper waveform (channel 1): input current of the filter (time scale is 10 ms/div); lower waveform: output voltage of the S9006 dc/dc converter

4.8.1 In-rush currents at the IPM input (at no load)

The IPM was switched on at no load by means of a switch placed between the output of the filter and the IPM input, i.e. performing the same functionality as the Kayser Relays Board in the actual PSS.

Fig. 4.90 shows (lower trace) the in-rush current at the input of the IPM. The peak values were between 8 and 9 A. The upper trace is the differential voltage at the input of the IPM.

In Fig. 4.91 here it is shown (lower trace) the in-rush current at the input of the IPM when switching off the unit; in this case, peak values between 2.5 and 6A were recorded. The upper trace is again the IPM input differential voltage.

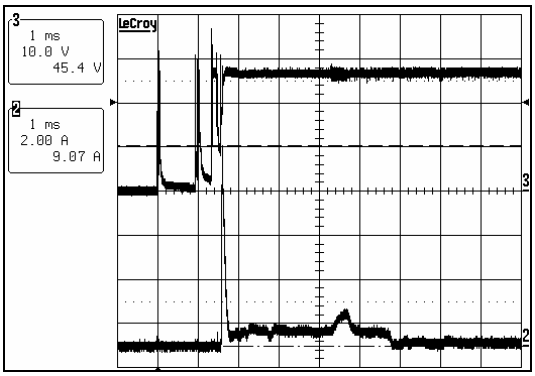


FIG. 4.90 See text.

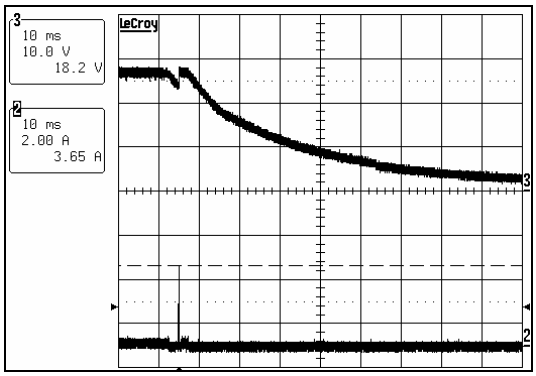


FIG. 4.91 See text.

4.8.2 In-rush currents at the IPM input (at full load)

These measurements were performed by switching on the power lines between the filter and the IPM by means of a switch, i.e. performing the same functionality as the Kayser Relays Board in the actual PSS. The IPM was fully loaded with a 3.4 Ω resistive load.

Fig. 4.92: here (lower trace) it is shown the "on" in-rush current at the input of the IPM. Peak values between 8 and 10 A were recorded. A stable regime is attained after ≈ 5.5 ms. The upper trace is the IPM input differential voltage.

Fig. 4.93: here (lower trace) it is shown the "off" in-rush current at the input of the IPM. The "zero current" state is attained after ≈ 2 ms. The observed peak values were between 9.5 e 11A .

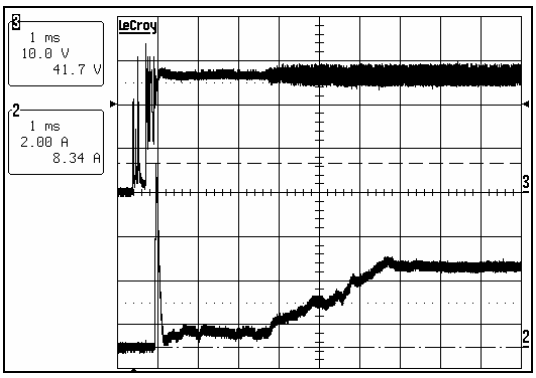


FIG. 4.92 See text.

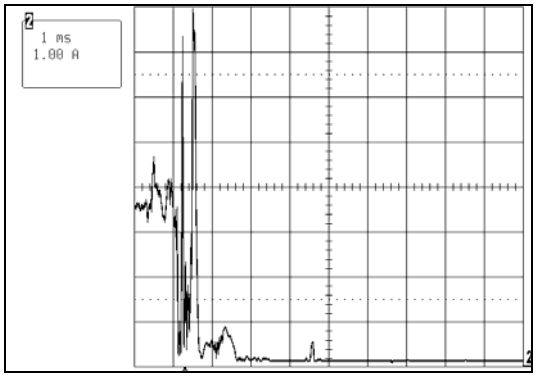


FIG. 4.93 See text

5. MEASUREMENTS WITH THE COMPLETE SYSTEM AND WITH RUSSIAN CABLES

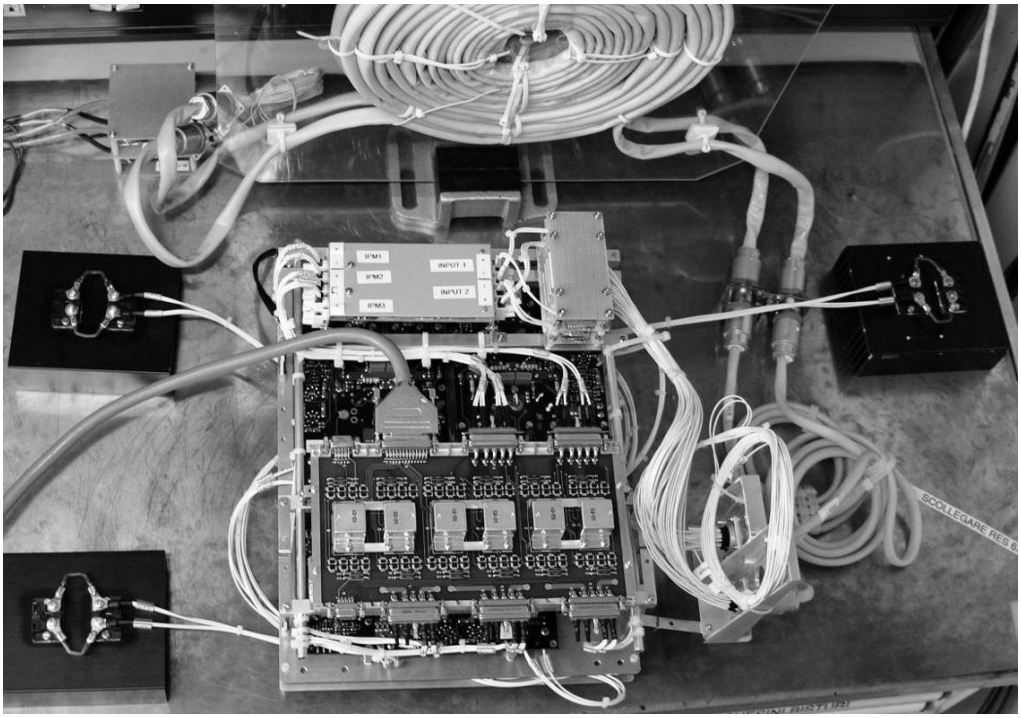


FIG. 5.1 Partial view of the measurement set-up, showing the Kayser Relays Board and one of the 10 m long Russian satellite power cable.

The following measurements were obtained with a complete system (CAEN filter + Kayser Relays Board + 3 IPM fully loaded with resistive loads). Figs. 5.1 and 5.2 are pictures showing part of the set up. The main scope of these tests were to check for the voltage drops when using the very long Russian cables foreseen for satellite operation and check if the noise at the main critical points of the system (filter's input, IPM inputs and outputs) remained basically unaltered with respect to the previous measurements.

5.1 Voltage drop measurements

Fig. 5.3 is a scheme of the set-up used for the voltage drop measurements. Russian space-qualified connectors, identical to those that will be mounted on the satellite, were used (XP1A, XP2A, XP1E, XP2E, XP1R, XP2R, XP1 and XP2), together with 10 m long and 2 m long Russian cables. The cables provide two independent supply lines (line 1 and Line 2) that are connected to the CAEN filter. The Kayser Relays Board is powered by the filtered supply and it provides the switching of the power lines of the IPMs.

In the set-up of Fig. 5.3 Line 1 supplies one IPM, whether Line 2 supplies the other two. The power supply was set to 23 V DC, and the voltage drops at the various points (A, B, etc.) of the chain were measured. The currents in Line 1 and Line 2 are I_1 = 4,3A e I_2 = 9,0A, respectively.

With reference to Fig. 5.3, we have a total voltage drop from point A to the IPM inputs: ΔV_{AF} = 1.17 V, ΔV_{AE} = 2.06V and ΔV_{AD} = 2.09 V for the 3 IPMs, respectively. Relevant voltage drops develop on the Russian cables and across the CAEN filter.

Therefore, since the IPM undervoltage threshold is about 19.5 V (see Section 4.6), the safety margin for IPM undervoltage for a satellite input voltage of 23 V (the minimum guaranteed voltage from the satellite in normal operations, according to the ICD) is about 1.4 V, which is not considered an entirely safe value.

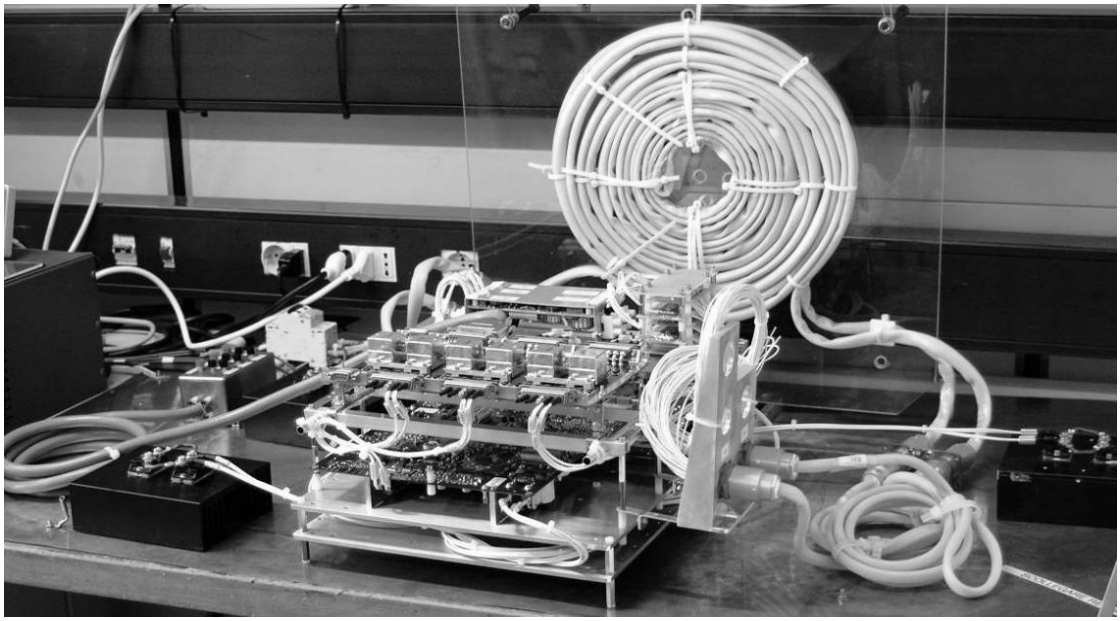


FIG. 5.2 Another picture of the set-up.

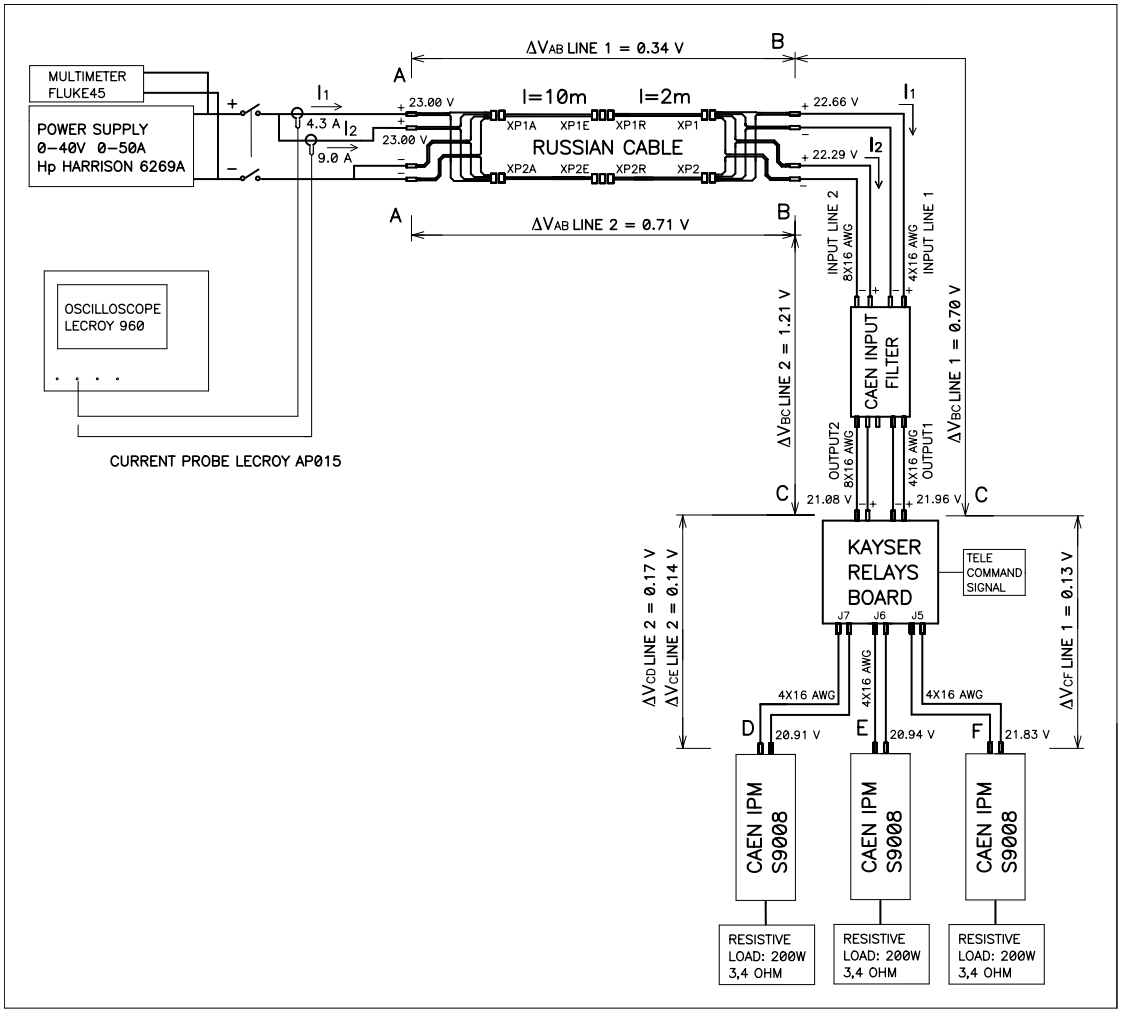


FIG. 5.3 Schematic block diagram of the voltage drop measurement set-up.

5.2 Noise at the CAEN filter's input.



FIG. 5.4 Detail of the CAEN filter.

The scheme used for these measurements is illustrated in Fig. 5.5.

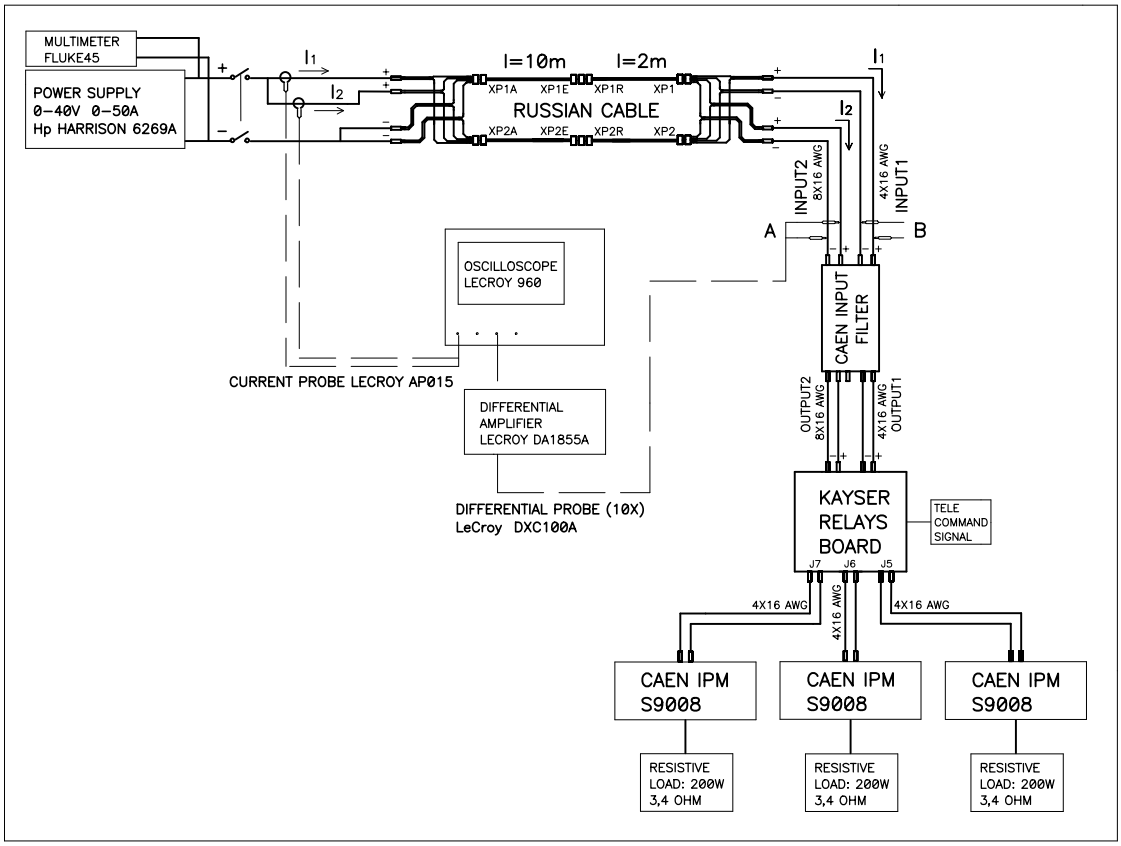


FIG. 5.5 Set-up used for the AC noise measurements at the filter's input.

Fig. 5.6 reports in the upper waveform (channel 3) the AC voltage (10 ms/div time scale, 50 mV/div vertical scale, BWL = 20 MHz) measured at the filter's input at point A. The lower waveform (channel 2) is the current I_2 measured at the beginning of the chain

(see Fig. 5.5). Fig. 5.7 displays the same waveforms as Fig. 5.6, but with the time scale set at 1 μs/div.

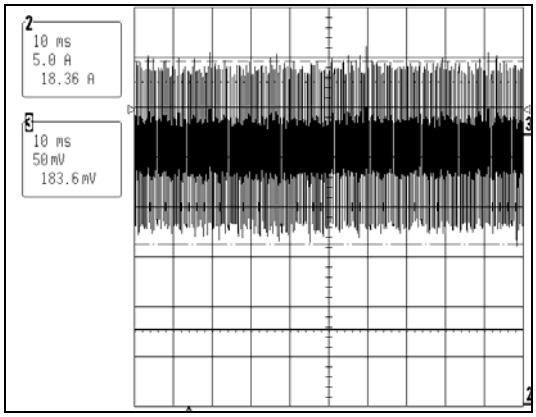


FIG. 5.6 See text.

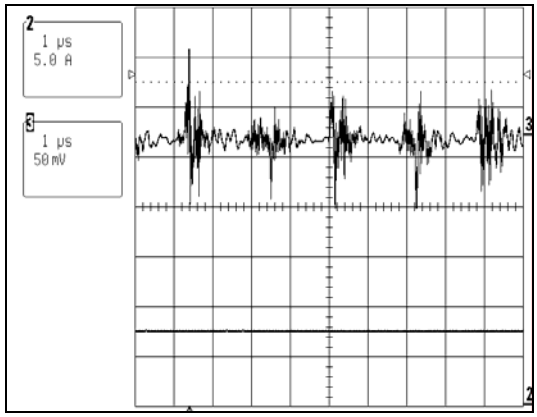


FIG. 5.7 See text.

Fig. 5.8: the upper waveform (channel 3) is the AC voltage (10 ms/div time scale, 50 mV/div vertical scale, BWL = 20 MHz) measured at the filter's input at point B of Fig. 5.5. The lower waveform (channel 2) is the current I_1 measured at the beginning of the chain.

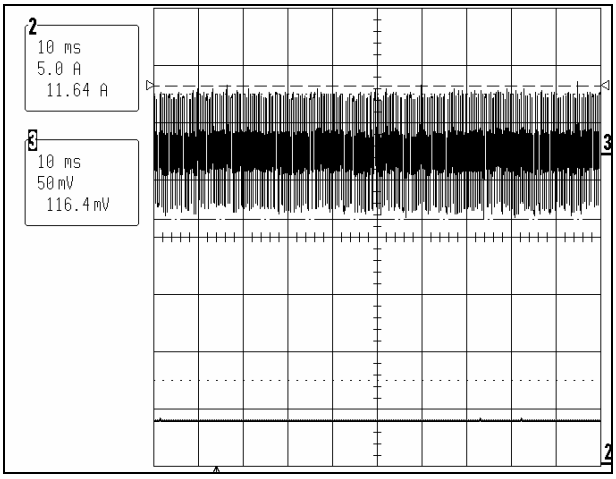


FIG. 5.8 Upper trace: AC voltage at filter's input B; lower trace: current I_1 (see Fig. 5.5)

5.3 Noise at the CAEN filter's output

Fig. 5.9 shows schematically the set up used for measurement of AC noise at the filter's output, i.e. at the input of the Kayser Relays Board.

The upper waveform (channel 3) in Fig. 5.10 is the AC voltage (10 ms/div time scale, 1 V/div vertical scale, BWL = 20 MHz) measured at the Kayser relays board's input at point A. The lower waveform (channel 2) is the current I_2 measured at the beginning of the chain.

Fig. 5.11 is analogous to Fig. 5.10, but with a different time scale (0.2 μs/div).

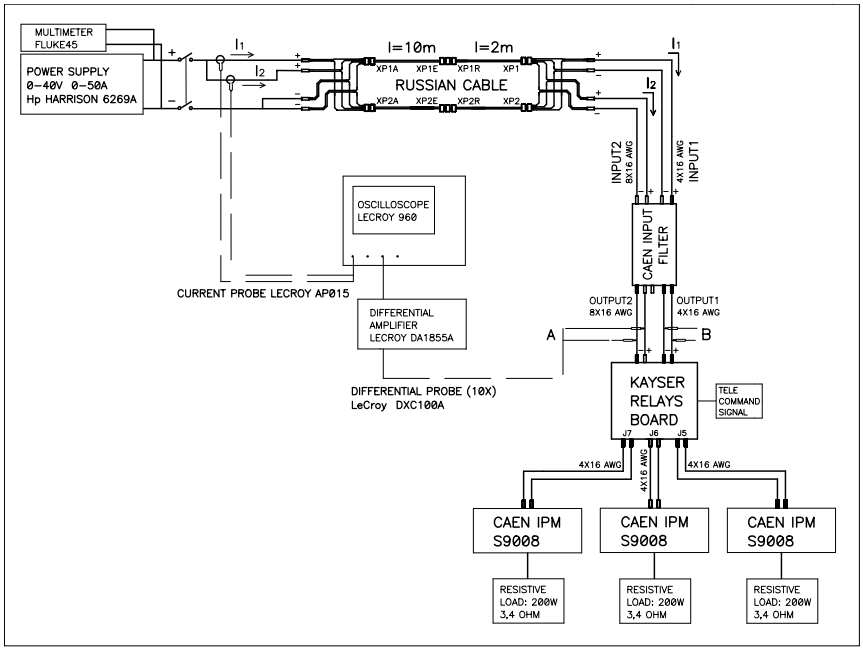


FIG. 5.9 Output filter's noise measurement scheme

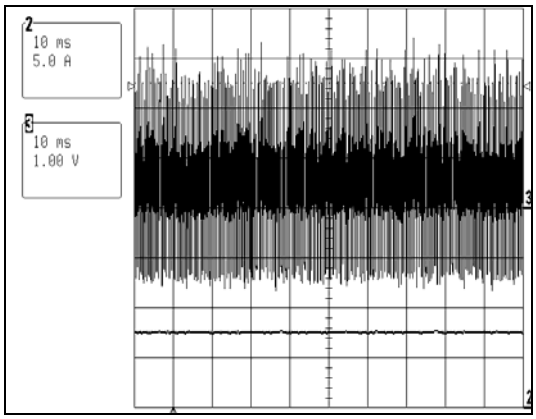


FIG. 5.10 See text.

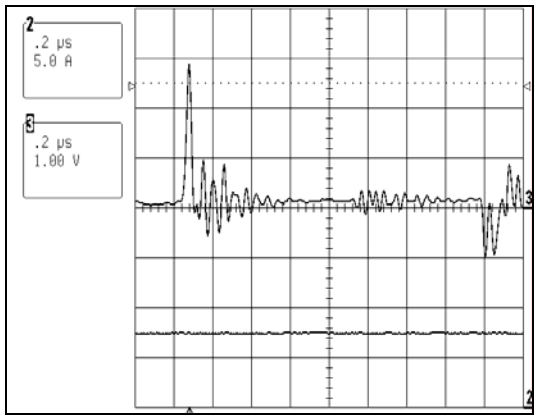


FIG. 5.11 See text.

Figure 5.12: the upper waveform (channel 3) is the AC voltage (10 ms/div time scale, 1 V/div vertical scale) measured at the Kayser relays board's input at point B. The lower waveform (channel 2) is the current I_1 measured at the beginning of the chain.

Figure 5.13: same as in Figure 5.12, but with time scale set at 0.2 µs/div.

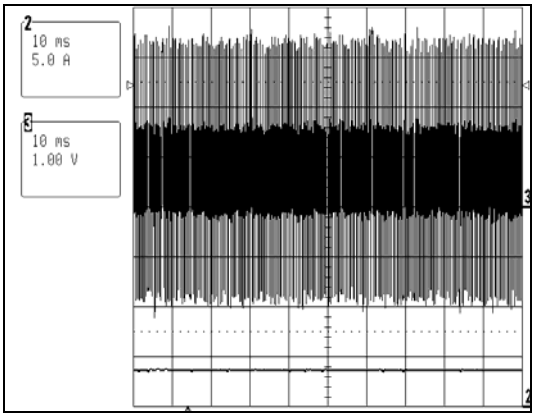


FIG. 5.12 See text.

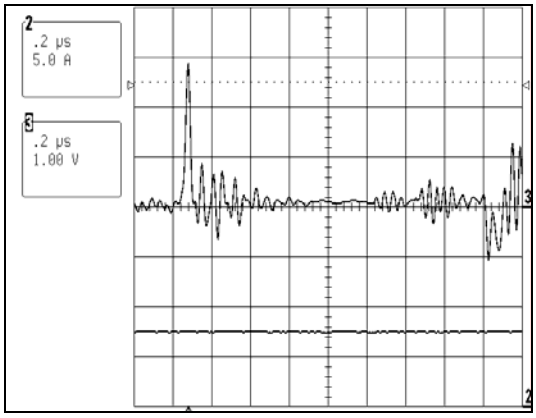


FIG. 5.13 See text.

5.4 Noise at the IPM output

The set-up used to measure the noise at the output of the IPM is shown schematically in Fig. 5.14 shows schematically the set up used for measurement of AC noise at the IPM output.

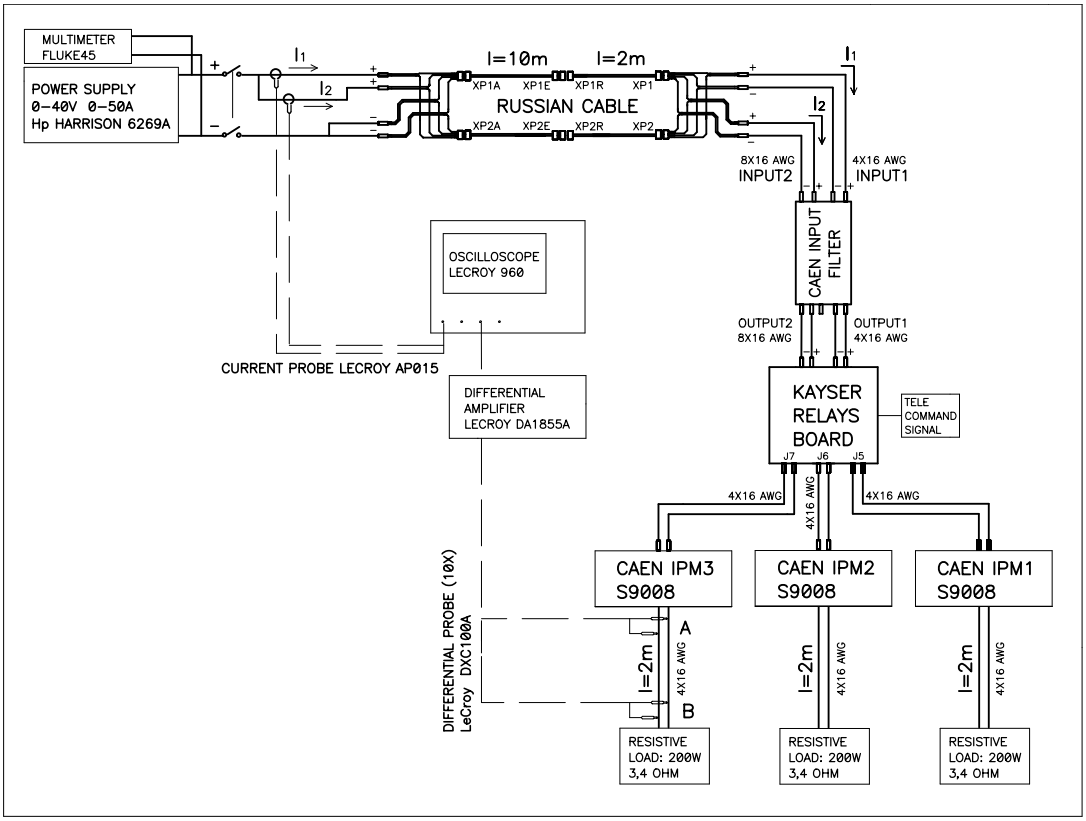


FIG. 5.14 IPM output noise measurement set-up.

In Fig. 5.15 the upper waveform (channel 3) is the AC voltage (10 ms/div time scale, 20 mV/div vertical scale) measured at the IPM3 output pin, with the unit fully loaded. The lower waveform (channel 2) is the current I_2 measured at the beginning of the chain.

In Fig. 5.16 the upper waveform (channel 3) is the AC voltage (10 ms/div time scale, 10 mV/div vertical scale) measured directly on the 3.4 Ω load of IPM3, after the 2 m long cable connecting the IPM output pin to the load. The lower waveform (channel 2) is again the current I_2 measured at the beginning of the chain.

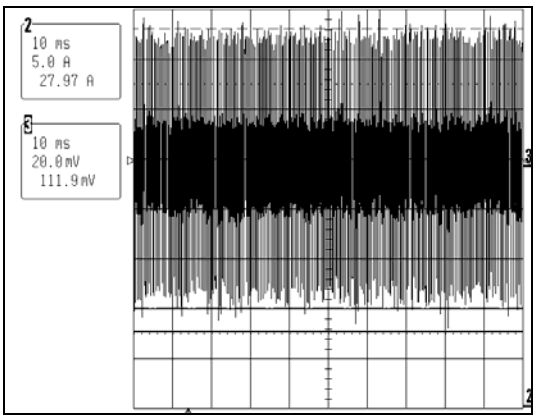


FIG. 5.15 See text (BWL = 20 MHz)

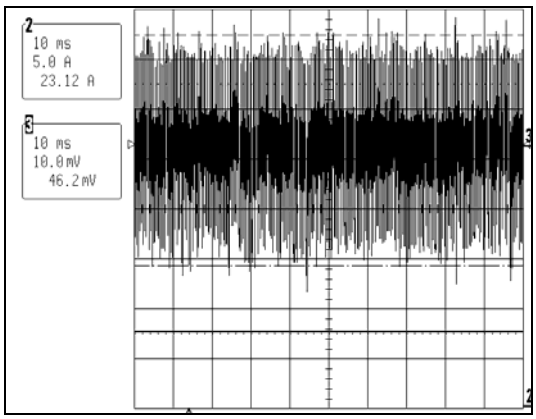


FIG. 5.16 See text (BWL = 20 MHz).

Fig. 5.17 is the same as Figure 5.16, but with time scale set at 2 μs/div.

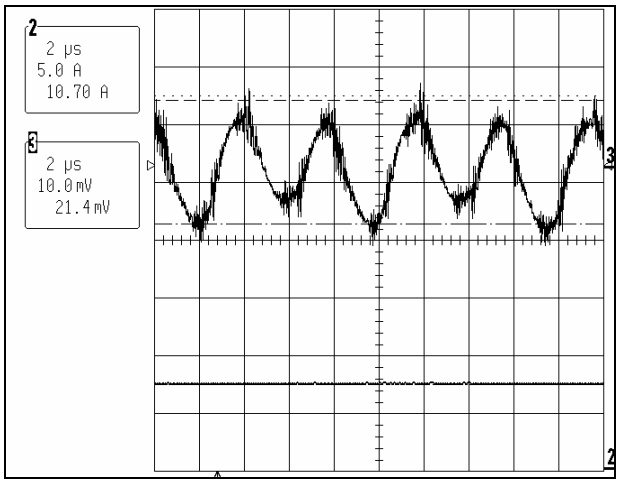


FIG. 5.17 Upper trace: AC voltage measured directly on the 3.4 Ω load of IPM3; lower trace: current I_2 measured at the beginning of the chain. BWL = 20 MHz.

By comparing Figs. 5.15, 5.16 and 5.17 with Figs. 4.4 and 4.5, we van conclude that the noise at the IPM output has remained virtually the same after completing the PSS under test with the "flight" cables of the proper length and with the KRB.

5.5 Measurement on the Kayser Relays Board

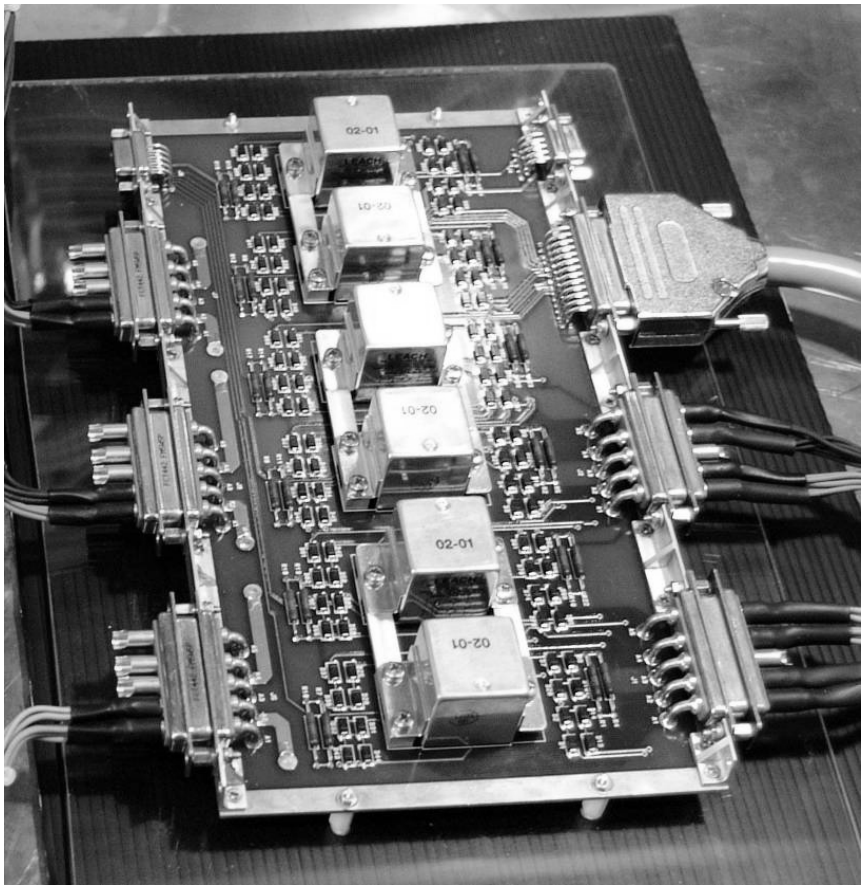


FIG. 5.18 The Kayser Relays Board.

The Kayser Relays Board (KRB, Fig. 5.18) is a crucial component of the PSS. It was therefore extremely important to characterize its performance thoroughly. Fig. 5.19 shows schematically the set up used for the switching measurements on the KRB.

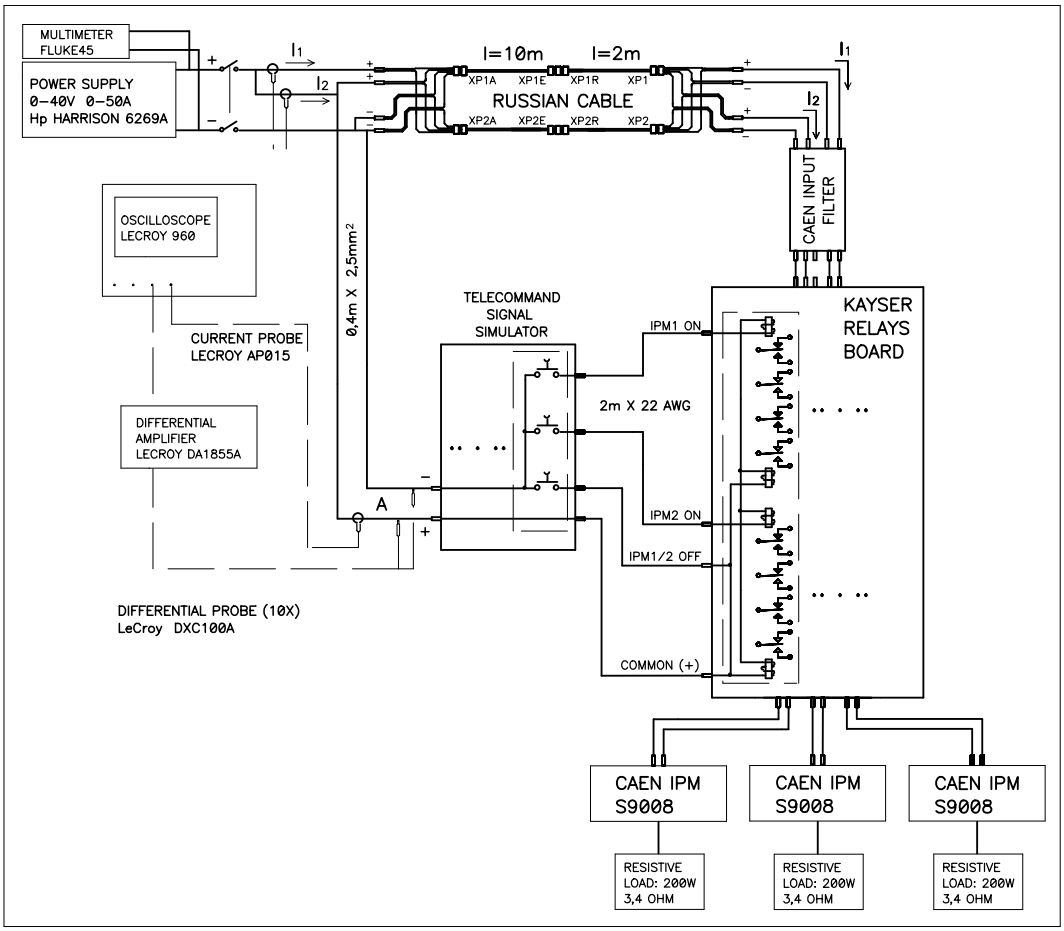


FIG. 5.19 Block scheme of the KRB test set-up

The upper waveform in Fig. 5.20 (channel 3) displays the voltage measured at point A of Figure 5.19, while the lower waveform (channel 2) is the current measured at the same point.

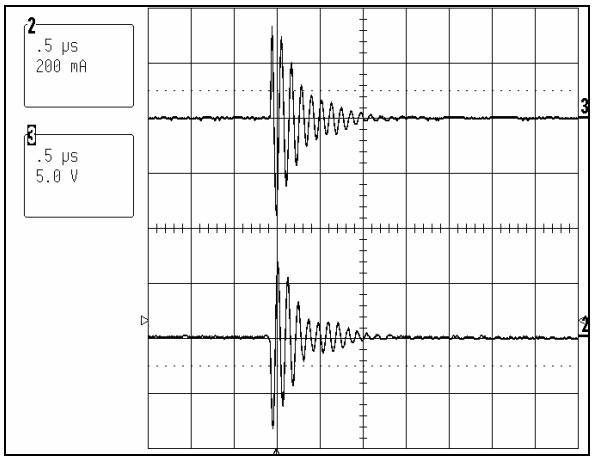


FIG. 5.20 Upper trace: voltage at point A in Fig. 5.19; lower trace: current at the same point.

As it can be seen from this Figure, the switching of the relays of KRB induce a relevant peak-to-peak ringing on the power lines towards the satellite. Therefore, this fact will have to be investigated during the EMI/EMC compatibility tests of PAMELA on the Resurs-DK1.

5.5.1 In-rush current tests with the KRB

Fig. 5.21 shows schematically the set up used for in-rush current measurement (current I_2 measured at the beginning of the chain). IPMs were switched on with the KRB.

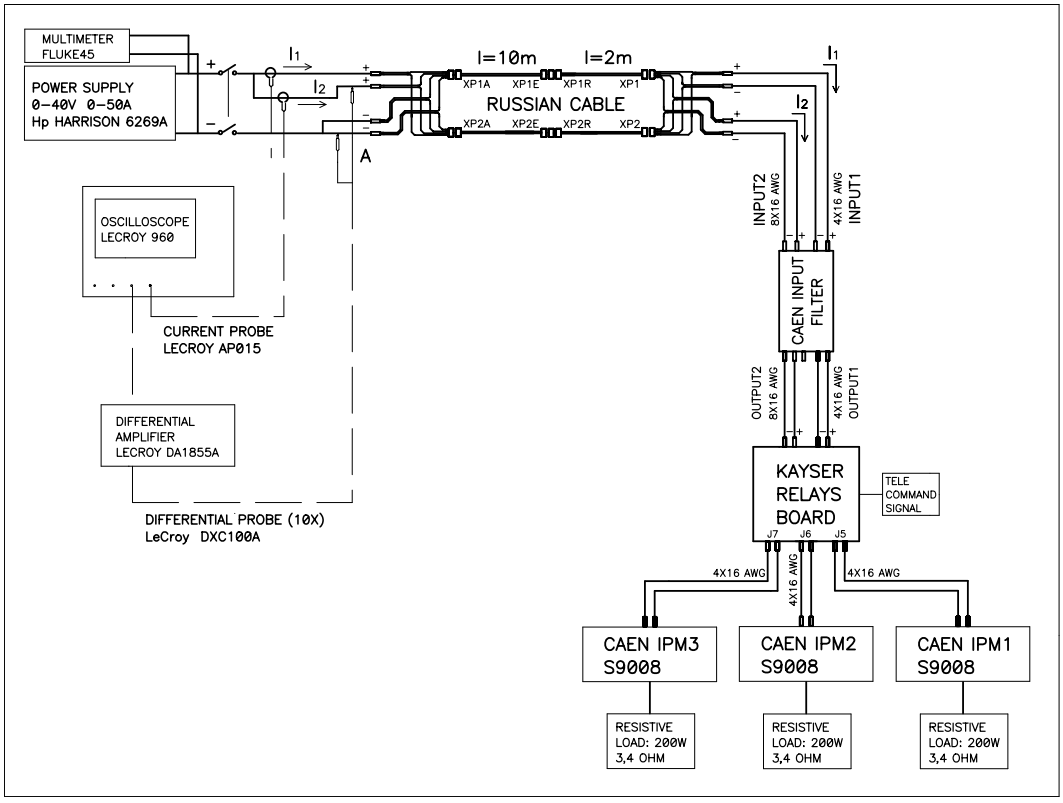


FIG. 5.21 Set-up used for in-rush current measurements with the KRB.

In Fig. 5.22 the upper waveform (channel 3) is the voltage measured at point A of Figure 5.19 when the IPM3 is switched on via the KRB, while the lower waveform (channel 2) is the current I_2 measured at the beginning of the chain. No relevant in-rush is present.

In Fig. 5.23 the upper waveform (channel 2) is the current I_2 measured at the beginning of the chain when IPM3 is switched off: an in-rush current (negative) of about 1.85A is present. The lower waveform (channel 3) is the voltage measured at point A of Fig. 5.21.

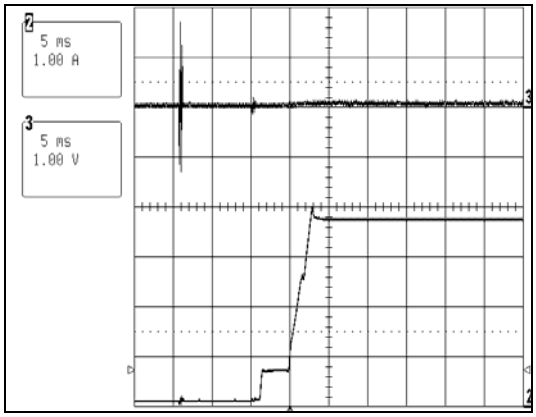


FIG. 5.22 IPM "on": see text

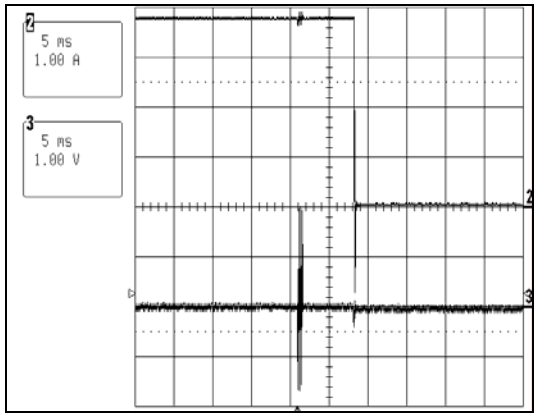


FIG. 5.23 IPM "off": see text

6 REFERENCES

(1) M. Boezio, V. Bonvicini et al, Nucl. Phys. B (Proc. Suppl.) **134**, 39, (2004).
(2) O. Adriani et al., Nucl. Instr. Meth. **A 511**, 72, (2003).
(3) M. Boezio, V. Bonvicini et al., Nucl. Instr. Meth. **A 487**, 407, (2002).
(4) M. Pearce et al., Proc. 28th Intern. Cosmic Ray Conference, Tsukuba, Japan, **OG 1.5**, 2125 (2003).
(5) D. Campana et al., 28th Intern. Cosmic Ray Conference, Tsukuba, Japan, **OG 1.5**, 2141 (2003).
(6) http://www.kayser.it
(7) All data sheets of the S9008 (IPM), S9003, S9004, S9005, S9006, S9019, S9029 and S9030 dc/dc converters used in the PAMELA PSS are available at CAEN web site (www.caen.it) under the "Aerospace" section.

APPENDIX A

Measurements in presence of supply voltage with single voltage pulse rushes of up to 10 µs duration and an amplitude of up to 80 V respect to the negative terminal of the power bus (i.e. differential mode disturbance).

After discussing some preliminary PSS test results with the Russian counterpart, it was decided to repeat the tests described in sub-section 4.7 also in differential mode.

A.1 Preliminary tests on the NG.

With the NG, as described in sub-section 3.2, it is possible to regulate both the peak level of the pulses and the output DC level of the primary supply lines (from + 23 to + 37 V. The set up used for the preliminary tests on the NG is depicted in Fig. A1. A 6.8 Ω load was placed directly at the NG output.

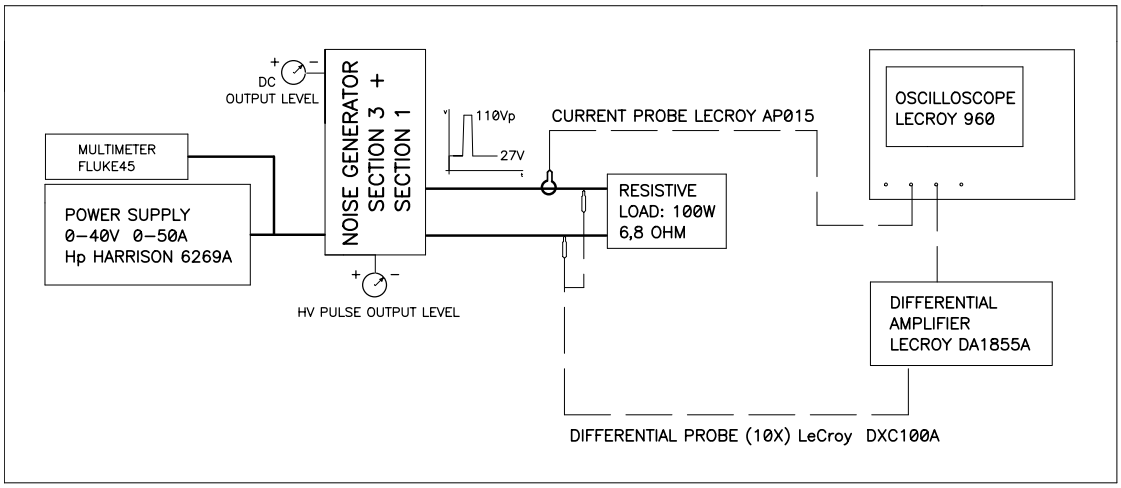


FIG. A1 Set-up used for the preliminary tests on the NG

Fig. A2 shows on channel 3 (upper trace) the output voltage at the load when applying a + 27 V dc level and a minimum high voltage pulse. The central trace is the current flowing to the load and the lower trace is the power delivered to the load under these conditions.

Fig. A3 shows the same quantities as Fig. A2, for the maximum deliverable pulse (+ 83 V). As it can be seen, under this condition, current and power peak values reach 16 A and 1.8 kW, respectively.

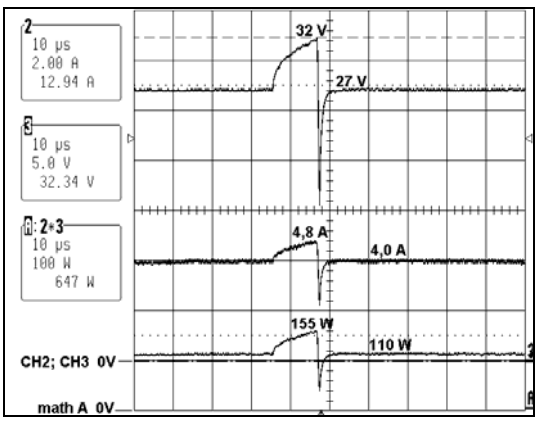


FIG. A2 See text.

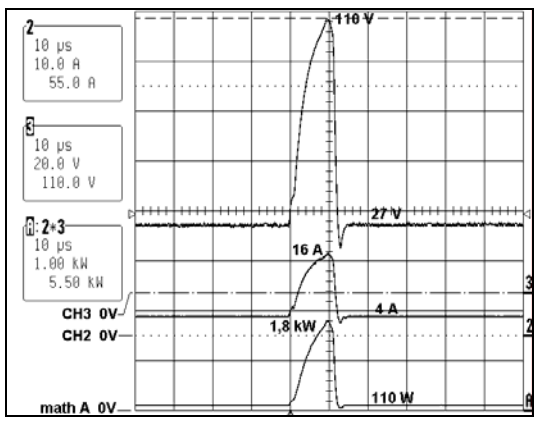


FIG. A3 See text.

A.2 Tests with the IPM connected to a resistive load and 3 dc/dc converters

For this set of measurements, the CAEN filter and the IPM were introduced in the chain. The IPM was connected, via the splitter, to a resistive load (6.8 Ω, corresponding to half power) and 3 dc/dc converters simultaneously: an S9004, an S9006 and an S9019. Each dc/dc converter was fully loaded with a resistive load. The set up is depicted in Fig. A4.

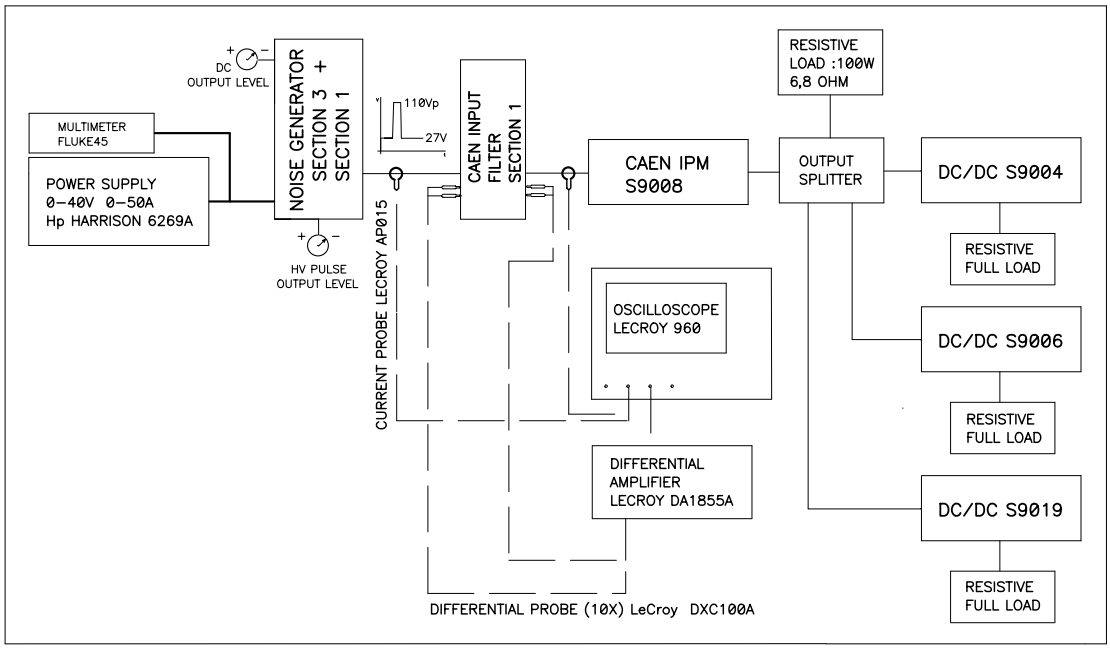


FIG. A4 Set-up used for the "differential voltage pulse rushes" test with the complete chain (filter-IPM-dc/dc converters)

The NG provides the DC supply, with superimposed pulse trains, with frequency 10 Hz and settable amplitude. The tests have shown that for pulse amplitude below a certain value, the filter cuts them off effectively and no effect appears at the output. Above about 45 V, however, disturbances appear at the filter's output.

Fig. A5 shows the voltage (channel 3, upper) and current (channel 2, central) waveform at the filter's input, while the lower waveform (channel A) displays the instantaneous power.

Fig. A6 shows, in the same way, the voltage, current and power at the filter's output. Notice the appearance of a 45 V glitch in the output voltage.

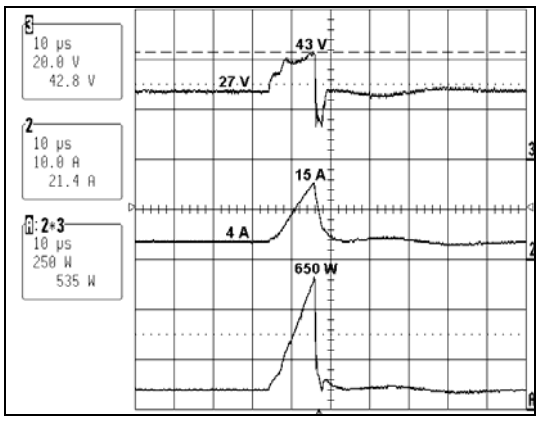


FIG. A5 Signals at filter's input. Upper trace: voltage; central trace: current; lower trace: instantaneous power.

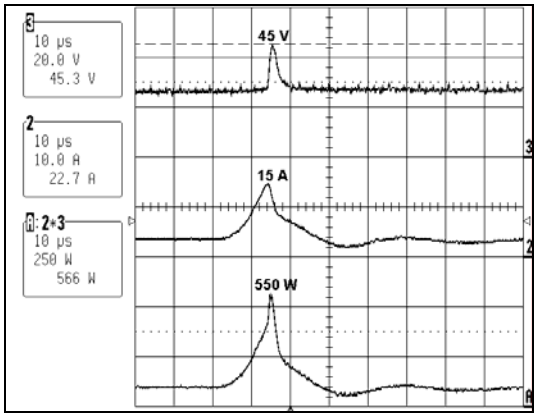


FIG. A6 As in Fig. A5 but at the filter's output.

To evaluate more exactly the pulse height beyond which the filter becomes ineffective, the NG was connected as in Fig. A1, directly to resistive loads of 6.8 ohm (Fig. A7) and of 180 ohm (Fig. A8), and set to deliver the same pulse height for which we started to observe disturbance transmission towards the filter's output. The results are displayed in Figs. A7 and A8 for the two loads used.

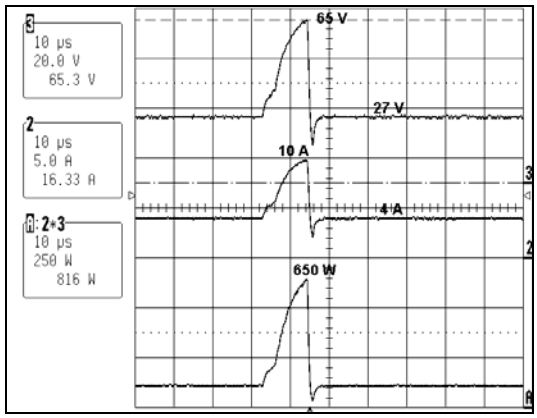


FIG. A7 NG directly connected to a 6.8 ohm load: voltage (upper trace), current (central trace) and power (lower trace) on the load.

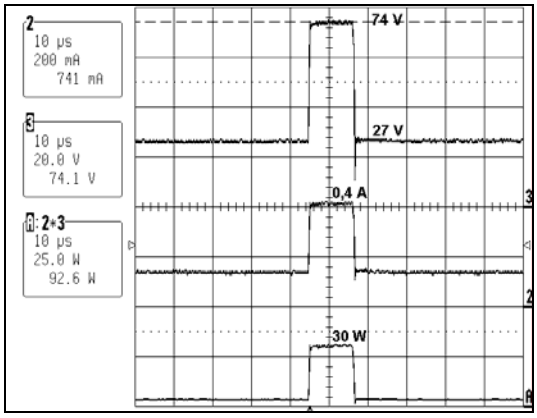


FIG. A.8 As in Fig. A7, but for a 180 ohm load.

For even larger pulses on the primary lines, the transmitted disturbances at the filter's output are large enough to cause the switching off of the IPM.

Fig. A9 shows the waveforms of the voltage (channel 3, upper) and current (channel 2, central) at filter's input when this condition occurs. The lower waveform, channel A, in the same picture is the instantaneous power.

Fig. A10 shows the same quantities as Fig. A9, referred to the filter's output. As said above, for pulses as large (or larger) as those shown in Fig. A10 the IPM switches off.

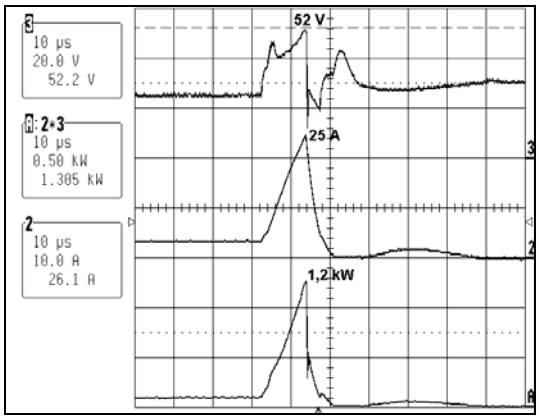


FIG. A9 See text.

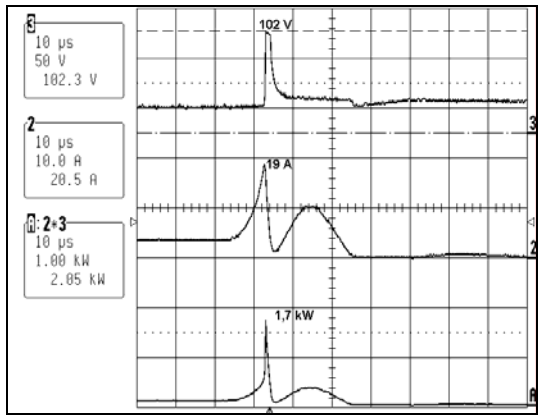


FIG. A10 See text.

To evaluate more exactly the pulse height that provokes the switching off of the IPM, the NG was connected as in Fig. A1, directly to resistive loads of 6.8 ohm (Fig. A11) and of 180 ohm (Fig. A12), and set to deliver the same pulse height level of Figs. A9 and A10. The results are displayed in Figs. A11 and A12 for the two loads used. In both pictures, the sequence is: voltage across the load (upper trace), current to the load (central trace) and power (lower trace.)

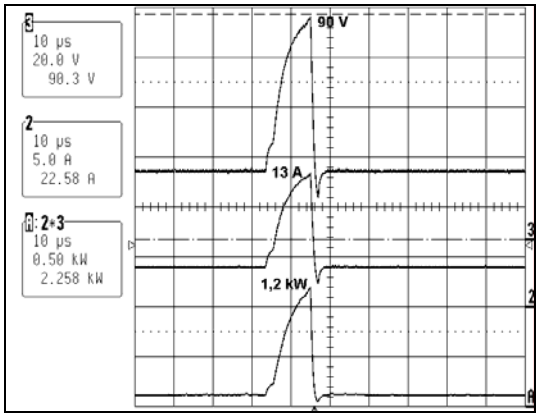


FIG. A11 See text.

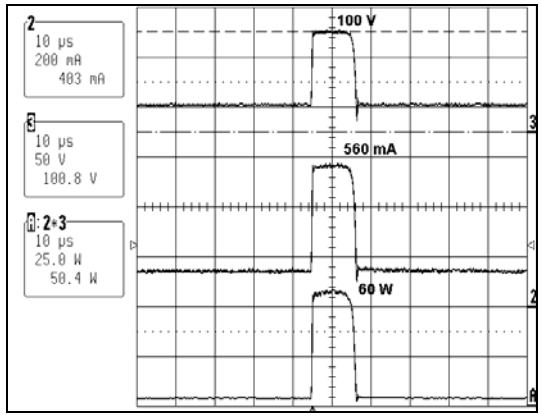


FIG. A12 See text.

Fig. A13 shows that the voltage pulses applied to the filter's input in the scheme of Fig. A4, are not propagated towards the IPM output (i.e. towards the PAMELA apparatus) even for pulse amplitudes close to the observed IPM switching off. In Fig. A13 the central and lower waveforms are the IPM input voltage (displaying a 100 V peak) and the IPM input current, respectively, while the upper waveform (channel 2) is the IPM output voltage (vertical scale of channel 2 is 200 mV/div).

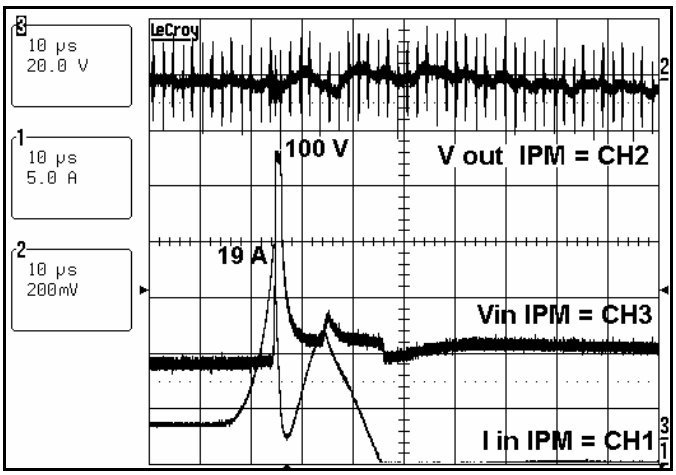


Figure A13 Upper trace: IPM output voltage; central trace: IPM input voltage; lower trace: IPM input current.

A last test performed with this type of pulse disturbances consisted of delivering continuously for 1 hour to the system filter- IPM – resistive load + 3 fully loaded dc/dc converters (set-up of Fig. A4) a series of pulses with the characteristics shown in Fig. A14. The upper waveform is the IPM input voltage and the lower trace is the IPM input current. The pulse period was 80 ms and the pulse height 55 V. No problems whatsoever were reported in the IPM or dc/dc units after this test.

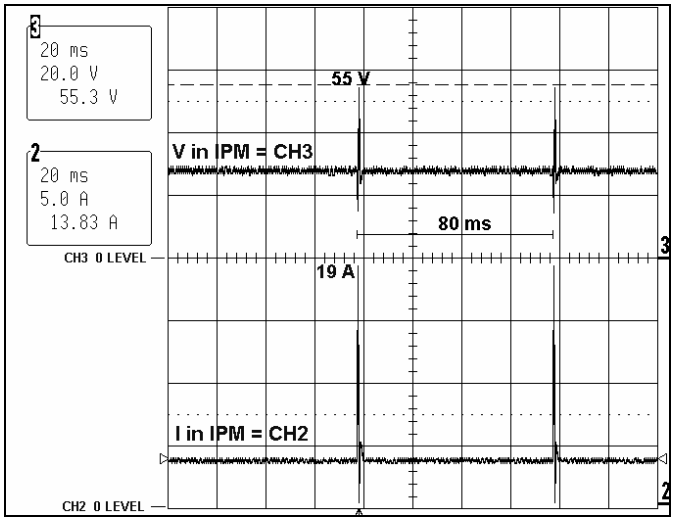


FIG. A14 Characteristics of the pulse disturbances applied to the filter – IPM – dc/dc converters system continuously for 1 hour. Upper waveform: IPM input voltage; lower trace: IPM input current.

At the end of this series of tests, to verify that the integrity and functionality of the filter had not been spoiled by the large pulses delivered to it during measurements, we have repeated a "frequency sweep" test as described in sub-section 4.5. Fig. A15 shows the set-up used for this measurement.

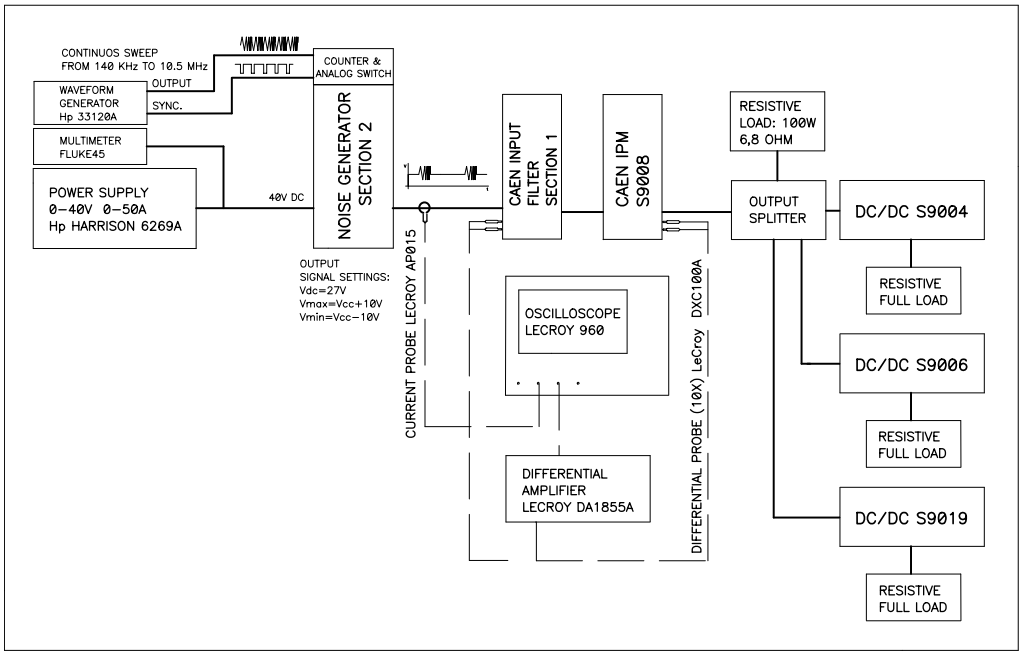


FIG. A15 Set-up for the integrity test on the filter

In both Figs. A16 and A17 the lower trace is the CAEN filter's input current, while the upper trace is the filter input (Fig. A16) and output (Fig. A17) voltage, respectively. The signal shapes as well as the resonance frequency of the filter are unaltered with respect to the measurements reported in sub-section 4.5. Figs. A16 and A17 should be compared with Figs. 4.59 and 4.60, respectively. We therefore conclude that the filter was not damaged by this test.

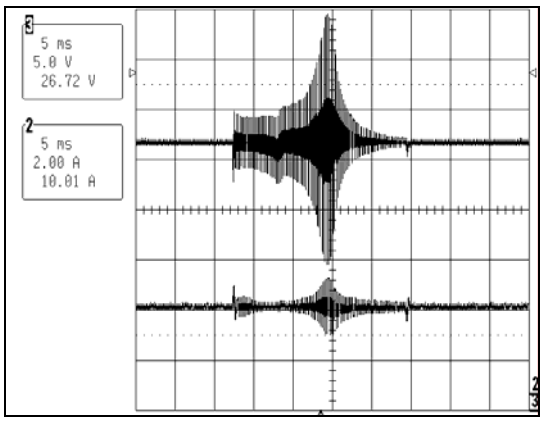


FIG. A16 See text.

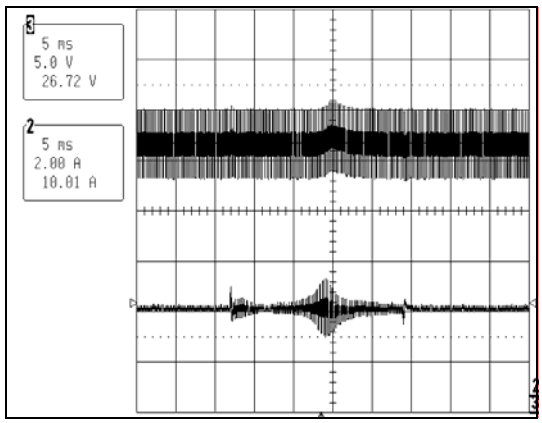


FIG. A17 See text

APPENDIX B

Measurements of maximum output current on dc/dc converters type S9004

The dc/dc converters S9004 deliver a regulated ± 5.7 V, which in PAMELA are used to supply the front-end electronics of the Imaging Calorimeter. Initially it was foreseen to use 2 S9004 hot units (+ 2 cold) for each of the 4 sections of the Calorimeter. During the design and construction of the PSS, it was decided to bias each section of the Calorimeter with only 1 S9004 (+ 1 cold), in order to reduce the cabling and interconnection problems. This meant that the maximum output current of the dc/dc converter should be increased from the initial values (0.8 A for the positive output and 1.2 A for the negative one) to 1.1A for the positive and 1.45 A for the negative output. That was judged a sufficiently safe value in view of the transients occurring at the Calorimeter switch-on. After the modifications performed on the board, we verified its output capability by means of the set-up shown in Fig. B1.

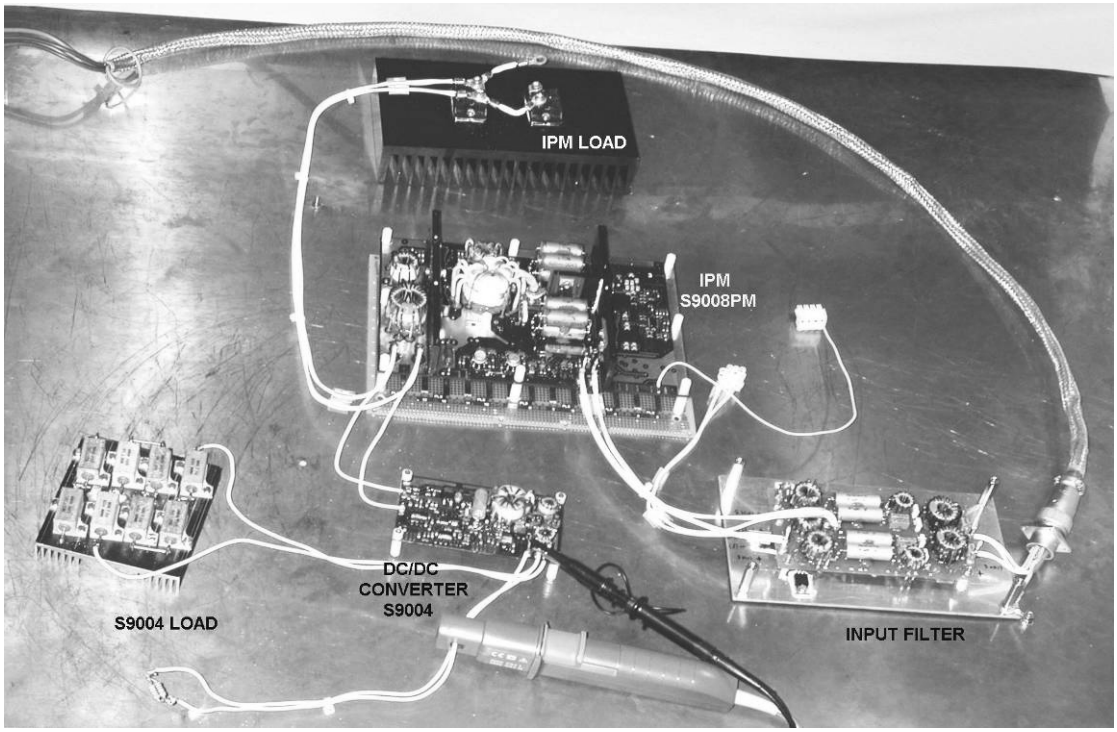


Figure B1 Picture of the set-up for output current measurements on the S9004 type dc/dc converter.

Tab. B1 summarizes the results of the measurements. In the Table, the current and voltage values were measured at full dc/dc load. As shown by the reported results, the target values for the maximum output currents were achieved.

TEST VALUES (S9004 s.n. 04- 05)			
Current		Voltage	
OUTPUT -	OUTPUT +	OUTPUT -	OUTPUT +
A	A	V	V
1.46	1.13	5.73	5.73

TAB. B1

APPENDIX C
Measurements on the IPM Control Board

The IPM Control Board (see the general PAMELA PSS block scheme of Appendix E) is a board that interfaces the IPM units with the PAMELA CPU. It has to set the initial operating conditions (that is, "hot" IPMs on and "cold" IPMs off) and, if needed, switch-off a malfunctioning unit and switch-on the corresponding cold unit upon receiving a command from the CPU. Since, obviously, the IPM Control Board must be "on" before actually turning on the IPMs, it must be powered directly from the unregulated primary voltage (nominally + 27 V DC, see section 2). This means that the IPM Control Board behavior had to be checked in presence of the disturbances on the primary line described throughout the paper.

Fig. C1 shows the measurement set-up that we used to perform the tests on the first version of the IPM Control Board. To simulate the so-called "HV command" signals from the PAMELA CPU (pulses of duration 100 ms and amplitude 26 V), we realized a 9-channel generator that provides the pulses "OFF", "HOT ON" and "COLD ON". By means of the NG, we gave to the primary power line (at 27 V DC) negative pulses with amplitude of 5 V, duration of 200 ms and repetition frequency of 1 s.

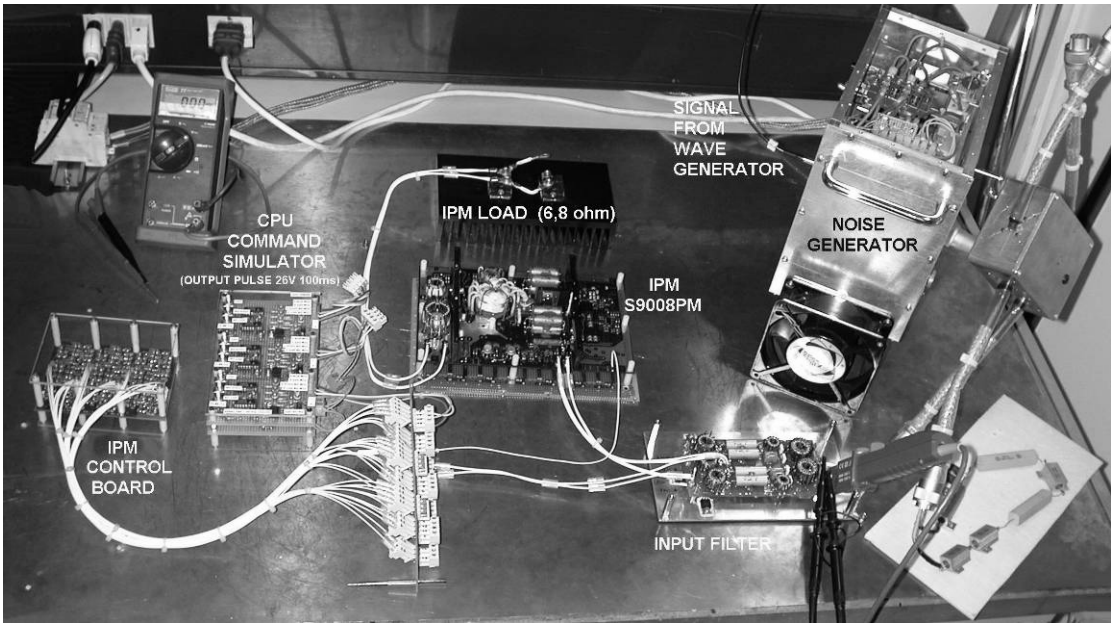


FIG. C1 Picture of the set-up used to test the first version of the IPM Control Board.

Fig. C2 shows the switching on of the IPM after an "on" command received from the "IPM Cold 0" output of the Control Board, in presence of negative pulses (with the characteristics described above) on the supply voltage. Channel 1 (upper trace) is the voltage measured at the filter's input and channel 2 (lower trace) is the corresponding filter's input current. Channel 3 (central trace) is the voltage measured at the "IPM Cold 0" output of the Control Board. Point "A" in Fig. C2 is the instant in which the correct switching on of the IPM takes place. The IPM remains correctly on despite the presence of the negative pulses on the primary supply voltage.

Fig. C3 shows the switching off of the IPM after an "off" command received from the "IPM Cold 0" output of the Control Board, in presence of negative pulses on the supply voltage. Channel 1 (upper trace) is the voltage measured at the filter's input and channel 2 (lower trace) is the corresponding filter's input current. Channel 3 (central trace)

is the voltage measured at the “IPM Cold 0” output of the Control Board. Point “A” in Fig. C3 is the instant in which the correct switching off of the IPM takes place. The IPM remains correctly off despite the presence of the disturbances on the primary supply voltage.

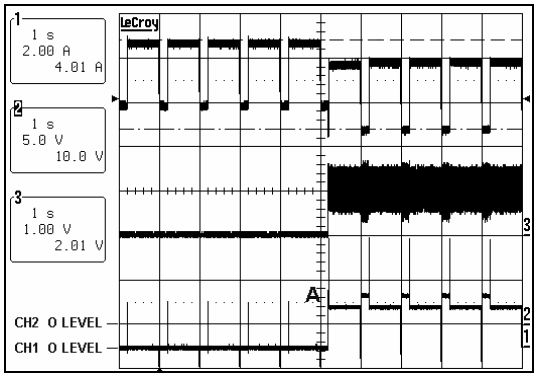


FIG. C2 See text.

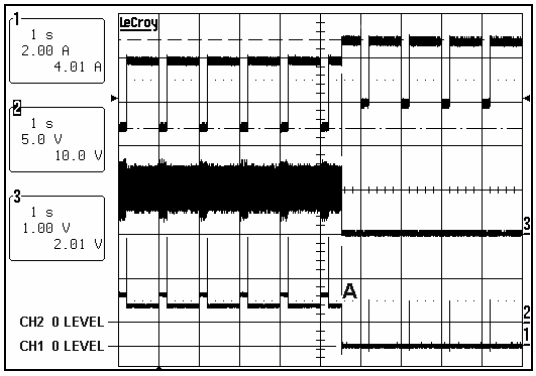


FIG. C3 See text.

On the other hand, a problem was detected on the ‘hot” section of the Control Board for the “off” commands in presence of the above described disturbances. Fig. C4 shows the switching off and the subsequent, erroneous switching on due to a pulse on the primary supply voltage. Channel 1 (upper trace) is the voltage measured at the input of the filter, while channel 2 (lower trace) is the corresponding filter input current. Channel 3 (central trace) is the voltage measured at the “IPM Hot 0” output of the Control Board. Point “A” in Fig. C4 is the instant in which the correct switching off of the IPM takes place. The IPM remains in the “off” state until a following disturbing pulse on the primary supply (point “B”) provokes an erroneous signal at the “IPM Hot 0” output of the Control Board (point “C”) and, consequently, an unwanted switch-on of the unit.

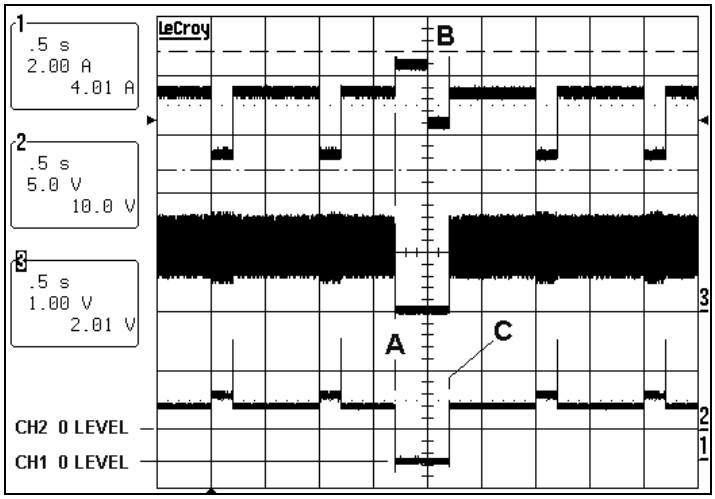


FIG. C4 Uncommanded switch-on of the IPM in presence of voltage drops on the primary supply lines after a successful switch-off command through the IPM Control Board (see text).

These tests allowed discovering this “fault” on the preliminary, test version of the IPM Control Board, which was corrected and eliminated on the final, “flight” version of the board.

APPENDIX D
Verification of the effective switch-off threshold on a "flight" IPM ("undervoltage condition")

Before starting the assembly of the PSS of the Flight Model of PAMELA, we performed some additional undervoltage tests on a "flight" IPM board. A first set of tests ("static measurements") was done by loading the IPM with a resistive load and gradually lowering the supply voltage. Fig. D1 shows the measurement set-up.

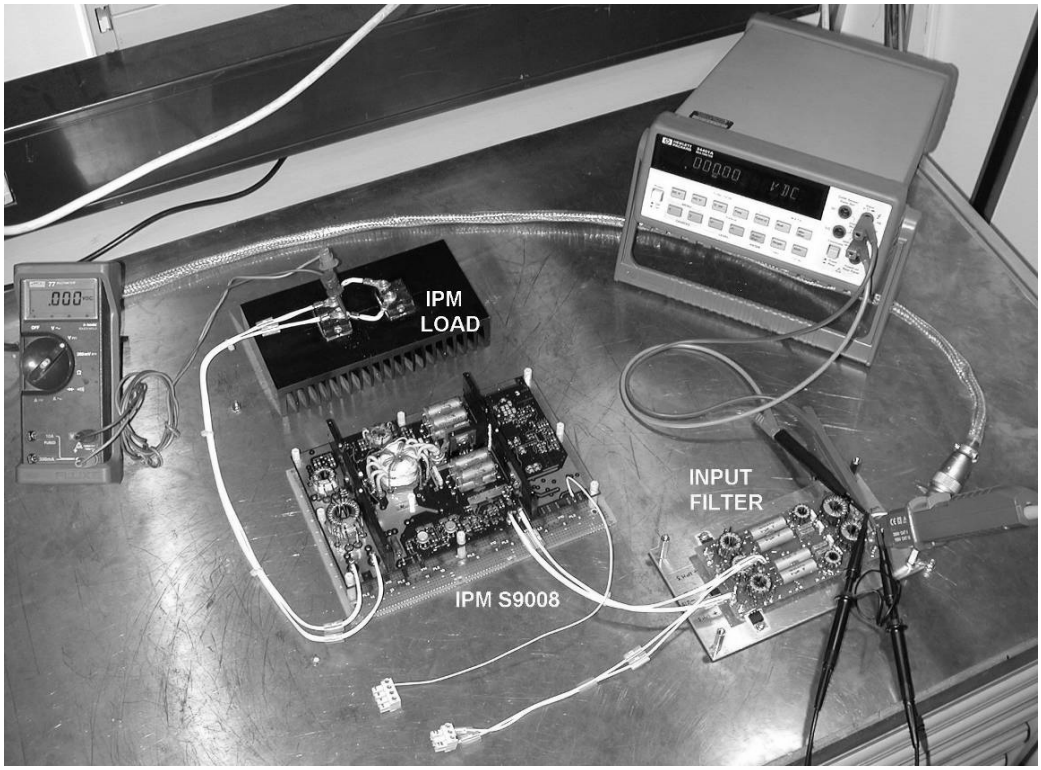


FIG. D1 Picture of the set-up used for the "static" undervoltage measurements.

The IPM was loaded with a 3.4ohm resistive load, corresponding to full-power operation of the unit. Fig. D2 displays on channel 2 the voltage measured at the input of the CAEN filter and on channel 1 the current measured at the input of the filter. The "off" threshold measured at the filter's input, in these conditions, was 20.7 V.

Fig. D3 shows, for the same conditions, the IPM input voltage (channel 2), while channel 1 is again the filter's input current. The "off" threshold measured at the IPM input was 20.1 V.

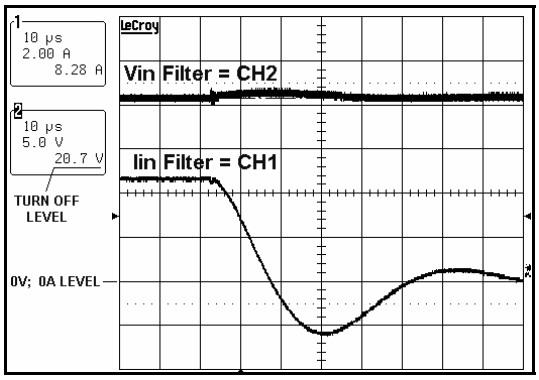


FIG. D2 See text.

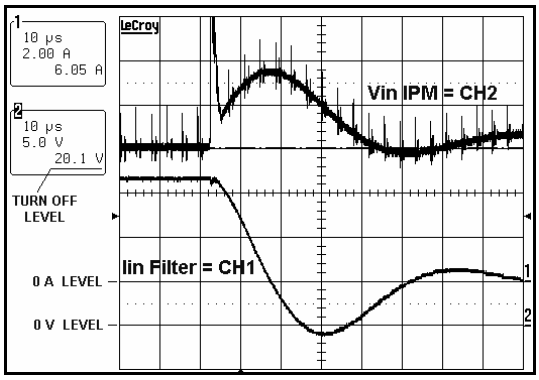


FIG. D3 See text.

A second set of tests was done by applying negative pulses (duration 200 ms, period 1 s) on the supply voltage. Through the NG, the lower level of the pulse was gradually decreased, until reaching the switching off of the IPM (see the set-up used in Fig. D4).

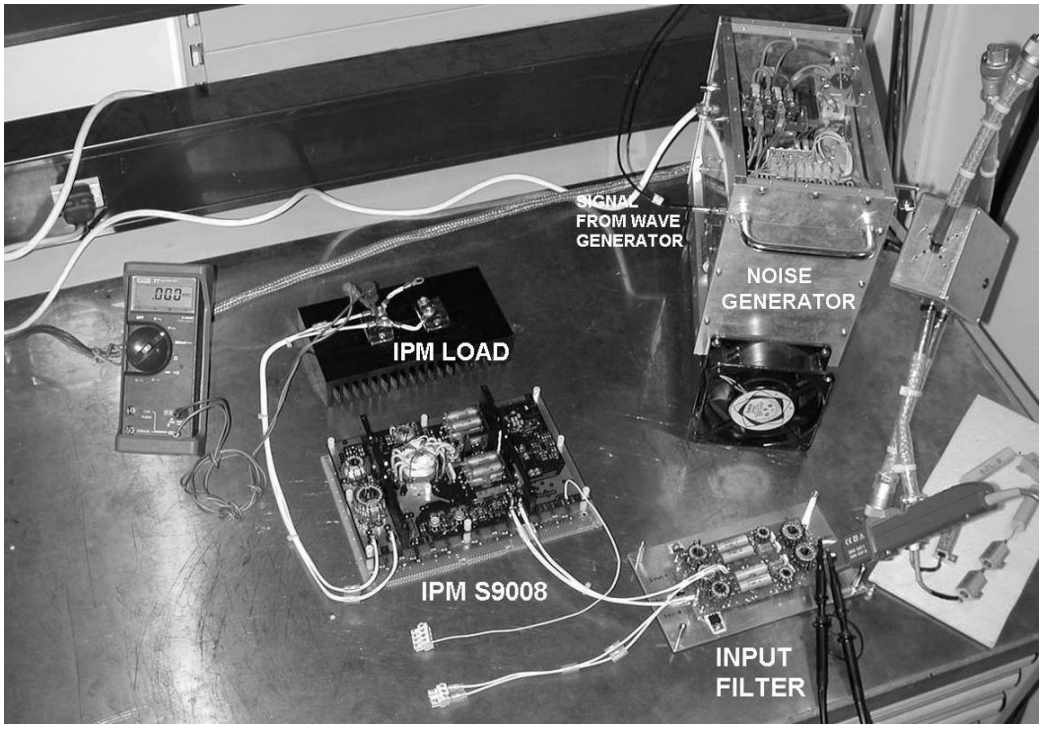


FIG. D4 Set-up used for the "dynamic" undervoltage measurements.

The results of these "dynamic" measurements are summarized in Fig. D5, where channel 2 is the voltage measured at the filter's input and channel 1 is the corresponding filter's input current. The "off" threshold measured at the filter's input, in these conditions, was 20.7 V, like in the previous case of the "static" measurement.

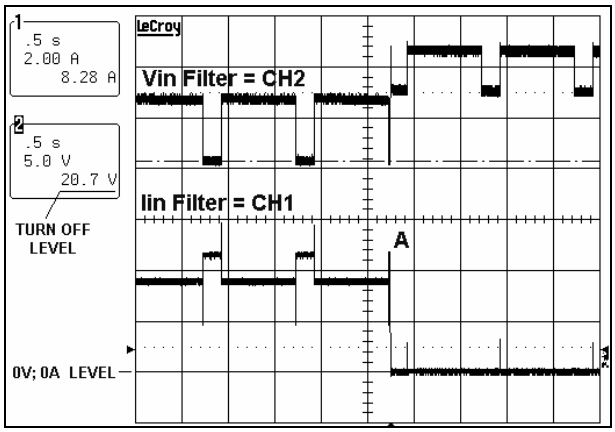
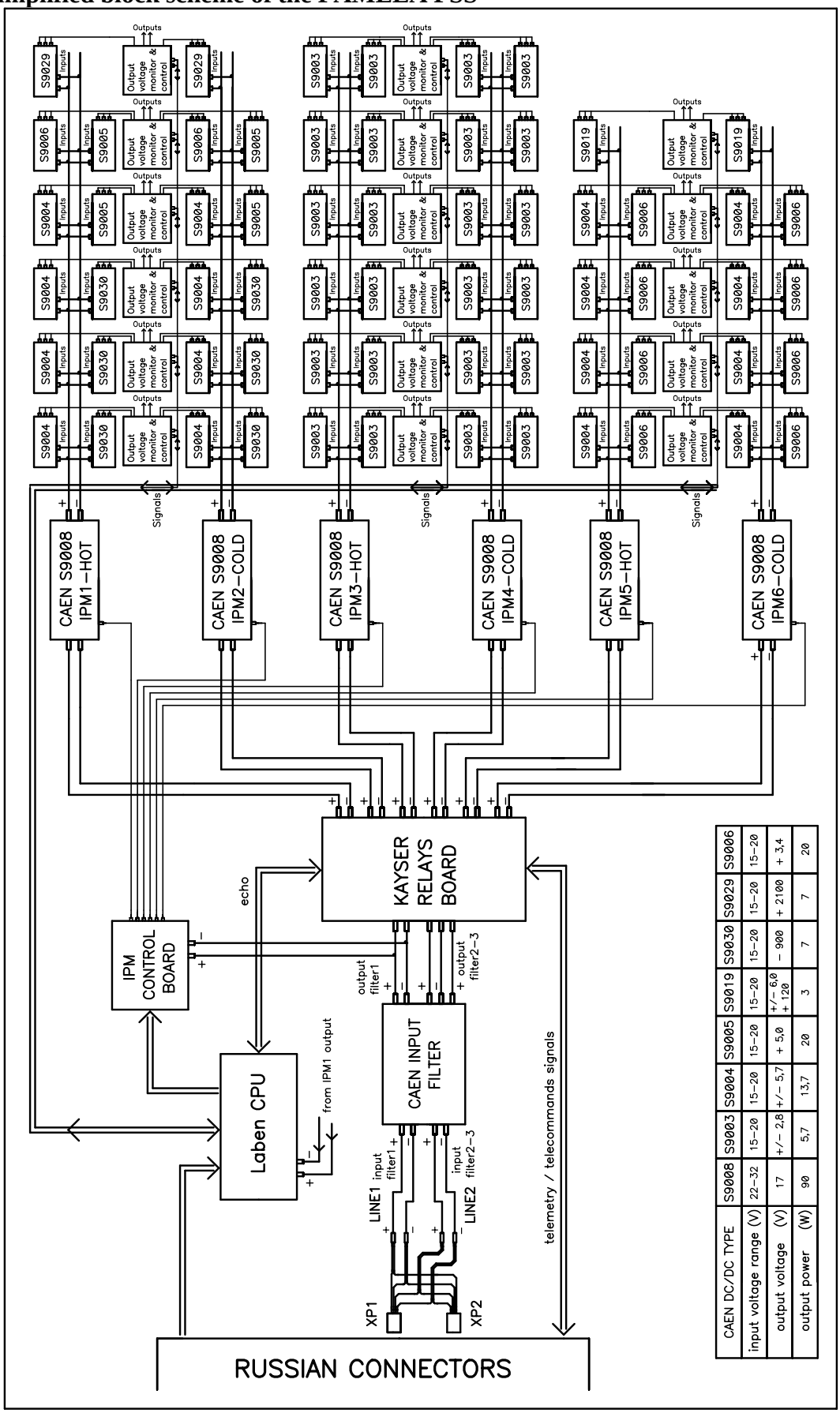


Figure D.5 Filter's input voltage (channel 2) and current (channel 1) measured in the "dynamic" undervoltage test.

APPENDIX E

Simplified block scheme of the PAMELA PSS



CAEN DC/DC TYPE	S9008	S9003	S9004	S9005	S9019	S9030	S9029	S9006
input voltage range (V)	22–32	15–20	15–20	15–20	15–20	15–20	15–20	15–20
output voltage (V)	17	+/– 2,8	+/– 5,7	+ 5,0	+/– 6,0 + 120	– 900	+ 2100	+ 3,4
output power (W)	90	5,7	13,7	20	3	7	7	20